

Transferrin mutations at the glycosylation site complicate diagnosis of congenital disorders of glycosylation type I

Mailys Guillard · Yoshinao Wada · Hana Hansikova · Isao Yuasa · Katerina Vesela ·
Nina Ondruskova · Machiko Kadoya · Alice Janssen ·
Lambertus P. W. J. Van den Heuvel · Eva Morava · Jiri Zeman · Ron A. Wevers ·
Dirk J. Lefeber

Received: 15 December 2010 / Revised: 17 February 2011 / Accepted: 21 February 2011 / Published online: 23 March 2011
© The Author(s) 2011. This article is published with open access at Springerlink.com

Abstract Congenital disorders of glycosylation (CDG) form a group of metabolic disorders caused by deficient glycosylation of proteins and/or lipids. Isoelectric focusing (IEF) of serum transferrin is the most common screening method to detect abnormalities of protein N-glycosylation. On the basis of the IEF profile, patients can be grouped into CDG type I or CDG type II. Several protein variants of transferrin are known that result in a shift in isoelectric point (pI). In some cases, these protein variants co-migrate with transferrin glycoforms, which complicates interpretation. In two patients with abnormal serum transferrin IEF profiles, neuraminidase digestion and subsequent IEF showed profiles suggestive of the diagnosis of CDG type I. Mass spectrometry of tryptic peptides of immunopurified transferrin, however,

revealed a novel mutation at the N-glycan attachment site. In case 1, a peptide with mutation p.Asn630Thr in the 2nd glycosylation site was identified, resulting in an additional band at disialotransferrin position on IEF. After neuraminidase digestion, a single band was found at the asialotransferrin position, indistinguishable from CDG type I patients. In case 2, a peptide with mutation p.Asn432His was found. These results show the use of mass spectrometry of transferrin peptides in the diagnostic track of CDG type I.

Abbreviations

CDG Congenital disorders of glycosylation
IEF Isoelectric focusing
LC-MS Liquid chromatography mass spectrometry

Communicated by: Verena Peters

Competing interest: None declared.

M. Guillard · A. Janssen · L. P. W. J. Van den Heuvel ·
R. A. Wevers · D. J. Lefeber (✉)
Institute for Genetic and Metabolic Disease,
Department of Laboratory Medicine / Department of Neurolog,
Radboud University Nijmegen Medical Centre,
Geert Grooteplein 10,
6525 GA Nijmegen, The Netherlands
e-mail: d.lefeber@neuro.umcn.nl

M. Guillard · D. J. Lefeber
Department of Neurology,
Radboud University Nijmegen Medical Centre,
Nijmegen, The Netherlands

E. Morava
Department of Paediatrics,
Radboud University Nijmegen Medical Centre,
Nijmegen, The Netherlands

Y. Wada · M. Kadoya
Osaka Medical Center and Research Institute
for Maternal and Child Health,
Osaka, Japan

I. Yuasa
Division of Legal Medicine, Tottori University,
Yonago, Japan

H. Hansikova · K. Vesela · N. Ondruskova · J. Zeman
Department of Pediatrics and Adolescent Medicine,
First Faculty of Medicine, Charles University in Prague
and General University Hospital in Prague,
Prague, Czech Republic

MALDI Matrix assisted laser desorption/ionisation
TOF Time-of-flight

Introduction

Congenital disorders of glycosylation (CDG) comprise a group of rare inherited metabolic disorders caused by deficient glycosylation of proteins and/or lipids. For N-glycan biosynthesis, a lipid-linked oligosaccharide is synthesized in the endoplasmatic reticulum, and transferred *en bloc* to a nascent protein. N-glycans are exclusively transferred to an asparagine in the consensus sequence Asn-Xxx-Ser/Thr, where Xxx is any amino acid except proline. The glycosylated protein is then transferred to the Golgi for further processing of the glycans. Defects in the biosynthesis and transfer of the lipid-linked oligosaccharide result in the loss of whole N-glycans on glycoproteins, resulting in a CDG type I (CDG-I).

Diagnostic screening of CDG is performed by isoelectric focusing (IEF) of transferrin. In its most abundant form, this serum glycoprotein carries two complex N-glycans attached to Asn432 and Asn630. Each N-glycan is terminated by two negatively charged sialic acids. Defects in the biosynthesis of N-glycans in the endoplasmatic reticulum cause a loss of one or two complete N-glycans, resulting in a typical IEF pattern of CDG-I, characterized by increased asialo- and disialotransferrin bands, and decreased tetrasialotransferrin. Secondary causes of hypoglycosylation such as galactosemia or fructosemia may cause an identical pattern and therefore must be excluded. Several transferrin protein polymorphisms result in a shifted IEF pattern, caused by *pI* differences of the polypeptide chain (Fujita et al. 1985; Kamboh and Ferrell 1987). Variant TF C is the most common form of transferrin, the anodic variant B and cathodic variant D are less common. In particular, heterozygous combinations of C and D variants may lead to misinterpretation in CDG diagnosis (Fujita et al. 1985; Marklova and Albahri 2009). Nevertheless, these polymorphisms can be identified by

neuraminidase treatment of serum, resulting in an IEF pattern with two distinct asialotransferrin bands (Fig. 1, lane 5).

To improve diagnostics of CDG, mass spectrometric methods for glycoprotein analysis are being developed because of their higher sensitivity and specificity (Hahn et al. 2006; Lacey et al. 2001; Wada 2006; Wada 2007). Liquid chromatography-mass spectrometry (LC-MS) of immunopurified transferrin was proven to be a sensitive screening method for CDG-I, showing distinct peaks for fully glycosylated transferrin, and transferrin lacking one or two oligosaccharide chains (Bunkenborg et al. 2004; Hulsmeier et al. 2007; Lacey et al. 2001; Wada et al. 1992). For CDG type II with abnormal processing of glycans, analysis of enzymatically removed glycans can be diagnostic (Guillard et al. 2011).

Here, we present the application of MS of transferrin peptides in the diagnosis of CDG and reveal two novel transferrin mutations in the N-glycan attachment site.

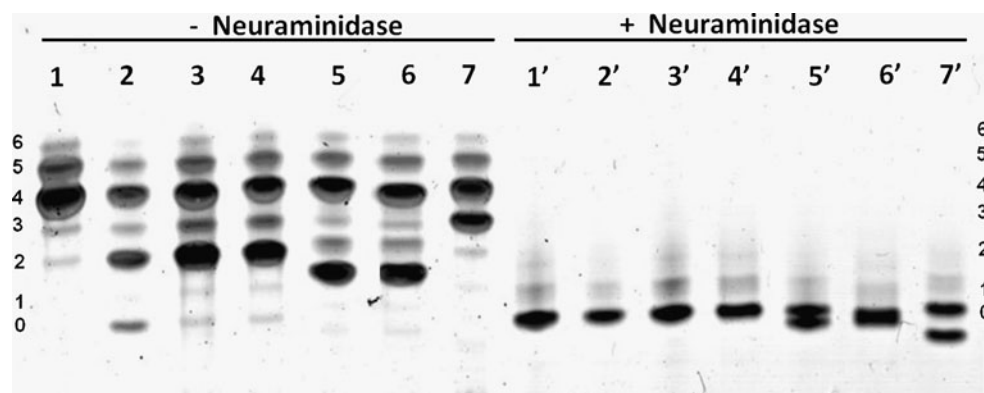
Patients and methods

IEF and SDS-PAGE of transferrin

IEF of transferrin was performed as described in two cases. Case 1 was suspected of CDG due to a clinical presentation of cyclic vomiting accompanied with ketosis and metabolic acidosis and the appearance of atypical fat pads and inverted nipples at the age of seven. Hemoglobin and mean corpuscular volume were normal. Case 2 was a healthy donor for blood transfusion, who participated in a large-scale screening for transferrin variants in populations of Japan and New Zealand (Yuasa et al. 1987). His mother was also healthy.

Five μL of plasma was incubated for 30 min with equal volumes of 6.7 mM Fe(III)citrate and 0.17 mM NaHCO_3 (Fluka, Buchs, Switzerland) in ultrapure water, then diluted ten times in saline. Two μL of each sample was transferred to a hydrated immobilin dry gel (GE Healthcare, Buckinghamshire, UK) with Servalyt, pH 5–7

Fig. 1 Transferrin isoelectric focusing profiles before and after neuraminidase incubation. Lane 1 and 1': control, lane 2 and 2': PMM2-CDG, lane 3 and 3': case 1, lane 4 and 4': mother of case 1, lane 5 and 5': case 2, lane 6 and 6': mother of case 2, lane 7 and 7': patient with a known "D variant" polymorphism. Left and right of the figure are the numbers of sialic acids present on transferrin C variant



(Serva, Heidelberg, Germany) and run on a PhastSystem (GE Healthcare). Different isoforms of transferrin were detected by immunoprecipitation in the gel with 60 μ L rabbit-anti-human transferrin antibody per gel (8.5 g/l; Dako, Glostrup, Denmark) for 30 min, followed by overnight washing in saline, fixation with 20% (w/v) trichloroacetic acid and Coomassie blue staining.

Removal of sialic acids was achieved by incubating 3 μ L of plasma for 30 min with the same volume of 6.7 mM Fe(III) citrate and 0.17 mM NaHCO₃ (Fluka) in water, prior to addition of 15 mU of neuraminidase (Roche diagnostics, Mannheim, Germany) and incubation for two hours at 37°C. IEF was then performed identically to non-treated samples.

Prior to SDS-PAGE analysis, plasma samples were centrifuged and diluted 100-fold with ultrapure water. Three μ L diluted sample was mixed with 100 μ L sample buffer (10 mM Tris-HCl, pH 8.0, 1 mM EDTA, 2.5% SDS, 2% DTT, and 0.01% bromophenol blue) and heated for 5 min at 95°C. The samples were then applied to a 12.5% Phastgel (GE Healthcare) and the proteins separated on a Phastsystem (GE Healthcare). After separation, the proteins were detected by western blotting using a primary rabbit anti-human transferrin antibody (Dako) and a secondary goat anti-rabbit peroxidase conjugated antibody, followed by electrochemiluminescence detection.

Matrix assisted laser desorption/ionization-MS (MALDI-MS) of transferrin

The purified transferrin was desalted by a ZipTip C4 (Millipore, Bedford, MA) and analysed by MALDI mass spectrometry using a Voyager DE Pro MALDI-time-of-flight mass spectrometer with a nitrogen pulsed laser (337 nm) (Applied Biosystems, Foster City, CA) (Wada et al. 1994). The sample matrix was 10 mg/mL sinapinic acid in a 0.1% (v/v) TFA and 30% (v/v) acetonitrile solution. The measurements were carried out in positive ion and linear TOF mode.

For electrospray MS of peptides, transferrin was dissolved in a solution of 6 M guanidine, 0.25 M Tris-HCl, pH 8.0, reduced with 0.13 M dithiothreitol at 50°C for 1 h and then S-carbamidomethylated with 0.22 M iodoacetamide for 30 min at room temperature. Tryptic peptides were desalted by ZipTip C18 (Millipore), dissolved in a 0.1% formic acid and 50% (v/v) acetonitrile solution and were directly infused into an LTQ XL ion trap mass spectrometer (Thermo-Fisher Scientific, San Jose, CA) using a nanospray tip. The CID MS/MS was carried out with helium gas and the spectra were acquired by 100 scans.

Genetic analysis

DNA from case 1 and his mother was isolated from whole blood samples by the commonly used salt-out method for

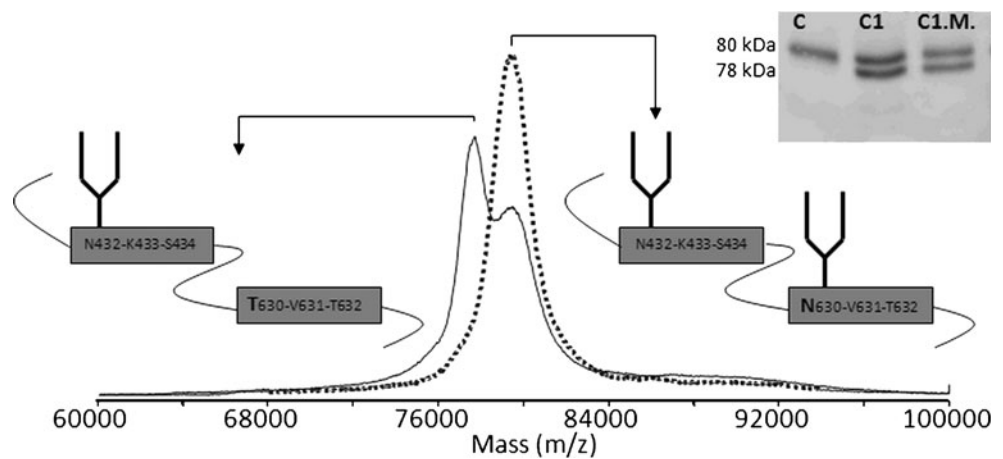
DNA isolation. DNA of other family members was isolated from archived dried blood spots on filter paper using the QIAamp DNA Micro Kit (Qiagen, Valencia, CA). The isolation process was performed according to the recommended manufacturer protocols. The primers were designed to the intronic regions surrounding the 17 protein coding exons of the transferrin gene (*TF* gene: OMIM 190000; NCBI gene ID: 7018; NG_013080.1; ENSG00000091513). Primer sequences are available upon request. The fragments were amplified using the Combi PPP Master Mix (Top-Bio s.r.o; Praha, Czech Republic) and purified by gel extraction using Wizard SV Gel and PCR clean-Up System (Promega, Madison, WI). All fragments were sequenced on ABI PRISM 3100-Avant Genetic Analyzer (Applied Biosystems, Carlsbad, CA) using the Big Dye Terminator v.3.1 Cycle Sequencing Kit (Applied Biosystems) according to the recommended manufacturer protocols. Sequence analyses were performed using SeqScape Software v2.5 (Applied Biosystems). The nucleotide numbering follows cDNA numbering with +1 corresponding to the A of the ATG translation codon in the reference sequence. The initiation codon is codon 1. For restriction analyses of the c.1889A > C mutation, the HpyCH4IV (New England BioLabs, Ipswich, MA) restriction endonuclease was used according to the manufacturer protocols of the enzyme.

Results

Clinical suspicion of CDG in case 1 triggered us to perform IEF of transferrin, which showed a type I profile (Fig. 1, lane 3) with increased disialotransferrin and decreased tetrasialotransferrin. Neuraminidase treatment resulted in a single band corresponding to asialotransferrin, suggesting that the double band in the untreated sample was not the result of a protein variant (Fig. 1, lane 3'). IEF of serum transferrin from case 2 and his mother showed two major bands in a 1:1 ratio with one band at the level of tetrasialotransferrin and one band just below disialotransferrin (Fig. 1, lanes 5 and 6). After neuraminidase treatment, two bands were visible at the asialotransferrin position (Fig. 1, lanes 5' and 6'). The distance between these two bands is much smaller than between the bands of sialylated transferrin.

Additional information was obtained by SDS-PAGE analysis of transferrin. In controls, transferrin SDS-PAGE shows a single band around 79 kDa corresponding to the glycoprotein with two N-glycans (Fig. 2). The transferrin of a PMM2-CDG (CDG-Ia) patient showed bands with non-glycosylated transferrin at 75 kDa, transferrin with one N-glycan at 77 kDa and the fully glycosylated transferrin at 79 kDa (Wada et al. 1994). In cases 1 and 2, two bands of equal intensity were observed at 77 kDa and 79 kDa. This

Fig. 2 MALDI-TOF profile of immunopurified transferrin, carrying 1 (m/z 77.3 kDa) or 2 (m/z 79.6 kDa) N-glycan chains. Dotted line: control, continuous line: case 1. The gray boxes represent the glycosylation consensus sequences of the transferrin protein. Right: SDS-PAGE of serum transferrin: C = control, C1 = case 1, C1.M. = mother of case 1



finding was confirmed by MALDI-MS of whole transferrin (Wada et al. 1994). Instead of a single peak at 79.6 kDa, peaks were observed at 77.3 kDa and 79.6 kDa, corresponding to transferrin with one and two N-glycans, respectively (Fig. 2).

Despite these indications for true CDG-I profiles, a number of clues suggested otherwise. On transferrin IEF, the disialo- and tetrasialotransferrin bands were present in a 1:1 ratio, while asialotransferrin was normal (<3%). In CDG-I patients, such severe profiles are commonly associated with an increase of asialotransferrin. IEF of thyroxin binding globulin (TBG), another serum glycoprotein used for screening of CDG, showed a normal pattern (data not shown). Additionally, transferrin IEF and SDS-PAGE in serum of the healthy mothers revealed similar patterns to their children's (Fig. 1, lanes 4 and 6; Fig. 2). In contrast to the results after neuraminidase digestion, these findings were indicative of a protein variant.

In order to obtain more insight into the structure of the transferrin protein in cases 1 and 2, transferrin was immunopurified from serum, trypsinized, and the peptides were analyzed by mass spectrometry. Glycopeptides, known to be present in the normal transferrin, were detected. In addition, a thus-far unreported nonglycosylated peptide was found in case 1 as doubly charged ion at m/z 1252.1 and triply charged ion at m/z 835.0. MS/MS analysis revealed the peptide sequence 622-QQHLFGSTVTDCSGNFCLFR-642, corresponding to the non-glycosylated glycopeptide 2 with a heterozygous p.Asn630Thr change (Fig. 3). This asparagine is the second N-glycosylation site of transferrin (underlined). In case 2, an unknown doubly charged ion with m/z 750.4 was found. MS/MS sequencing indicated a p.Asn432His change in the first glycosylation site: 421-CGLVPVLAENYHK-433 (Fig. 4).

Thus, in both cases, MS/MS analysis of transferrin peptides showed a heterozygous amino acid change in one of the N-glycan attachment sites, resulting in a transferrin molecule with a single N-glycan. As a result, the mutated

transferrin will lack two sialic acids and therefore be located at the disialotransferrin level on IEF. The imidazole group of the histidine in case 2 causes a slight pI difference between the common disialotransferrin and the mutated form.

For case 1, sequencing of the *TF* gene revealed the heterozygous c.1889A > C mutation, thereby confirming the p.Asn630Thr alteration at the amino acid level. RFLP analysis in family members of case 1 showed the heterozygous mutation in the mother of case 1, her sister and the grandmother. This p.Asn630Thr mutation was not found in 130 controls.

Case 2 was not available for further investigations at the molecular level. Yet, based on the amino acid sequence, a c.1294A > C mutation may have occurred, resulting in the substitution from Asn (AAT) to His (CAT).

Discussion

In the diagnosis of CDG, it is important to exclude secondary causes of hypoglycosylation of transferrin, as well as transferrin variants which show an IEF pattern suggestive of CDG. In this study, we showed that the current method to identify a protein variants by treatment of serum samples with neuraminidase can be misleading when the mutation is located in one of the amino acids of the consensus sequence of N-glycosylation for transferrin. The loss of the N-glycan in half of the transferrin proteins in serum resulted in a pattern with equal amounts of disialo- and tetrasialotransferrin. Although this resembles a CDG type I pattern, the approximate 1:1 ratio between the two isoforms in combination with low levels of asialotransferrin (<3%), should trigger one to consider a mutation in one of the glycosylation sites. If neuraminidase treatment is inconclusive, IEF of another glycoprotein, like TBG, may provide additional information about a generalized glycosylation defect. When serum of the patient's parents is

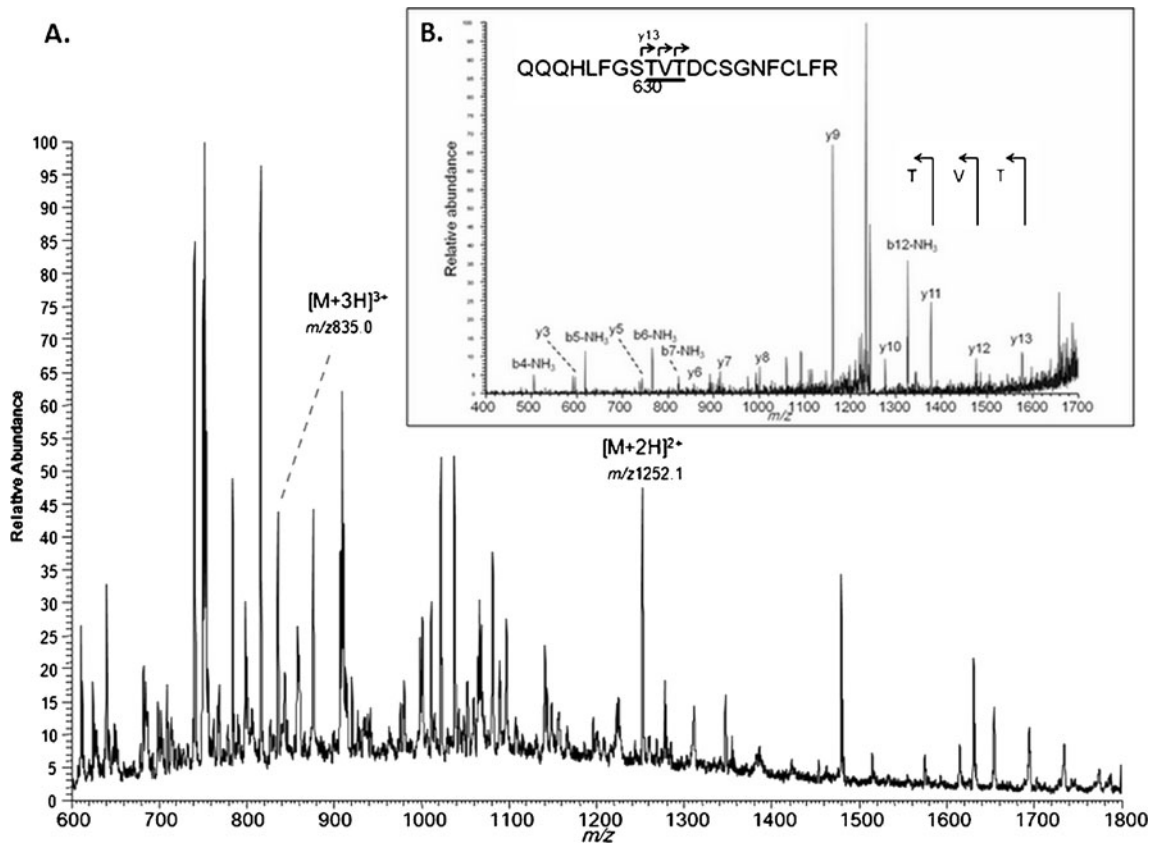


Fig. 3 Analysis of transferrin peptides in case 1. **a** identification of doubly- and triply charged species, not present in controls. **b** MS/MS analysis of m/z 1252.1 indicates a p.N630T mutation

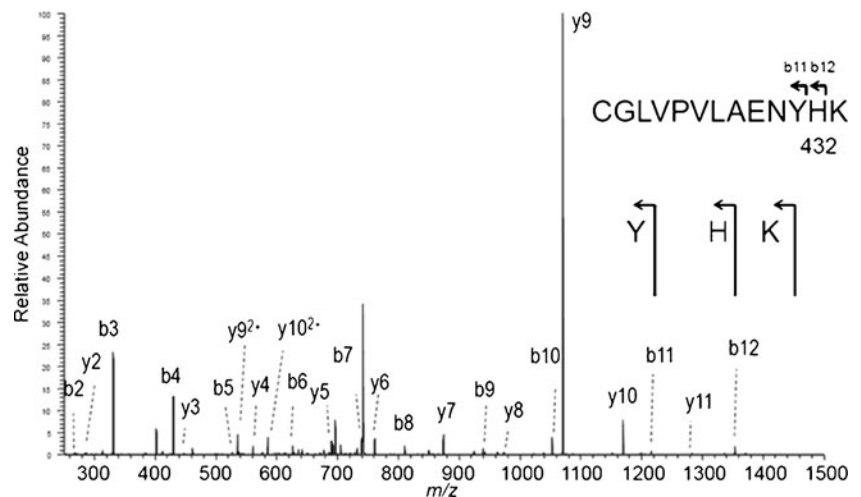
in the second transferrin glycosylation site, thus peptide 622-QQQLFGSNVTDCSGNFCLFR-642 is mutated to 622-QQQLFGSTVTD~~CSGNFCLFR~~-642

available, IEF of transferrin in these samples can also help to exclude such a mutation.

Currently, mass spectrometry is increasingly used in diagnostics of inborn errors of metabolism. For CDG diagnosis, MS opportunities are growing (Lacey et al. 2001;

Wada 2007; Guillard et al. 2011). Here, we show that the application of MS of transferrin (glyco)peptides reveals a non-glycosylated peptide with a mutated N-glycosylation consensus sequence Asn-Xxx-Thr/Ser. Alternatively, identification of non-glycosylated peptides with normal sequence

Fig. 4 Identification of a protein mutation in case 2. MS/MS analysis of m/z 750.4 indicated a p.N432H mutation in the first transferrin glycosylation site in case 2, thus peptide 421-CGLVPVLAENYNK-433 is mutated to 421-CGLVPVLAENYHK-433



will direct the diagnostics toward CDG-I. These analyses do not require additional serum sampling and provide unambiguous results.

Our findings indicate the potential for mass spectrometric analysis of transferrin (glyco)peptides, not only in CDG-II, but also in the diagnostic track of CDG-I patients. It allowed the detection of two novel mutations in the consensus glycosylation sites, which influence the screening by transferrin IEF.

Acknowledgement This work was supported by the European Commission (LSHM-CT2005-512131, Euroglycanet) and Metakids and a grant from the Ministry of Education, Youth and Sports of the Czech Republic MSM 0021620806.

Open Access This article is distributed under the terms of the Creative Commons Attribution Noncommercial License which permits any noncommercial use, distribution, and reproduction in any medium, provided the original author(s) and source are credited.

References

- Bunkenborg J, Pilch BJ, Podtelejnikov AV, Wisniewski JR (2004) Screening for N-glycosylated proteins by liquid chromatography mass spectrometry. *Proteomics* 4(2):454–465
- Fujita M, Satoh C, Asakawa J, Nagahata Y, Tanaka Y, Hazama R, Krasteff T (1985) Electrophoretic variants of blood proteins in Japanese. VI. Transferrin. *Jpn J Hum Genet* 30(3):191–200
- Guillard M, Morava E, van Delft FL, Hague R, Korner C, Adamowicz M, Wevers RA, Lefeber DJ (2011) Plasma N-Glycan profiling by mass spectrometry for congenital disorders of glycosylation type II. *Clin Chem*
- Hahn SH, Minnich SJ, O'Brien JF (2006) Stabilization of hypoglycosylation in a patient with congenital disorder of glycosylation type Ia. *J Inherit Metab Dis* 29(1):235–237
- Hulsmeier AJ, Paesold-Burda P, Hennet T (2007) N-glycosylation site occupancy in serum glycoproteins using multiple reaction monitoring liquid chromatography-mass spectrometry. *Mol Cell Proteomics* 6(12):2132–2138
- Kamboh MI, Ferrell RE (1987) Human transferrin polymorphism. *Hum Hered* 37(2):65–81
- Lacey JM, Bergen HR, Magera MJ, Naylor S, O'Brien JF (2001) Rapid determination of transferrin isoforms by immunoaffinity liquid chromatography and electrospray mass spectrometry. *Clin Chem* 47(3):513–518
- Marklova E, Albahri Z (2009) Transferrin D protein variants in the diagnosis of congenital disorders of glycosylation (CDG). *J Clin Lab Anal* 23(2):77–81
- Wada Y (2006) Mass spectrometry for congenital disorders of glycosylation, CDG. *J Chromatogr B Analyt Technol Biomed Life Sci* 838(1):3–8
- Wada Y (2007) Mass spectrometry in the detection and diagnosis of congenital disorders of glycosylation. *Eur J Mass Spectrom (Chichester, Eng)* 13(1):101–103
- Wada Y, Nishikawa A, Okamoto N, Inui K, Tsukamoto H, Okada S, Taniguchi N (1992) Structure of serum transferrin in carbohydrate-deficient glycoprotein syndrome. *Biochem Biophys Res Commun* 189(2):832–836
- Wada Y, Gu J, Okamoto N, Inui K (1994) Diagnosis of carbohydrate-deficient glycoprotein syndrome by matrix-assisted laser desorption time-of-flight mass spectrometry. *Biol Mass Spectrom* 23(2):108–109
- Yuasa I, Saneshige Y, Suenaga K, Ito K, Gotoh Y (1987) Transferrin variants in Japan and New Zealand. Report of an unusually sialylated TF variant. *Hum Hered* 37(1):20–25



Brief Communication

Clinical picture of S-adenosylhomocysteine hydrolase deficiency resembles phosphomannomutase 2 deficiency

Tomáš Honzík^{a,b}, Martin Magner^b, Jakub Krijt^a, Jitka Sokolová^a, Oliver Vugrek^c, Robert Belužić^c, Ivo Barić^d, Hana Hansíková^b, Milan Elleder^{a,1}, Kateřina Veselá^b, Lenka Bauerová^e, Nina Ondrušková^b, Pavel Ješina^a, Jiří Zeman^{a,b}, Viktor Kožich^{a,*}

^a Institute of Inherited Metabolic Disorders, First Faculty of Medicine, Charles University in Prague and General University Hospital in Prague, Czech Republic

^b Department of Pediatrics, First Faculty of Medicine, Charles University in Prague and General University Hospital in Prague, Czech Republic

^c Department of Molecular Medicine, Institute "Ruđer Bošković", Zagreb, Croatia

^d Department of Pediatrics, University Hospital Center Zagreb and School of Medicine, Zagreb, Croatia

^e Institute of Pathology, First Faculty of Medicine, Charles University in Prague and General University Hospital in Prague, Czech Republic

ARTICLE INFO

Article history:

Received 20 June 2012

Received in revised form 14 August 2012

Accepted 14 August 2012

Available online 23 August 2012

Keywords:

S-adenosylhomocysteine hydrolase

S-adenosylhomocysteine

S-adenosylmethionine

Phosphomannomutase 2

Congenital disorders of glycosylation

ABSTRACT

We report on the seventh known patient with S-adenosylhomocysteine hydrolase (SAHH) deficiency presenting at birth with features resembling phosphomannomutase 2 (PMM2-CDG Ia) deficiency. Plasma methionine and total homocysteine levels were normal at 2 months and increased only after the 8th month of age. SAHH deficiency was confirmed at 4.5 years of age by showing decreased SAHH activity (11% in both erythrocytes and fibroblasts), and compound heterozygosity for a known mutation c.145C>T (p.R49C) and a novel variant c.211G>A (p.G71S) in the *AHCY* gene. Retrospective analysis of clinical features revealed striking similarities between SAHH deficiency and the PMM2-CDG Ia.

© 2012 Elsevier Inc. All rights reserved.

1. Introduction

S-adenosylhomocysteine hydrolase (SAHH; EC 3.3.1.1) is an enzyme that catalyzes the last step in the conversion of methionine to homocysteine [1]. Deficiency of this enzyme has been reported in the literature in only six cases [2–6] (OMIM # 180960). Herein, we report on the seventh patient diagnosed with SAHH deficiency and highlight the remarkable resemblance of SAHH deficiency to PMM2 deficiency. The marked similarities in the clinical course are striking. In addition to the neurological manifestation with hypotonia, psychomotor retardation and strabism, these similarities are mainly seen in

the systemic presentation of both diseases with severe coagulopathy, hepatopathy and myopathy. The differential diagnosis may be particularly difficult in early infancy, when the typical changes of fat pads and inverted nipples and the elevated levels of homocysteine and methionine may be absent in PMM2 deficiency and SAHH deficiency, respectively.

2. Laboratory methods

See electronic supplements (Supplement 1).

3. Patients

3.1. Case report of the young female patient with SAHH deficiency

3.1.1. Clinical presentation

This female patient was born after uneventful pregnancy to non-consanguineous parents of Caucasian origin with birth weight of 3180 g and length of 48 cm. She required intubation and mechanical ventilation immediately after birth due to severe hypotonia. Spontaneous movements were significantly reduced. Her Moro's reflex and tendon reflexes were absent. Mechanical ventilation was required until 35 days of life, but poor sucking persisted and she was fed *via* a nasogastric tube until the 3rd month of life. The brain and heart ultrasounds,

Abbreviations: AdoHcy, S-adenosyl-L-homocysteine; AdoMet, S-adenosyl-L-methionine; *AHCY*, S-adenosyl-L-homocysteine hydrolase gene; ALT, alanine transaminase (alanine aminotransferase or serum glutamic pyruvic transaminase); AST, aspartate transaminase (aspartate aminotransferase or serum glutamic oxaloacetic transaminase); CDG, congenital disorder of glycosylation; CK, creatine kinase; GDP, guanosine diphosphate; INR, international normalized ratio; tHcy, total homocysteine; Met, methionine; PMM2, phosphomannomutase 2; SAHH, S-adenosyl-L-homocysteine hydrolase.

* Corresponding author at: Institute of Inherited Metabolic Diseases, Charles University, First Faculty of Medicine, Ke Karlovu 2, 128 08 Praha 2, Czech Republic. Fax: +420 224967119.

E-mail address: Viktor.Kozich@LF1.cuni.cz (V. Kožich).

¹ Deceased.

² The author serving as a guarantor for the article.

brain MRI and electromyography were all normal. Convergent strabismus was noted at the age of 8 months and persisted thereafter. At 4.5 years, she had a microcephaly with severe developmental delay corresponding to the level of a six-month-old infant. She did not develop the ability to sit unsupported, was unable to pull herself to stand or walk and exhibited some vocalizations without syllables. The brain MRI results obtained at the age of 4.5 years were normal and did not demonstrate any white matter changes.

3.1.2. Laboratory data (for details see Supplementary Table 1)

In routine laboratory tests the international normalized ratio (INR) was prolonged since birth (1.29–2.6, controls 0.8–1.25). Early on, mild elevations of serum aminotransferases – ALT (0.73–1.41 $\mu\text{kat/l}$, controls <0.6) and AST (0.61–1.60 $\mu\text{kat/l}$, controls <0.63) – were attributed to the muscle disease because the activity of creatine kinase (5.88–19.56 $\mu\text{kat/l}$, controls <2.27) was also markedly elevated. At the age of 4.5 years, an acute decompensation with progression of hepatopathy was observed (see below).

Metabolic screening at the age of 2 months revealed mild hyperalaninemia (645 $\mu\text{mol/l}$, controls <500), but her plasma methionine (27 $\mu\text{mol/l}$) and total homocysteine (5 $\mu\text{mol/l}$) levels were within the reference ranges. Analysis of serum transferrin by isoelectric focusing yielded normal results. A skin biopsy was taken to establish a fibroblast culture for the examination of a suspected mitochondrial disorder, but the activities of the oxidative phosphorylation complexes in the cultured fibroblasts were normal. Electron microscopy of the skin biopsy revealed that some capillaries had severe endothelial cell damage with plasma membrane destruction and cell rupture (Supplementary Fig. 1). Gradual elevation of methionine (259–547 $\mu\text{mol/l}$, controls 12–45) and mild elevation of total homocysteine (16.1–22.4, controls 3.5–10) appeared only after the age of 8 months. The late occurrence of these metabolic abnormalities and only mild elevation of plasma tHcy were not suggestive for a primary defect in homocysteine metabolism and were thus attributed to the observed hepatopathy.

Acute decompensation was observed at the age of 4.5 years when the patient was admitted to our hospital with an acute gastrointestinal infection and mild dehydration. The laboratory signs of disseminated intravascular coagulopathy were present (INR > 10.0, controls 0.8–1.25; APTT > 180.0, controls 25.9–40; fibrinogen < 0.1–0.4 g/l, controls 2–4; D-dimers 1444–5712, controls < 190). After the administration of vitamin K and freshly frozen plasma, the coagulopathy improved. After admission the elevation of aminotransferases was only mild, and there were no signs of acute rhabdomyolysis. The next day, activities of aminotransferases increased more than 10-fold, whereas the creatine kinase activity had only doubled. The serum glucose, albumin, bilirubine and ammonia concentrations remained within the normal reference ranges.

SAHH deficiency was suspected based on the elevated plasma levels of S-adenosylhomocysteine and S-adenosylmethionine documented at the age of 4.5 years. The AdoMet and AdoHcy concentrations in the patient's plasma were 23 and 84 times higher than the upper reference range value for the corresponding metabolite (P-AdoMet 3.2 $\mu\text{mol/l}$, controls 0.013–0.141; P-AdoHcy 6.8 $\mu\text{mol/l}$, controls 0.004–0.081). The SAHH activity levels in erythrocytes (0.7 nmol/h per mg of hemoglobin, controls 5.7 ± 1.7 nmol/h per mg of hemoglobin; $n = 3$) and fibroblasts (7.2 nmol/h per mg of protein, control 66 nmol/h per mg of protein) were both decreased to 11% of the control levels, thereby confirming SAHH deficiency in the patient.

The low methionine diet (20–25 mg methionine/kg/day corresponding to 0.7–0.9 g protein/kg/day) with methionine-free amino acid supplements (1 g/kg/day), creatine (2 g/day) and vitamin K supplementation have been administered since the diagnosis of SAHH deficiency was confirmed. Although no major neurological improvement was observed, the levels of AdoHcy, AdoMet, methionine and tHcy decreased, and the levels of the latter two metabolites have

reached the reference range. In addition, improvements in her liver and coagulation tests were also observed.

3.1.3. Molecular analysis

Molecular analysis of the *AHCY* gene in the patient and her parents revealed the compound heterozygosity for a previously described mutation c.145C>T (p.R49C), and a novel variant c.211G>A (p.G71S). To elucidate whether the novel variant is pathogenic, we expressed the p.G71S variant enzyme in *Escherichia coli*. Due to the low yield, we were not able to assess the catalytic activity of the p.G71S variant purified by Ni-NTA (Supplementary Fig. 2). The mutant protein was substantially less soluble than the wild type SAHH, and it formed inclusion bodies, indicating impaired folding. Because misfolding and/or rapid degradation of mutant proteins is a common mechanism in human genetic diseases, we also analyzed the amount of SAHH antigen in the patient's fibroblasts, which revealed that the amount of SAHH was decreased to 5% of the control level when normalized to actin (Supplementary Fig. 2). Together, these data indicate that the novel p.G71S variant is indeed pathogenic and potentially is misfolded forming aggregates that are rapidly degraded.

3.2. PMM2-CDG Ia patients

Between 2002 and 2011, a total of 17 Czech patients with PMM2 deficiency, including 8 males and 9 females, were diagnosed by our group at both the enzymatic and molecular levels. Two children died at the ages of 9 and 12 months, and the age range of the living patients spans from 1 year to 22 years with a median of 11 years. The typical clinical findings, i.e., muscle hypotonia, psychomotor delay, strabism, ataxia due to cerebellar hypoplasia and combined coagulopathy, observed in nearly all patients with PMM2 deficiency [7] were also present in each of these Czech patients. The characteristic inverted nipples and atypical fat pads were absent in one of our patients at the time of diagnosis and disappeared in six patients during childhood. Strabism and severe muscle hypotonia were present at birth in all patients. Ataxia manifested in all patients after 12 months of life, although no obvious regression of psychomotor development was observed. Six patients suffered from seizures, and four patients showed temporary neurological deterioration after stroke-like episodes. Psychomotor development was delayed in all patients, with the delay being mild in two, moderate in four, severe in two and profound in 3 patients. The factor XI concentration was decreased in all patients. However, there was a tendency towards an improvement in coagulopathy during the course of the disease; in two patients, we even observed a normalization of the coagulation parameters (including factor XI levels) at the 8th and 15th years of life. Clinical similarities of two series of PMM2-CDG Ia patients (unpublished Czech cohort, and a group published by De Lonlay et al. [7]) and seven known SAHH-deficient patient are shown in Table 1.

4. Discussion

We report on the seventh known patient with S-adenosylhomocysteine hydrolase (SAHH) deficiency with the findings of novel mutation which caused an impaired enzyme folding in an *E. coli* expression system. Multisystemic manifestation with neonatal onset of severe hypotonia, poor sucking, hepatopathy, marked myopathy and severe coagulopathy and the absence of elevated methionine and homocysteine during the first two months of life prompted us to search for disorders of glycosylation. This case demonstrates that establishing diagnosis in patients with SAHH deficiency may be intriguing.

Firstly, the clinical manifestation of SAHH deficiency may resemble the PMM2-CDG Ia (e.g. fetal hydrops, hypotonia with myopathy, cerebellar hypoplasia, strabism, hepatopathy or coagulopathy [6,8,9]). White matter changes are typical for SAHH deficiency in contrast to PMM2-

Table 1

Comparison of the clinical data obtained from SAHH- and PMM2-deficient patients (n.a. – data not available).

	SAHH-deficient patient	Other SAHH-deficient patients	PMM2-deficient patients	
Reported	Current report	[2–6]	Czech patients (2002–2011) current report	[7]
		Total (n = 7, including patient reported here)	Total (n = 17)	Total (n = 20)
Hypotonia	++	7/7	17/17	17/20
Psychomotor retardation	+	7/7	17/17	19/20
Cerebellar hypoplasia	–	2/7	13/13	n.a.
Strabism	+	4/7	17/17	16/20
Hypo/Areflexia	+	4/5	7/13	11/20
Seizures	–	0/7	6/17	5/20
Microcephaly	+	3/5	14/17	n.a.
Hepatomegaly/ hepatopathy	++	7/7	14/17	12/20
Cardiomyopathy	–	1/7	0/20	2/20
White matter abnormalities	++	5/6	1/9	n.a.
Coagulopathy	++	6/6	17/17	n.a.

CDG Ia, for which cerebellar hypoplasia is a common sign (Table 1). However, white matter abnormalities were not present in the repeated brain MRIs in this Czech SAHH-deficient patient, and cerebellar hypoplasia was previously documented in two severely affected SAHH-deficient neonates [6]. On the other hand, MR imaging in one of the Czech PMM2-CDG Ia patients showed white matter abnormalities in addition to cerebellar hypoplasia. Although coagulopathy is present in both diseases, the vitamin K-independent clotting factor XI level is typically decreased in PMM2-CDG Ia but not in SAHH deficiency (our observation). Dysmorphic features including inverted nipples and atypical fat pads are characteristic signs of PMM2-CDG Ia patients but any or all of these signs can be missing or may develop only later ([8], our observation).

Secondly, the methionine and homocysteine levels in this SAHH patient were unexpectedly within the reference range during the neonatal period, and have risen only later in infancy due to unknown reasons. Thus, normal homocysteine and methionine levels in neonatal period or early infancy thus do not exclude SAHH deficiency.

Take-home message

SAHH deficiency should be considered in early infancy when PMM2-CDG Ia deficiency is suspected but appropriate laboratory tests do not reveal altered glycosylation pattern.

Competing interest statement

All authors confirm that they have no competing interests to declare.

Details of funding

The authors confirm independence from the sponsors; the content of the article has not been influenced by the sponsors.

Details of ethics approval

The study was performed in accordance with the Declaration of Helsinki of the World Medical Association. Due to the nature of the study, no ethical approval was requested from the local ethics committee.

Acknowledgments

The authors acknowledge the technical help of Ms. A. Dutá and P. Melenovská, MSc. and V. Simunović, PhD. Institutional support was provided by research programs PRVOUK-P24/LF1/3 and UNCE 204011; by the Research Project RVO-VFN64165/2012; by the grant IGA NT12166-5/2011, 108-1081870-1885 (to IB) and the IPA-project “Creation of Research Infrastructure for Translational Medicine and Applied Genomics” (IPA2007/HR/16IPO/001-040305).

Appendix A. Supplementary data

Supplementary data to this article can be found online at <http://dx.doi.org/10.1016/j.ymgme.2012.08.014>.

References

- [1] G. De La Haba, G.L. Cantoni, The enzymatic synthesis of S-adenosyl-L-homocysteine from adenosine and homocysteine, *J. Biol. Chem.* 234 (1959) 603–608.
- [2] I. Barić, K. Fumić, B. Glenn, S-adenosylhomocysteine hydrolase deficiency in a human: a genetic disorder of methionine metabolism, *Proc. Nat. Acad. Sci. U.S.A.* 101 (2004) 4234–4239.
- [3] I. Barić, M. Cuk, K. Fumić, O. Vugrek, R.H. Allen, B. Glenn, M. Maradin, L. Pazanin, I. Pogribny, M. Rados, V. Sarnavka, A. Schulze, S. Stabler, C. Wagner, S.H. Zeisel, S.H. Mudd, S-Adenosylhomocysteine hydrolase deficiency: a second patient, the younger brother of the index patient, and outcomes during therapy, *J. Inherit. Metab. Dis.* 28 (2005) 885–902.
- [4] N.R. Buist, B. Glenn, O. Vugrek, C. Wagner, S. Stabler, R.H. Allen, I. Pogribny, A. Schulze, S.H. Zeisel, I. Barić, S.H. Mudd, S-adenosylhomocysteine hydrolase deficiency in a 26-year-old man, *J. Inherit. Metab. Dis.* 29 (2006) 538–545.
- [5] M. Cuk, M. Lovric, K. Fumić, S.H. Mudd, O. Vugrek, V. Sarnavka, I. Barić, The fourth S-adenosylhomocysteine hydrolase deficient patient: further evidence of congenital myopathy, *Clin. Chem. Lab. Med.* 45 (2007) A43.
- [6] R. Grubbs, O. Vugrek, J. Deisch, C. Wagner, S. Stabler, R. Allen, I. Barić, M. Rados, S.H. Mudd, S-adenosylhomocysteine hydrolase deficiency: two siblings with fetal hydrops and fatal outcomes, *J. Inherit. Metab. Dis.* 33 (2010) 705–713.
- [7] P. De Lonlay, N. Seta, S. Barrot, A broad spectrum of clinical presentations in congenital disorders of glycosylation I: a series of 26 cases, *J. Med. Genet.* 38 (2001) 14–19.
- [8] S. Grunewald, The clinical spectrum of phosphomannomutase 2 deficiency (CDG-Ia), *Biochim. Biophys. Acta* 1792 (2009) 827–834.
- [9] B. Perez-Duenas, A. Garcia-Cazorla, M. Pineda, P. Poo, J. Campistol, V. Cusi, E. Sschollen, G. Matthijs, S. Grunewald, P. Briones, C. Pérez-Cerdá, R. Artuch, M.A. Vilaseca, Long-term evolution of eight Spanish patients with CDG type Ia: typical and atypical manifestations, *Eur. J. Paediatr. Neurol.* 13 (2009) 444–451.

Online supplement to the article Honzik et al.

Clinical picture of *S*-adenosylhomocysteine hydrolase deficiency resembles phosphomannomutase 2 deficiency

Supplement 1. Methods

1. *Amino Acid and S-adenosyl-L-homocysteine/S-adenosyl-L-methionine analyses.* Amino acid analyses were performed using the Amino Acid Analyzer (Ingos s.r.o, Czech Republic) with ninhydrine detection. Total homocysteine levels were determined using the previously published HPLC method [1] following the reduction of disulfide bonds with Tris (2-carboxyethyl) phosphine (TCEP) and the derivatization of –SH groups with ammonium 7-fluorobenzo-2-oxa-1, 3-diazole-4-sulfonate (SBD-F). *S*-adenosyl-L-homocysteine/*S*-adenosyl-L-methionine was determined by LC-MS/MS using a previously published method [2].

2. *SAHH activity.* SAHH activity was assayed according to a modified version of a previously published method [3]. SAHH activity was measured in the synthetic direction in hemolyzed erythrocytes and fibroblast extracts using isotopically labeled adenosine and homocysteine as substrates. In brief, 0.1 mL of a reaction mixture containing 79.5 μ L of 25 mM phosphate buffer (pH 7.0), 5 μ L of 10 mM adenosine [$^{13}\text{C}_1$]-ribose, 0.5 μ L of 1 mM EHNA (erythro-9-[2-hydroxy-3-nonyl]adenine), 5 μ L of 100 mM D,L-(3,3,3',4,4,4')- $^2\text{H}_8$ -homocysteine in 300 mM D,L-dithiothreitol and 10 μ L of erythrocyte hemolysate (diluted in water 1:4) or fibroblast extract (protein concentration of 2 mg/mL) was incubated for 15 minutes at 37°C. After incubation, the reaction was stopped by the addition of 25 μ L of 6% perchloric acid. The reaction product, [$^{13}\text{C}_1$, $^2\text{H}_4$]-*S*-adenosylhomocysteine, was detected using the LC-MS/MS method described previously [2] with mass spectrometric detection in the multiple-reaction monitoring mode (m/z 390 \rightarrow 136 setting for the [$^{13}\text{C}_1$, $^2\text{H}_4$]-AdoHcy).

3. *Transferrin isoelectric focusing.* The isoelectric focusing (IEF) of serum transferrin was performed as described by Guillard [4].

4. *Molecular genetic analyses.* All exons and adjacent intronic regions of the *AHCY* gene were amplified using genomic DNA and PCR primer pairs containing sequences of the

universal sequencing primers T7 and RP. All PCR reactions were performed in the DNA Engine Dyad PTC-220 (MJ Research, Waltham, Massachusetts) using PPP master mix (Top-Bio s.r.o., Prague, Czech Republic) and a final primer concentration of 0.25 μ M each. The following cycling conditions were used: an initial step at 95°C for 2 min; 35 cycles of 95°C for 10 s, 62°C for 10 s and 68°C for 50 s; and a final step at 68°C for 5 min. The PCR products were purified using the High Pure PCR Product Purification kit (Roche diagnostics, Mannheim, Germany) and then sequenced using the BigDye Terminator Cycle Sequencing v.3.1 kit on the ABI 3500xL sequencer (Applied Biosystems, Carlsbad, CA). The PCR and sequencing primers are shown below in the table.

Table. PCR and sequencing primers. The numbering of the exons is in agreement with the reference GenBank sequence NG_012630.1.

Exon	Primer sequence (5'→3')		Length of PCR product (bp)
1	PCR-S	T7 - CCAGCCCAGCGGTGACTTCGAG	535 bp
	PCR-AS	RP - CTGAAAGCTGCCCTGGACGTTA	
2	PCR-S	T7 - GGGAAAGTGAAGTGGCGGAATTT	649 bp
	PCR-AS	RP - GGGGCATGCTGGGACTTGTAGT	
3	PCR-S	T7 - GAATGCGGTGACAGAGTGCTAA	438 bp
	PCR-AS	RP - CCCACCCTGGCACAGTCGTCTT	
4	PCR-S	T7 - TCCCCAGCCTGTGATCCTAGAG	523 bp
	PCR-AS	RP - CTCCGCTTCATCATGTAGTTCC	
5	PCR-S	T7 - TGGGAGTTGGGAAGGAGGTAGT	572 bp
	PCR-AS	RP - GCCTCTGCACTCTGCGTACCTG	
6	PCR-S	T7 - TAAAGATGAGGAATTTGCATGA	421 bp
	PCR-AS	RP - TCTTCTCCCAAAGCCATAAAG	
7,8,9	PCR-S	T7 - AATACTCTGAGGCCAAGTTGTC	829 bp
	PCR-AS	RP - CCCCATCCCCCTGCACAGGT	
	Seq-S	TAGGGCAAGGGTTGGTTGTC	
	Seq-AS	GCCAAGGATGATGTCAATA	
10	PCR-S	T7 - ATGTGCTGGAGGTTGTTTTGGA	521 bp
	PCR-AS	RP - TGTCAATGGGGAGAATGACTTC	
11	PCR-S	T7 - TGAGGCTGGGTGTGAGGATAGA	508 bp
	PCR-AS	RP - TCTGTTCCCGCTGCCACATTTG	

PCR-S, PCR-AS; sense and antisense PCR primers, respectively
 Seq-S, Seq-AS; internal sense and antisense sequencing primers, respectively
 T7, RP; the overhang containing sequence of the universal sequencing primers; T7: 3'-AATACgACTCACTATAg - 5' and RP: 3'-gAAACAgCTATgACCATg - 5'

5. *Cloning of Recombinant Mutant SAHH for Expression in E. coli.* The expression vector harboring the wild-type SAHH gene (p32AHHwt) [5] was used as a template for site-directed mutagenesis to create the pG71S vector using the GeneTailor™ system (Invitrogen, Carlsbad,

CA, USA). Oligonucleotides (SAHHG71Sf: 5'- TCGTCACCCTGGATGCTGTGGTGCAGT and SAHHG71Sr: 5'- ACCACTGCACCACAGCATCCAGGGTGA) were designed to introduce the point mutation. Successful mutagenesis was confirmed by dideoxy sequencing using BigDye® chemistry (Applied Biosystems, Foster City, CA, USA).

6. Over-expression and affinity purification of recombinant p.G71S enzyme. The soluble fraction of both the wild-type and G71S AH CY proteins in *E. coli* Bl-21 (DE3) RIL was prepared and purified as described in detail by Belužić and co-workers [5]. Due to the low yield of the variant protein, we used a modified protocol from de Marco and co-workers, which was previously used for the expression of mutant proteins showing significantly reduced solubility [6]. Briefly, bacterial cultures at $OD_{600} > 0.7$ were cooled to 28°C and supplemented with 0.1% benzyl-alcohol to induce endogenous chaperones. After approximately 30 minutes, protein expression was induced by the addition of 0.5 mM IPTG. To further increase the solubility, we lowered the temperature to 20°C with a 30-h incubation. To demonstrate that G71S is expressed as an insoluble protein in *E. coli*, we purified and solubilized the inclusion bodies from induced cultures, according to the protocol of the iFold Protein Refolding System 1 (Novagen, Madison, WI, USA). Recombinant proteins from solubilized inclusion bodies were further purified by Ni-NTA affinity chromatography, as described above [5] (Figure 2B). SDS-PAGE and the determination of protein concentrations were performed according to standard laboratory procedures. Additionally, the purity and electrophoretic behavior of the recombinant AH CY protein was analyzed using native polyacrylamide gel electrophoresis (native PAGE) with the reducing agent DTT (data not shown). Protein staining was performed with the eStain™ protein staining system (Genscript Inc., Piscataway, NJ, USA). S-Adenosylhomocysteine hydrolase activity in the purified enzyme preparations was assayed according to the method of Takata et al. [7].

7. Electron microscopy of skin biopsy samples. The biopsy samples were fixed in 4% buffered paraformaldehyde followed by 1% buffered osmium tetroxide. Thereafter, the samples were dehydrated in ethanol and embedded in a Durcupan-Epone mixture. Thin sections were cut with a diamond knife, double-contrasted with uranyl acetate and lead nitrate, and examined under a JEOL – 1200EX electron microscope.

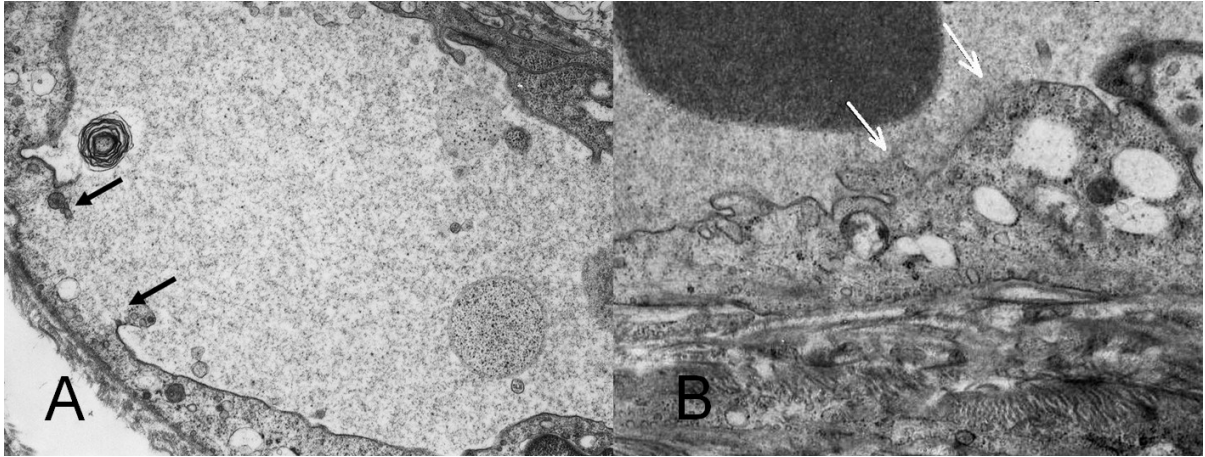
8. Western blot analysis. Fibroblast lysates (40 µg protein per lane) were separated under denaturing conditions in Novex 3-8% Tris-Acetate Mini Gels (Invitrogen, Carlsbad, CA) with Tris-Acetate SDS running buffer (final concentration of 50 mM tricine, 50 mM Tris base, 3.5

mM SDS) at 15 mA per gel. The separated proteins were transferred onto a polyvinylidene difluoride membrane (Immobilon-P, Millipore, Billerica, MA) using the semi-dry blotting transfer technique. SAHH was detected using a mouse monoclonal SAHH antibody (A11) diluted at 1:100 (Santa Cruz Biotechnology, Inc.) followed by a secondary goat anti-mouse IgG antibody conjugated to HRP diluted at 1:5000 (Pierce Biotechnology, Rockford, IL). The signal was visualized using the Super Signal West Femto Maximum Sensitivity Substrate (Pierce Biotechnology, Rockford, IL) and the bioimaging system ChemiGenius-Q (Syngene Inc., Frederick, MD) with a cooled CCD camera. The amount of SAHH was quantified using the Gene Tools software (Syngene Inc.) after performing background subtraction. In parallel, using the same protocol, actin was visualized using a rabbit anti-actin N-terminal antibody (Sigma-Aldrich, St. Louis, MO) diluted at 1:1000 and a secondary goat anti-rabbit IgG antibody conjugated to HRP diluted at 1:5000 (Pierce Biotechnology, Rockford, IL). The actin signal was used to normalize the amount of SAHH antigen.

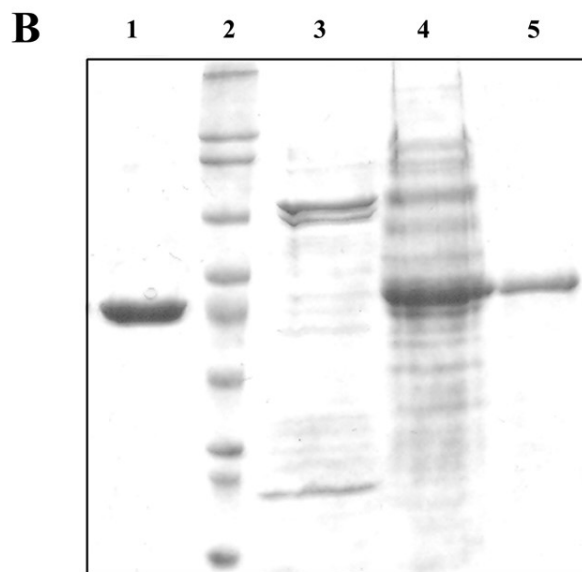
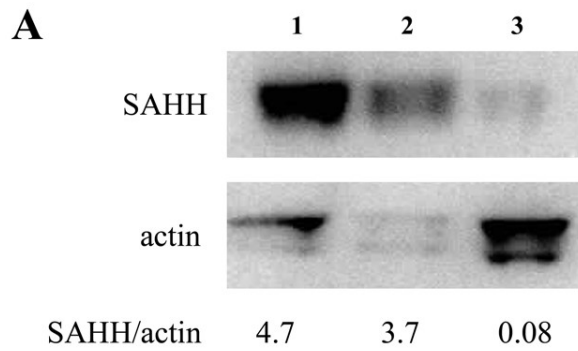
References for methods

- [1] J. Krijt, M. Vackova, V. Kozich, Measurement of homocysteine and other aminothiols in plasma: advantages of using tris(2-carboxyethyl)phosphine as reductant compared with tri-nbutylphosphine, *Clin. Chem.* 47 (2001) 1821-8.
- [2] J. Krijt, A. Duta, V. Kozich, Determination of S-Adenosylmethionine and S-Adenosylhomocysteine by LC-MS/MS and evaluation of their stability in mice tissues, *J. Chromatogr. B. Analyt. Technol. Biomed. Life Sci.* 877 (2009) 2061-6.
- [3] M.S. Hershfield, N.M. Kredich, D.R. Ownby, H. Ownby, R. Buckley, In vivo inactivation of erythrocyte S-adenosylhomocysteine hydrolase by 2'-deoxyadenosine in adenosine deaminase-deficient patients, *J. Clin. Invest.* 63 (1979) 807-11.
- [4] M. Guillard, Y. Wada, H. Hansikova, I. Yuasa, K. Vesela, N. Ondruskova, M. Kadoya, A. Janssen, L.P. Van den heuvel, E. Morava, J. Zeman, R.A. Wevers, D.J. Lefeber, Transferrin mutations at the glycosylation site complicate diagnosis of congenital disorders of glycosylation type I, *J. Inherit. Metab. Dis.* 34 (2011) 901-6.
- [5] R. Beluzić, M. Cuk, T. Pavkov, K. Fumić, I. Barić, S.H. Mudd, I. Jurak O. Vugrek, A single mutation at Tyr143 of human S-adenosylhomocysteine hydrolase renders the enzyme thermosensitive and affects the oxidation state of bound cofactor nicotinamide-adenine dinucleotide, *Biochem. J.* 400 (2006) 245-53.
- [6] O. Vugrek, R. Belužić, N. Nakić, S.H. Mudd, S-Adenosylhomocysteine hydrolase (AHCY) deficiency: Two novel mutations with lethal outcome, *Human. Mut.* 30 (2009) E555-E565.

[7] Y. Takata, T. Yamada, Y. Huang, J. Komoto, T. Gomi, H. Ogawa, M. Fujioka, F. Takusagawa, Catalytic mechanism of S-adenosylhomocysteine hydrolase. Site-directed mutagenesis of Asp-130, Lys-185, Asp-189, and Asn-190, *J. Biol. Chem.* 25 (2002) 22670-6.



Supplementary Figure 1. Electron micrographs of a skin biopsy from the patient with SAHH deficiency. Panels A and B. Two different capillaries, with arrows showing endothelial cells with plasma membrane destruction and cell rupture (magnification 10,000 x).



Supplementary Figure 2. Analysis of SAHH antigen in fibroblasts and following heterologous expression. Panel A. SDS-PAGE and western blot analysis of SAHH in fibroblast lysates. The SAHH signal was normalized against the actin signal. Lanes: 1 and 2, control fibroblasts; 3, patient fibroblasts. Panel B. SDS-PAGE and western blot analysis of wild-type and G71S SAHH protein expressed in *E. coli*. Lanes: 1, Ni-NTA affinity-purified recombinant SAHH wild-type protein; 2, molecular weight marker; 3, Ni-NTA-purified soluble fraction of G71S SAHH-harboring bacterial strain (shows no enzymatic activity); 4, solubilized inclusion bodies from G71S SAHH-harboring bacterial strain; 5, Ni-NTA-purified G71S SAHH mutant protein from inclusion bodies.

Supplementary Table 1. Laboratory data in the SAHH deficient patient.

Age		2 months	8 months – 4 years	Acute decompens ation at 4.5 years	4.5 years, on the low methionine diet	controls
Analyte/unit						
S-ALT	μkat/l	0.73-1.41	2.35- 10.05	2.2-30.44	1.93	<0.6
S-AST		0.61-1.60	1.90-6.63	2.35-30.55	2.14	<0.63
S-CK		5.88-19.56	7.67-45.01	8.18-20.66	27.68	<2.27
S-Creatinine	μmol/l	< 17	< 20	9	23	6weeks- 1year: 21-55 1-15 years: 27-88
INR		1.29	1.45-2.6	> 10.0	1.1	0.8-1.25
APTT	seconds	31.3	27.2-43.4	> 180.0	37.9	25.9-40
fibrinogen	g/l	n.d.	0.5-1.44	< 0.1-0.4	2.33	2-4
D dimer	μg/l	n.d.	25-70	1444-5712	111	0-190
antithrombin III	%	n.d.	39-67	23-44	105	70-140
Protein C		n.d.	26-47	198	84	70-140
Protein S		n.d.	59-88	60	90	65-140
F II		n.d.	52-61	20	95	70-120
F V		n.d.	132-144	26	133	70-120
F VII		n.d.	12-25	< 10	65	70-120
F VIII		n.d.	85	47	80	70-150
F IX		n.d.	63	32	70	70-120
F X		n.d.	82- 122	49	75	70-120
F XI		n.d.	104- 127	67	71	70-120
F XII		n.d.	73	32	94	60-150
P-Met		μmol/l	27	259-547	n.d.	18
P-tHcy	5.1		16.1-22.4	n.d.	4.6	3.5-10
P-AdoMet	n.d.		3.2	n.d.	0.35	0.013-0.141
P-AdoHcy	n.d.		6.8	n.d.	0.45	0.004-0.081

U-Hypoxanthine	mmol/	n.d.	48-89	n.d.	24.4	<30
U-Xanthine	mol creat	n.d.	26-39	n.d.	24.7	<25

(ALT – alanine aminotransaminase, AST – aspartate aminotransaminase, CK – creatine kinase, INR - international normalized ratio, APTT – activated partial thromboplastin time, AT III - antithrombin III, F II - XI – coagulation factors II - XI, Met – methionine, tHcy – total homocysteine, AdoMet – S-adenosylmethionine, AdoHcy – S-adenosylhomocysteine, n.d. – not determined, creat - creatinine, S-serum, P-plasma, U- urine)



Brief Communication

RFT1-CDG in adult siblings with novel mutations

Nina Ondruskova, Katerina Vesela, Hana Hansikova, Martin Magner, Jiri Zeman, Tomas Honzik*

Department of Pediatrics and Adolescent Medicine, First Faculty of Medicine, Charles University in Prague and General University Hospital in Prague, Prague, Czech Republic

ARTICLE INFO

Article history:

Received 26 August 2012

Received in revised form 7 October 2012

Accepted 7 October 2012

Available online 13 October 2012

Keywords:

RFT1-CDG

lipid-linked oligosaccharide

deafness

ABSTRACT

RFT1-CDG is a rare N-glycosylation disorder. Only 6 children with RFT1-CDG have been described, all with failure to thrive, feeding problems, hypotonia, developmental delay, epilepsy, decreased vision, deafness and thrombotic complications. We report on two young adult siblings with RFT1-CDG, compound heterozygotes for the novel missense mutations c.1222A>G (p.M408V) and c.1325 G>A (p.R442Q) in *RFT1* gene. Similar to the previously described patients, these siblings have profound intellectual disability but no feeding problems or failure to thrive. Their epilepsy is well controlled and coagulopathy is mild without clinical consequences. In addition, visual acuity is normal in both patients and hearing impairment is present only in one. Our findings extend the phenotype associated with RFT1-CDG.

© 2012 Elsevier Inc. All rights reserved.

1. Introduction

Glycosylation is one of the basic protein posttranslational modifications in eukaryotes leading to attachment of oligosaccharide chains to polypeptide. N-linked glycoproteins are formed in the endoplasmic reticulum (ER) and further processed in the Golgi apparatus. Synthesis of the lipid linked oligosaccharide (LLO) starts at the cytoplasmic side of the ER membrane by covalently linking N-acetylglucosamine-1-phosphate (GlcNAc-1-P) to dolichol phosphate (Dol-P). The product of this first assembly step Dol-PP-GlcNAc serves as the acceptor for the addition of the second GlcNAc residue and hence formation of Dol-PP-GlcNAc2, followed by addition of five mannosyl residues from UDP-mannose in reaction catalysed by five different mannosyltransferases. An asymmetric intermediate product, Dol-PP-GlcNAc2Man5, is then switched or “flipped” from the cytoplasmic to the luminal side of the ER membrane, a process catalysed by an integral ER membrane RFT1 protein [1,2]. Dol-P-Man and Dol-P-Glc become consecutively the donor substrates to four more mannosyltransferases and to three glucosyltransferases in the ER. The complete structure Dol-PP-GlcNAc2Man9Glc3 is transferred to selected asparagines on newly synthesized glycoproteins by the oligosaccharyltransferase (OST) complex. Disturbances of any step in the glycosylation process may result in severe disorders.

The first patient with a congenital disorder of glycosylation (CDG) syndrome caused by RFT1 deficiency was described in 2008 [1]. In conditions with limiting RFT1 activity, Dol-PP-GlcNAc2Man5 accumulates at the cytosolic side of the ER membrane, whereas the small amounts of flipped oligosaccharide are extended to Dol-PP-GlcNAc2Man9Glc3 and transferred to proteins. That results in the underglycosylation of N-glycoproteins [1].

Only 6 patients with RFT1-CDG have been described [1,3–6]. Symptoms included feeding problems, failure to thrive, hypotonia, developmental delay, epilepsy, decreased visual activity and sensorineural deafness since birth or within first year of life. All had coagulation factor abnormalities, and thrombotic complications in three of them. The oldest patient according to the date of publication might be now about 9 years old [5].

Herein we report on two affected young adult siblings (19 and 21 years old). They are compound heterozygotes for two novel missense mutations in the exon 12 of the *RFT1* gene. Both of them have intellectual disability, but they have no feeding problems or failure to thrive. Their visual acuity is normal and hearing impairment is present in only one of them. In addition, epilepsy in both siblings is well controlled and they have not presented bleeding or thrombotic episodes. Our findings extend the RFT1-CDG phenotype.

2. Laboratory methods – see electronic supplement

2.1. Patient reports

Patients are siblings born to healthy non-consanguineous Czech parents.

The patient 1 is a 21-years old man born at term with birth weight 2900 g and length 49 cm. His early postnatal adaptation was uneventful, but muscle hypotonia and developmental delay was recognized since the age of 8 months. He was able to sit unsupported

Abbreviations: CDG, congenital disorder of glycosylation; DolP, dolichol phosphate; ER, endoplasmic reticulum; LLO, lipid-linked oligosaccharide; MPI, phosphomannose isomerase; NLO, N-linked oligosaccharide; PMM, phosphomannomutase; RFT1-CDG, congenital disorder of glycosylation due to RFT1 deficiency.

* Corresponding author at: Department of Pediatrics and Adolescent Medicine, First Faculty of Medicine, Charles University and General University Hospital, Ke Karlovu 2, 128 08 Praha 2, Czech Republic. Fax: +420 224 967 713.

E-mail address: tomas.honzik@vfn.cz (T. Honzik).

at the age of 1.5 year and to walk at 3 years. Tonic-clonic seizures were first observed at the age of 12 months. They were reasonably controlled by valproic acid, but he intermittently had short tonic-clonic fits till the age of 8 years. Bilateral hearing loss (> 70 dB) was recognized at the age of 13 years. Brain magnetic resonance imaging was normal.

Nowadays he has mild dysmorphism, kyphoscoliosis and obesity. He has a short stature 169 cm (is 5th centile), weight 82 kg, body mass index 28.6 (is >97th centile), head circumference 56.8 cm (is 40th centile) and the Tanner stage is 5. He has neither strabismus or inverted nipples nor atypical fat pads. He has profound intellectual disability (IQ < 20), ataxia, axial hypotonia and mild spasticity with hyperreflexia. He vocalizes but does not use words. Visual evoked potentials excluded visual impairment. Abdominal ultrasound revealed mild hepatosplenomegaly.

Clotting factor abnormalities have been documented since toddler period and persist until now. They are mild and did not lead to any thrombotic or bleeding event. At present, protein C and factor XI are mildly decreased (62% and 41%, respectively, controls > 70%), the prothrombin time, activated partial thromboplastin time, anti-thrombin III and fibrinogen level are within the reference range. Serum aminotransferases are normal, creatine kinase is slightly increased (3.14 μ kat/l, controls < 2.8) and thyroid hormone levels are normal.

The patient 2 is a 19-years old girl born at term with birth weight 3050 g and length 49 cm. Her early postnatal adaptation was uneventful. She was responsive to smile since 8 weeks of age and she was able to reach objects by hands at the age of 4 months. Thereafter her psychomotor development slowed down. Similar to her brother, she was able to sit at the age of 15 months and to walk at the age of 3 years. She started to use some words around 2 years and controlled her bladder and bowels since 9 years. At the age of 12 years, she had two short attacks of myoclonic seizures, but since then her epilepsy is well controlled by valproic acid. In contrast to her brother she developed no hearing impairment.

Her weight at the age of 19 years is 54.5 kg, height 155 cm (< 3rd centile), BMI 22.7 (70th centile) and head circumference 54 cm (25th centile). She has mild dysmorphism and kyphoscoliosis. Tanner stage is 5. She has no inverted nipples or fat pads. She has ataxia, axial hypotonia and mild spasticity with hyperreflexia. Psychological investigation revealed severe developmental delay with actual development corresponding to the age between 24 and 36 months. MRI of the brain was normal. Ophthalmological investigation including visual evoked potentials was normal. Abdominal ultrasound revealed mild hepatosplenomegaly. Parents expressed no concerns regarding her hearing, saying that she is able to hear even whispering, but BAEP showed slightly abnormal findings.

The girl has mild coagulopathy with decreased levels of protein C (53%), factor VIII (68%), IX (54%) and XI (35%) respectively. Prothrombin time, activated partial thromboplastin time, antithrombin III and fibrinogen were normal. Liver function tests, thyroid hormones levels and activity of creatine kinase are normal.

Clinical and laboratory data are summarized in Table 1.

3. Results

Isoelectrofocusing of serum transferrin showed a type 1 pattern. A test with neuraminidase excluded a transferrin polymorphism. Phosphomannomutase (PMM2) and phosphomannose isomerase (MPI) activities measured in isolated lymphocytes and cultivated fibroblasts were normal, thus excluding PMM2-CDG and MPI-CDG.

The lipid-link oligosaccharide profile in fibroblasts of patient 2 showed an accumulation of Dol-PP-GlcNAc2Man5 and virtually no fully assembled oligosaccharide precursor Dol-PP-GlcNAc2Man9Glc3 was detected (not shown). Analysis of protein-linked glycans was normal (not shown). The accumulation of Dol-PP-GlcNAc2Man5 on LLO

combined with normal protein-linked glycans can be caused by a defect in the translocation of Dol-PP-GlcNAc2Man5 to the ER lumen, and thus RFT1 was analysed.

Both patients are compound heterozygote for two novel missense mutations in the exon 12 of *RFT1* gene. The c.1222A>G, inherited from the mother, leads to replacing of the methionine at position 408 by valine (p.M408V). The second mutation, inherited from the father, is the c.1325 G>A, which leads to a codon for glutamine at position 442 instead of arginine (p.R442Q). Both mutations were not detected in 200 healthy controls.

4. Discussion

All reported patients with RFT1-CDG showed a very similar phenotype (Table 1) [1,3–6]. Common features were feeding problems, failure to thrive, profound developmental delay, poor to absent visual contact, epilepsy, hypotonia and sensorineural deafness [5].

Our young adult siblings similar to all described patients with RFT1-CDG [1,3–6] have mild dysmorphism, profound intellectual disability (< 20 IQ points), epilepsy, hypotonia and coagulopathy. Although the epilepsy developed in both siblings, it was very mild in the girl, who had only two short attacks of myoclonic seizures during puberty. The hearing impairment was diagnosed at age of 13 years in patient 1 but his sister contrary to all described patients [1,3–6] developed no hearing problems of clinical importance. Also the visual acuity is normal in both siblings and neither of them has feeding problems or failure to thrive.

Five of the described patients carry homozygous missense mutation, while the sixth patient is compound heterozygote for the two missense changes at the same nucleotide. In the predicted model of the protein [7], all the described mutations are located in the protein loop sections facing to the ER lumen. The explanation for the milder phenotype and prolonged survival in our patients might be based on the position of the novel mutations. Both mutations in our patients lead to exchanges of two amino acids located in the transmembrane [7].

Competing interest statement

All authors confirm that they have no competing interests to declare.

Details of funding

The authors confirm independence from the sponsors; the content of the article has not been influenced by the sponsors.

Details of ethics approval

The study was performed in accordance with the Declaration of Helsinki of the World Medical Association. Due to the nature of the study, no ethical approval was requested from the local ethics committee.

Acknowledgments

The authors acknowledge the technical help of prof. Gert Matthijs, M.D., Ph.D. from Laboratory for Molecular Diagnosis, Center for Human Genetics, University of Leuven, Leuven, Belgium. Institutional support was provided by grant IGA MZ NT/12166-5/2011 and research programs PRVOUK-P24/LF1/3 and GAUK 638512.

Appendix A. Supplementary data

Supplementary data to this article can be found online at <http://dx.doi.org/10.1016/j.ymgme.2012.10.002>.

Table 1
Clinical and laboratory data in two siblings with RFT1 deficiency in comparison to six previously described patients.

	Imtiazi et al. 2000 and Clayton et al. 2009 [3,4]	Vleugels et al. 2009 [5]			Jaeken et al. 2009 [6]		new cases 2012 (current report)	
	patient 1 (KS*)	patient 2	patient 3	patient 4	patient 5	patient 6	patient 7 (P1)#	patient 8 (P2)#
RFT1 gene mutations	c.199C>T/ c.199C>T	c.199C>T/ c.199C>T	c.454A>G/ c.892 G>A	c.454A>G/ c.892 G>A	c.454A>G/ c.454A>G	c.887 T>A/ c.887 T>G	c.1222A>G/ c.1325 G>A	c.1222A>G/ c.1325 G>A
Amino acid changes	p.R67C/ p.R67C	p.R67C/ p.R67C	p.K152E/ p.E298 K	p.K152E/ p.E298 K	p.K152E/ p.K152E	p.I296K/ p.I296R/	p.M408V/ p.R442Q	p.M408V/ p.R442Q
Sex	female	female	male	male	male	female	male	female
Prenatal data								
prematurity	+	n.a	n.a	n.a	+	+	-	-
IUGR	+	n.a	n.a	n.a	+	-	-	-
Postnatal data								
onset of first symptoms	birth	birth	during 1st year	birth	birth	birth	8 months	6 months
failure to thrive	+	+	+	+	+	+	-	-
feeding problems& dysmorphism	+♣	+	+	+	+	-	+	+
inverted nipples	+	-	+	+	-	+	-	-
short stature	n.a	n.a	n.a	n.a	+	+	+	+
hypotonia	+	+	+	+	+	+	+	+
psychomotor delay	+	+	+	+	+	+	+	+
microcephaly	n.a	+	+	-	+	+	-	-
deafness	+	+	+	+	+	+	+	-
visual impairment	+	+	+	+	+	+	-	-
seizures	+	+	+	+	+	+	+	+
ataxia	-	n.a	n.a	n.a	n.a	n.a	+	+
abnormal brain MRI	+ ^a	- ^b	+ ^c	-	-	+ ^d	-	-
hepatomegaly	+	n.a	n.a	n.a	-	-	+	+
Laboratory data								
increased creatine kinase	n.a	n.a	n.a	n.a	-	-	-	-
increased transaminases	-	-	-	-	-	-	-	-
bleeding or thrombosis	+	n.a	+	n.a	-	+	-	-
coagulation factors abnormalities	+	n.a	+	n.a	+	+	+	+
Age at time of publication	4 years and 3 months	died aged 8 months	5.5 years	2.2 years	8 months	11 months	21 years	19 years

n.a - data not available.

* the patient designated by the abbreviation KS.

the patient designated as patient 1 or 2 in this report.

& poor feeding, incoordinate sucking, severe gastroesophageal reflux, food aspiration, gastrostomy.

♣ very severe, arthrogryposis.

a-brain MRI: atrophy of both the cerebral hemispheres and the posterior fossa structures.

b-MRI was performed at early age. However, at autopsy cerebral atrophy was reported.

c-brain MRI showed progressive cortical and subcortical atrophy; brain CT revealed a stroke-like episode affecting the frontal lobe.

d-brain MRI showed symmetrical lesions of the basal ganglia, cortical atrophy, diffuse supratentorial white-matter hyperintensity, unmyelinated capsula interna, normal cerebellum.

References

- [1] M.A. Haeuptle, F.M. Pujol, C. Neupert, B. Winchester, A.J. Kastaniotis, M. Aebi, T. Hennet, Human RFT1 deficiency leads to a disorder of N-linked glycosylation, *Am. J. Hum. Genet.* 82 (3) (2008) 600–606.
- [2] J. Helenius, D.T. Ng, C.L. Marolda, P. Walter, M.A. Valvano, M. Aebi, Translocation of lipid-linked oligosaccharides across the ER membrane requires Rft1 protein, *Nature* 415 (6870) (2002) 447–450.
- [3] F. Imitiaz, V. Worthington, M. Champion, C. Beesley, J. Charlwood, P. Clayton, G. Keir, N. Mian, B. Winchester, Genotypes and phenotypes of patients in the UK with carbohydrate-deficient glycoprotein syndrome type 1, *J. Inherit. Metab. Dis.* 23 (2) (2000) 162–174.
- [4] P. Clayton, S. Grunewald, Comprehensive description of the phenotype of the first case of congenital disorder of glycosylation due to RFT1 deficiency (CDG In), *J. Inherit. Metab. Dis.* (Mar 11 2009) [Epub ahead of print].
- [5] W. Vleugels, M.A. Haeuptle, B.G. Ng, J.C. Michalski, R. Battini, C. Dionisi-Vici, M.D. Ludman, J. Jaeken, F. Foulquier, H.H. Freeze, G. Matthijs, T. Hennet, RFT1 deficiency in three novel CDG patients, *Hum. Mutat.* 30 (10) (2009) 1428–1434.
- [6] J. Jaeken, W. Vleugels, L. Régál, C. Corchia, N. Goemans, M.A. Haeuptle, F. Foulquier, T. Hennet, G. Matthijs, C. Dionisi-Vici, RFT1-CDG: Deafness as a novel feature of congenital disorders of glycosylation, *J. Inherit. Metab. Dis.* (Oct 24 2009) [Epub ahead of print].
- [7] M.A. Haeuptle, T. Hennet, Congenital disorders of glycosylation: an update on defects affecting the biosynthesis of dolichol-linked oligosaccharides, *Hum. Mutat.* 30 (12) (2009) 1628–1641.

Online supplement to the article Ondruskova et al.

RFT1-CDG in adult siblings with novel mutations

Supplement 1. Methods

Isoelectric focusing (IEF) of serum transferrin

IEF of serum transferrin was carried out as described by van Eijk and van Noort [1]. 2 µl of serum were incubated for 30 min. with equal volumes of 6.7 mM Fe(III) citrate and 0.17 mM NaHCO₃ (Sigma) and then diluted ten times in water. 1 µl of iron-saturated serum was separated on a PAGE gel (5%T, 3%C) (pH 5- 7) on a Mini IEF Cell, Model 111 (Biorad system). After IEF transferrin isoforms were detected by immunoprecipitation in the gel anti-human transferrin antibody (DAKO) and the gels were stained with Commassie Blue.

Neuraminidase treatment for detection of polymorphism in transferrin-glycoprotein

Iron-saturated serum was incubated overnight at 37°C with neuraminidase from *Clastridium perfringens* (Boehringer), separated on a PAGE gel (5%T, 3%C) (pH 3-10) on a Mini IEF Cell, Model 111 (Biorad system). After IEF transferrin isoforms were detected by immunoprecipitation in the gel anti-human transferrin antibody (DAKO) and the gels were stained with Commassie Blue.

Phosphomannomutase (PMM)- and phosphomannose isomerase (MPI)- assay

PMM and MPI activities were measured in isolated lymphocytes according to the procedure described by Van Schaftingen and Jaeken [2].

Lipid-linked and protein N-linked oligosaccharide (LLO, NLO) analysis

N-linked (NLO) and lipid-linked oligosaccharide (LLO) analysis was carried out in fibroblasts as described [3]. In brief, fibroblasts from patient 2 (the girl) were pulse radiolabeled with 2-[³H]-mannose. After metabolic labeling, the glycoproteins were obtained by differential extraction. The glycoprotein fraction was digested overnight with trypsin. The resulting glycopeptides were treated with PNGase F to release the oligosaccharides from the peptides. The LLO fraction was also obtained after sequential extraction with different solvents, after which the oligosaccharides were released from the lipid carrier by mild acid

treatment. The oligosaccharides (NLO and LLO) were separated by HPLC and identified on the basis of their retention times compared to standard glycans [4].

Molecular methods

Genomic DNA and cDNA (mRNA) were isolated from peripheral blood samples. The primers for gDNA were designed to cover the 13 exons and the flanking intronic regions of *RFTI* gene (primer sequences are available on request). The cDNA primers were designed as 5 pairs to amplify all cDNA in 5 overlapping fragments. Samples were analyzed on capillary instrument, the 3500 Genetic Analyzer from Applied Biosystems. Mutation c.1222A>G was confirmed by restriction digestion using LweI (Fermentas) restriction endonuclease. For confirmation of c.1325G>A the BspPI (Fermentas) enzyme was used. Restriction digestion was also used for 200 control samples.

References

- [1] H.G. van Eijk, W.L. van Noort, The analysis of human serum transferrins with the PhastSystem: quantitation of microheterogeneity, *Electrophoresis* 13(6) (1992) 354-8
- [2] E. van Schaftingen, J. Jaeken, Phosphomannomutase deficiency is a cause of carbohydrate-deficient glycoprotein syndrome type I, *FEBS Lett.* 377(3) (1995) 318-20.
- [3] W. Vleugels, E. Schollen, F. Foulquier, G. Matthijs, Screening for OST deficiencies in unsolved CDG-I patients, *Biochem. Biophys. Res. Commun.* 390(3) (2009) 769-74
- [4] F. Foulquier, A. Harduin-Lepers, S. Duvet, I. Marchal, A.M. Mir, P. Delannoy, F. Chirat, R. Cacan, The unfolded protein response in a dolichyl phosphate mannose-deficient Chinese hamster ovary cell line points out the key role of a demannosylation step in the quality-control mechanism of N-glycoproteins, *Biochem. J.* 362(Pt2) (2002) 491-8.

Glycogen storage disease-like phenotype with central nervous system involvement in a PGM1-CDG patient

Nina ONDRUSKOVA, Tomas HONZIK, Alzbeta VONDRACKOVA,
Marketa TESAROVA, Jiri ZEMAN, Hana HANSIKOVA

Department of Pediatrics and Adolescent Medicine, First Faculty of Medicine, Charles University in Prague and General University Hospital in Prague, Prague, Czech Republic

Correspondence to: Hana Hansikova, MSc., PhD.
Department of Pediatrics and Adolescent Medicine, First Faculty of Medicine,
Charles University in Prague and General University Hospital in Prague
Ke Karlovu 2, 128 08, Prague, Czech Republic.
TEL: +420 224 967 748; E-MAIL: hana.hansikova@lf1.cuni.cz

Submitted: 2014-01-13 *Accepted:* 2014-02-23 *Published online:* 2014-05-05

Key words: **phosphoglucomutase 1; glycoconjugate; congenital disorders of glycosylation; glycogen; intellectual disability**

Neuroendocrinol Lett 2014; **35**(2):137-141 PMID: 24878975 NEL350214A10 © 2014 Neuroendocrinology Letters • www.nel.edu

Abstract

OBJECTIVES: A 10-year-old boy presented with cleft palate, hepatopathy, cholecystolithiasis, myopathy, coagulopathy, hyperlipidemia, hypoglycemia, hyperuricemia, short stature, obesity, hypothyroidism, microcephaly and mild intellectual disability. The multi-systemic manifestation involving certain distinct clinical features prompted us to search for a subtype of congenital disorders of glycosylation (CDG).

METHODS: The patient was screened for CDG by examining the distribution of transferrin (TRF) and apolipoprotein C-III (ApoC-III) sialylated isoforms using isoelectric focusing of serum. This was followed by spectrophotometric measurement of phosphoglucomutase 1 (PGM1) activity in fibroblasts and molecular analysis including sequencing and PCR-RFLP of *PGM1* gene. Selected bioinformatics tools were used to evaluate the data.

RESULTS: Increased relative levels of di-, mono- and asialotransferrin reflected a defect of *N*-glycosylation in the patient. Markedly decreased activity of PGM1 corresponding to less than 5% of control's was found. Sequencing of *PGM1* gene revealed the presence of two heterozygous missense mutations c.1010C>T (p.T337M) and c.1508G>A (p.R503Q), whose pathogenicity was confirmed by *in silico* analysis.

CONCLUSION: We report the first Czech patient with a glycosylation disorder due to PGM1 deficiency. Compared to the described cases, no dilated cardiomyopathy was noted in our patient. However, he suffered from a mild neurological impairment, which is an uncommon feature that extends the phenotype associated with PGM1-CDG. Lactose-rich diet, which was previously reported to have ameliorated the clinical symptoms in some PGM1-CDG patients, did not result in any improvement in our patient.

Abbreviations:

ALT	- alanine transaminase
ApoC-III	- apolipoprotein C-III
APTT	- activated partial thromboplastin time
AST	- aspartate transaminase
BMI	- body mass index
CDG	- congenital disorders of glycosylation
DNA	- deoxyribonucleic acid
ft4	- free thyroxine
GSD	- glycogen storage disease
IEF	- isoelectric focusing
IQ	- intelligence quotient
PCR	- polymerase chain reaction
PCR-RFLP	- polymerase chain reaction-restriction fragment length polymorphism
PGM1	- phosphoglucomutase 1
PMI	- phosphomannoisomerase
PMM2	- phosphomannomutase 2
SD	- standard deviation
SDS-PAGE	- sodium dodecyl sulfate polyacrylamide gel electrophoresis
TBG	- thyroxine binding globulin
TRF	- transferrin
TSH	- thyroid-stimulating hormone

INTRODUCTION

The family of disorders, labeled congenital disorders of glycosylation (CDG), is a rapidly expanding group of multisystemic and clinically heterogeneous diseases, characterized by defective glycosylation of proteins and lipids. In 1984, Dr. Jaeken was the first to report a case of twin patients with decreased transferrin sialylation (Jaeken *et al.* 1984), a novel syndrome later found to be caused by pathological mutations in the phosphomannomutase 2 gene. This disorder, now referred to as PMM2-CDG, is the most frequently diagnosed form of CDG. Since then, defects in more than 80 different genes leading to various degrees of glycoconjugate hypoglycosylation have been described (Freeze 2013). Considering the large number of genes potentially involved in the glycosylation process, more novel CDG types are expected to be discovered in the near future.

Diagnosing CDG is quite challenging, due to both the extreme variability of clinical symptoms and the non-specific manifestations of the disease. Common symptoms of CDG include psychomotor delay and intellectual disability, muscle hypotonia, seizures, strabismus, dysmorphism, microcephaly, growth retardation, hepatopathy and coagulopathy (Grunewald *et al.* 2002). Often, more typical signs such as inverted nipples and abnormal fat distribution are noted (Jaeken 2010; Honzik *et al.* 2012). Some CDG present cutis laxa, blindness, deafness or urogenital anomalies (Jaeken 2010; Ondruskova *et al.* 2012). The standard selective screening method consists of isoelectric focusing (IEF) of serum transferrin (TRF) and apolipoprotein C-III (ApoC-III). Based on the results of these tests and subsequent analyses, several CDG types can be recognized. However, many cases remain unsolved and are labeled CDG-Ix or CDG-IIx.

The current approach to disease gene identification increasingly relies on the application of next-generation sequencing techniques. Recently, a novel type of CDG due to phosphoglucomutase 1 (PGM1; EC 5.4.2.2) deficiency was identified in four patients from three families (Timal *et al.* 2012; Stojkovic *et al.* 2009; Pérez *et al.* 2013). Herein, we report the first Czech patient with novel mutations in the *PGM1* gene. The patient presented with multi-organ dysfunction including attacks of ketotic hypoglycemia. No dilated cardiomyopathy was documented. Central nervous system involvement observed in our patient is an uncommon feature that extends the phenotype associated with PGM1-CDG.

MATERIAL AND METHODS

Clinical report

The patient was born after 37 weeks of gestation, with a birth weight of 2.75 kg and length of 47 cm, following an uneventful pregnancy. He is the second child of non-consanguineous parents of Caucasian origin. His early postnatal adaptation was complicated by hypotonia and cleft palate involving both the soft palate and part of the hard palate. At 6 months, he presented with a developmental delay and persistent muscular hypotonia. Although his motor milestones were significantly delayed, he made gradual progress during the first two years of life. He was able to walk with support at 17 months of age. At that time, he was diagnosed with cholelithiasis and hypothyroidism (ft4 12.4 pmol/l, controls 11.5–22.7; TSH 6.4 mIU/l, controls 0.5–6.0) with low levels of thyroxine-binding globulin (TBG 13 mg/l, controls >19). Surgical closure of the cleft palate was postponed 15 times due to recurrent otitis media.

At 6 years old, upon evaluation by a psychologist, the patient was reported to have borderline intellectual functioning (IQ 78). Short stature (108 cm; –2.85 SD), obesity (23.5 kg; +2.79 SD) and microcephaly (49.5 cm; 3rd centile) were also documented. Laboratory investigations showed elevated serum transaminases (ALT 1.69 μ kat/l, controls <0.69; AST 4.0 μ kat/l, controls <0.63), creatine kinase (12 μ kat/l, controls <2.3), uric acid (413 μ mol/l, controls <340), triglycerides (6.7 mmol/l, controls <1.5), and lactate (5 mmol/l, controls <2.3), as well as mild coagulopathy (APTT 41.8 sec; antithrombin III 32%; protein C 44%; protein S 67%, controls 70–120) with low factor XI (19%; controls 70–120). In addition, a low fasting glucose level (2.4 mmol/l, controls >3.3) accompanied with ketonuria was noted. Abdominal ultrasound demonstrated mild hepatomegaly. Echocardiography was normal.

On his most recent routine clinical visit at the age of 10.5 years, the height of the patient remained far below the 3rd centile (126 cm; –2.73 SD), and he had severe obesity (51 kg; BMI 32; +5.7 SD) and a head circumference of 52 cm (20th centile). He displayed distractibility, hyperactivity and inattentiveness. At school, he struggles in reading and requires special assistance.

Psychological showed IQ decline in the patient, confirming mild intellectual disability (IQ 66). Abdominal ultrasound revealed one gallstone within the gallbladder and showed mild hepatomegaly. Treatments include dietary intervention to prevent hypoglycemia, allopurinol to keep uric acid within the reference range and levothyroxine substitution to normalize thyroid gland function. However, hepatopathy (transaminases 4- to 6-fold above upper control values), hyperlipidemia, mild coagulopathy and mildly elevated creatine kinase persist.

Ethics

This study was approved by the Ethics Committee of the General University Hospital in Prague. All blood and tissue samples were analyzed with informed consent from the parents of the patient.

CDG screening in serum

The patient was screened for defective *N*-glycosylation using IEF and SDS-PAGE of TRF. To detect alterations in protein *O*-glycosylation, IEF of ApoC-III was performed. The methods were carried out as previously described (Wopereis *et al.* 2007).

Enzyme assays

Cultivated fibroblasts were grown in DMEM (E15-843, PAA Laboratories GmbH) supplemented with 10% fetal calf serum and antibiotics (P11-002, PAA Laboratories GmbH). The cells were harvested by trypsinization and stored at -80°C .

Phosphoglucomutase (PGM1) activity was measured in cultivated fibroblasts as previously described (Timal *et al.* 2012) with minor modifications. Activity assay was performed in the final volume of 500 μl reaction mixture and 20 μl of the cell extract, corresponding to 60–80 μg of protein, was used for one measurement. Phosphoglucomutase activities were expressed as nmol/min/mg protein. The protein level was determined according to Lowry (Lowry *et al.* 1951). Phosphomannoisomerase (PMI) activity was measured as a control enzyme, according to (Van Schaftingen & Jaeken 1995).

Molecular analysis

Using the Primer3Plus software, primers were designed to amplify the 11 exons and their flanking regions of the *PGM1* gene. Primer sequences and specific PCR conditions are available on request. Genomic DNA was extracted from peripheral blood using the standard procedures of protease digestion, phenol-chloroform extraction and ethanol precipitation. PCR amplicons were then sequenced using the ABI PRISM 3100/3100-Avant Genetic Analyzer (Applied Biosystems). The frequency of the identified causal missense sequence variants was ascertained by PCR-RFLP (BssSI, Hpy188I) in 100 healthy Czech control samples. The web servers SIFT, PolyPhen-2, MutPred, SNPs&GO, nsSNPAna-

lyzer and PANTHER were used to evaluate the possible pathogenicity of the identified missense substitutions as described elsewhere (Sim *et al.* 2012; Adzhubei *et al.* 2010; Li *et al.* 2009; Calabrese *et al.* 2009; Bao *et al.* 2005; Mi *et al.* 2013).

RESULTS

Biochemical findings

Elevated levels of di-, mono- and asialotransferrin relative to fully glycosylated TRF forms were found in patient's serum (type 2 pattern; Figure 1A); a TRF polymorphism was excluded by IEF of TRF after neuraminidase treatment. Analysis of TRF by SDS-PAGE showed a shift towards lower molecular weights, representative of TRF isoforms with incomplete glycan chains (Figure 1B). A physiological distribution of ApoC-III glycoforms was detected. Fibroblasts from the patient showed a clearly deficient phosphoglucomutase activity (2.2 nmol/min per mg protein; controls 53–87; $n=5$). IEF of TRF in serum samples taken after 5 months of lactose treatment showed no changes in the profile of TRF hyposialylated isoforms (data not shown).

Molecular analysis

Two heterozygous missense variations c.1010C>T (p.T337M) and c.1508G>A (p.R503Q) were identified in the *PGM1* gene of the patient. In 100 healthy Czech controls, neither of the sequence variants was detected by PCR-RFLP. Protein alignment revealed that the affected codons are evolutionary conserved. All applied online bioinformatics tools unanimously assessed the p.T337M and p.R503Q substitutions in the *PGM1* gene as disease-causing. Unfortunately, PANTHER was not able to classify the effect of p.R503Q.

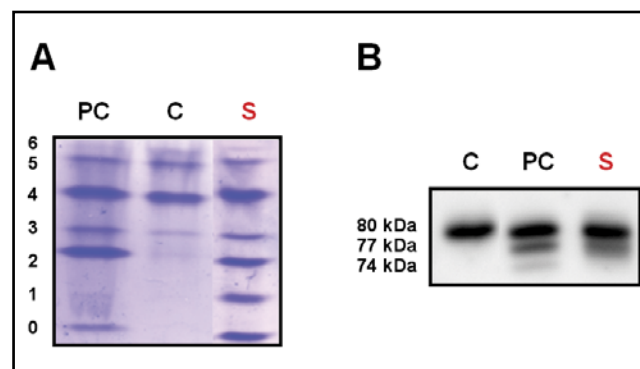


Fig. 1. Biochemical screening for CDG in serum from the patient. **A:** Samples from a patient with PMM2-CDG syndrome (PC), a healthy control (C) and our subject (S) were analyzed by isoelectric focusing of transferrin (pH 5-7). Numbers on the left indicate sialic acid content on protein (asialo- to hexasialotransferrin). **B:** Transferrin analyzed by SDS-PAGE (12% gel) in sera of a control (C), PMM2-CDG patient (PC) and the subject (S).

DISCUSSION

We report the first Czech patient with PGM1-CDG. He demonstrated multi-organ dysfunction, including impairment of the liver and gallbladder (hepatomegaly, hepatopathy and gallstone), muscle (exercise intolerance, elevated creatine kinase), the endocrine system (hypothyroidism, short stature, obesity and ketotic hypoglycemia), the brain (microcephaly, mild intellectual disability, hyperactivity and attention deficit), blood clotting and metabolism of uric acid (elevated uric acid), lipids (hyperlipidemia) and lactate (hyperlactacidemia). Although craniofacial dysmorphism, inverted nipples and atypical fat pads were not present, it is worthwhile to note that the patient had a cleft palate. Our finding of a mild impairment of the central nervous system is an uncommon feature that broadens the spectrum of PGM1-CDG previously reported as a non-neurological CDG (Pérez *et al.* 2013), however we cannot fully exclude other causes not related to PGM1 deficiency. In contrast to the four cases reported in the literature, dilated cardiomyopathy and attacks of myoglobinuria were not documented in our patient (Table 1).

Clinical and laboratory abnormalities such as short stature, hepatomegaly, hepatopathy, myopathy, hypertriglyceridemia, hyperlactacidemia, hyperuricemia and ketotic hypoglycemia prompted the diagnosis of a glycogen storage disease. The mild course of disease and absence of nephromegaly were not compatible with the diagnosis of GSD type I. GSD type III, VI and IX were excluded. Stojkovic *et al.* (Stojkovic *et al.* 2009) found

a remarkable similarity of PGM1 deficiency in their patient to McArdle's disease (glycogen storage disease type V) due to recurrent muscle cramps, exercise intolerance and attacks of myoglobinuria. The authors suggested that PGM1 deficiency be added to the list of rare glycogenolytic disorders and designated it as GSD type XIV (Stojkovic *et al.* 2009). In 2013, Preisler *et al.* observed increased exercise tolerance in the same PGM1-CDG patient after glucose infusion (Preisler *et al.* 2013).

Screening for CDG in our patient revealed a pathological transferrin profile, namely a type 2 pattern because of the increase of monosialotransferrin, pointing to a defect in the *N*-glycan remodeling in the Golgi. However it has to be noted that a type 2 pattern can hide a type 1 pattern (CDG I/II, as seen in galactosemia (Sturiale *et al.* 2005)). Thus, an associated *N*-glycan assembly defect is possible. Because the patient exhibited clinical symptoms suggestive of a glycogen storage disease, we investigated phosphoglucomutase activity. The PGM1 assay confirmed markedly decreased PGM1 activity (<5%) compared to healthy controls.

Based on molecular analysis, the patient was found to be a compound heterozygote for c.1010C>T (p.T337M) and c.1508G>A (p.R503Q) in the *PGM1* gene. The mutation c.1010C>T is unique and had not been characterized before. By utilizing selected *in silico* servers, the detected sequence variations were confirmed to be deleterious.

According to the study done by van Scherpenzeel and colleagues (van Scherpenzeel *et al.* 2012), galactose treatment in PGM1-CDG patients seems to be benefi-

Tab. 1. Clinical and laboratory data in our patient compared to previously described patients.

	Stojkovic <i>et al.</i> 2009	Timal <i>et al.</i> 2012	Timal <i>et al.</i> 2012	Pérez <i>et al.</i> 2012	Current report (2014)
	Patient 1	Patient 2	Patient 3	Patient 4	Patient 5
<i>PGM1</i> gene mutations	c.343A>G/ c.1145-1G>C	c.1507C>T	c.415G>C	c.871G>A/ c.1144+3A>T	c.1010C>T/ c.1508G>A
Amino acid changes	n.d.	p.R503X	p.G121R	p.G291R/ p.R343fs	p.T337M/ p.R503Q
Gender	male	male	female	male	male
Age at time of publication	35 years	died at 8 years	16 years	13 years	10 years
Cleft palate/ Pierre-Robin sequence	n.d.	-	+/+	+/+*	+/-
Short stature	n.d.	n.d.	n.d.	+	+
Intellectual disability	n.d.	n.d.	n.d.	-	mild (IQ 66)
Myopathy	+	-	+	+	+
Dilated cardiomyopathy	n.d.	+	+	-	-
Hypoglycemia	n.d.	-	-	-	+
Hepatopathy	n.d.	+	+	+	+
Coagulopathy	n.d.	+	+	n.d.	+

abbreviations: n.d.: not determined; * described as first branchial arch syndrome

cial. Because galactose as a prescription medication is not available in Czech Republic, we started the patient on a lactose-rich diet (40–50 g of lactose during therapy, 10 g before). Unfortunately, during the 5-month period of treatment, the diet modification did not result in either clinical improvement or amelioration of laboratory abnormalities, and his obesity severely worsened.

Our findings update the clinical and mutational spectrum of PGM1 deficiency and enable us to provide genetic counseling to the affected family.

ACKNOWLEDGMENTS

We thank the patient and his family for participating in the study. This study was supported by the grants GAUK 638512 (Charles University in Prague); IGA MZ CR NT/12166-5, SVV260022 and PRVOUK P24/LF1/3.

REFERENCES

- Adzhubei IA, Schmidt S, Peshkin L, Ramensky VE, Gerasimova A, Bork P, Kondrashov AS, Sunyaev SR (2010). A method and server for predicting damaging missense mutations. *Nat Methods* **7**: 248–249.
- Bao L, Zhou M, Cui Y (2005). nsSNPAnalyzer: identifying disease-associated nonsynonymous single nucleotide polymorphisms. *Nucleic Acids Res* **33**: W480–482.
- Calabrese R, Capriotti E, Fariselli P, Martelli PL, Casadio R (2009). Functional annotations improve the predictive score of human disease-related mutations in proteins. *Hum Mutat* **30**: 1237–1244.
- Freeze HH (2013). Understanding human glycosylation disorders: biochemistry leads the charge. *J Biol Chem* **288**: 6936–6945.
- Grunewald S, Matthijs G, Jaeken J (2002). Congenital disorders of glycosylation: a review. *Pediatr Res* **52**: 618–624.
- Honzik T, Magner M, Krijt J, Sokolová J, Vugrek O, Belužić R, Barić I, Hansíková H, *et al.* (2012). Clinical picture of S-adenosylhomocysteine hydrolase deficiency resembles phosphomannomutase 2 deficiency. *Mol Genet Metab* **107**: 611–613.
- Jaeken J (2010). Congenital disorders of glycosylation. *Ann N Y Acad Sci* **1214**: 190–198.
- Jaeken J, Van Eijk HG, Van Der Heul C, Corbeel L, Eeckels R, Eggermont E (1984). Sialic acid-deficient serum and cerebrospinal fluid transferrin in a newly recognized genetic syndrome. *Clin Chim Acta* **144**: 245–247.
- Li B, Krishnan VG, Mort ME, Xin F, Kamati KK, Cooper DN, Mooney SD, Radivojac P (2009). Automated inference of molecular mechanisms of disease from amino acid substitutions. *Bioinformatics* **25**: 2744–2750.
- Lowry OH, Rosebrough NJ, Farr AL, Randall RJ (1951). Protein measurement with the Folin phenol reagent. *J Biol Chem* **193**: 265–275.
- Mi H, Muruganujan A, Thomas PD (2013). PANTHER in 2013: modeling the evolution of gene function, and other gene attributes, in the context of phylogenetic trees. *Nucleic Acids Res* **41**: D377–386.
- Ondruskova N, Vesela K, Hansikova H, Magner M, Zeman J, Honzik T (2012). RFT1-CDG in adult siblings with novel mutations. *Mol Genet Metab* **107**: 760–762.
- Pérez B, Medrano C, Ecaj MJ, Ruiz-Sala P, Martínez-Pardo M, Ugarte M, Pérez-Cerdá C (2013). A novel congenital disorder of glycosylation type without central nervous system involvement caused by mutations in the phosphoglucomutase 1 gene. *J Inher Metab Dis* **36**(3): 535–42.
- Preisler N, Laforêt P, Echaniz-Laguna A, Orngreen MC, Lonsdorfer-Wolf E, Doutreleau S, Geny B, Stojkovic T, *et al.* (2013). Fat and carbohydrate metabolism during exercise in phosphoglucomutase type 1 deficiency. *J Clin Endocrinol Metab* **98**: E1235–1240.
- Sim NL, Kumar P, Hu J, Henikoff S, Schneider G, Ng PC (2012). SIFT web server: predicting effects of amino acid substitutions on proteins. *Nucleic Acids Res* **40**: W452–457.
- Stojkovic T, Vissing J, Petit F, Piraud M, Orngreen MC, Andersen G, Claeys KG, Wary C, *et al.* (2009). Muscle glycogenosis due to phosphoglucomutase 1 deficiency. *N Engl J Med* **361**: 425–427.
- Sturiale L, Barone R, Fiumara A, Perez M, Zaffanello M, Sorge G, Pavone L, Tortorelli S, *et al.* (2005). Hypoglycosylation with increased fucosylation and branching of serum transferrin N-glycans in untreated galactosemia. *Glycobiology* **15**: 1268–1276.
- Timal S, Hoischen A, Lehle L, Adamowicz M, Huijben K, Sykut-Cegielska J, Paprocka J, Jamroz E, *et al.* (2012). Gene identification in the congenital disorders of glycosylation type I by whole-exome sequencing. *Hum Mol Genet* **21**: 4151–4161.
- Van Schaftingen E, Jaeken J (1995). Phosphomannomutase deficiency is a cause of carbohydrate-deficient glycoprotein syndrome type I. *FEBS Lett* **377**: 318–320.
- Wopereis S, Grünewald S, Huijben KM, Morava E, Mollicone R, Van Engelen BG, Lefeber DJ, Wevers RA (2007). Transferrin and apolipoprotein C-III isofocusing are complementary in the diagnosis of N- and O-glycan biosynthesis defects. *Clin Chem* **53**: 180–187.

Diagnostic serum glycosylation profile in patients with intellectual disability as a result of MAN1B1 deficiency

Monique Van Scherpenzeel,¹ Sharita Timal,² Daisy Rymen,³ Alexander Hoischen,⁴ Manfred Wuhrer,^{5,6} Agnes Hipgrave-Ederveen,⁵ Stephanie Grunewald,⁷ Romain Pianne,³ Ann Saada,⁸ Shimon Edvardson,⁹ Sabine Grønberg,¹⁰ George Ruijter,¹¹ Anna Kattentidt-Mouravieva,¹¹ Jaime Moritz Brum,¹² Mary-Louise Freckmann,¹³ Susan Tomkins,¹⁴ Anil Jalan,¹⁵ Dagmar Prochazkova,¹⁶ Nina Ondruskova,¹⁷ Hana Hansikova,¹⁷ Michel A. Willemsen,² Paul J. Hensbergen,⁵ Gert Matthijs,³ Ron A. Wevers,¹ Joris A. Veltman,⁴ Eva Morava¹⁸ and Dirk J. Lefeber^{1,2}

1 Laboratory of Genetic, Endocrine and Metabolic Diseases, Radboud University Medical Centre, Nijmegen, The Netherlands

2 Department of Neurology, Radboud University Medical Centre, Nijmegen, The Netherlands

3 Centre for Human Genetics, University of Leuven, Leuven, Belgium

4 Department of Human Genetics, Radboud University Medical Centre, Nijmegen, The Netherlands

5 Centre for Proteomics and Metabolomics, Leiden University Medical Centre, Leiden, The Netherlands

6 Division of BioAnalytical Chemistry, VU University, Amsterdam, The Netherlands

7 Great Ormond Street Hospital, London, UK

8 Monique and Jacques Roboh Department of Genetic Research and the Department of Genetics and Metabolic diseases, Hadassah-Hebrew University Medical Centre, Jerusalem, Israel

9 Monique and Jacques Roboh Department of Genetic Research and the Paediatric Neurology Unit, Hadassah-Hebrew University Medical Centre, Jerusalem, Israel

10 Department of Clinical Genetics, Centre for Rare Diseases, Copenhagen University Hospital, Copenhagen, Denmark

11 Department of Clinical Genetics, Erasmus Medical Centre, Rotterdam, The Netherlands

12 Molecular Pathology Laboratory, Sarah Network of Hospitals for Rehabilitation, Brasilia, Brazil

13 Department of Clinical Genetics, The Canberra Hospital, Canberra ACT Australia

14 Clinical Genetics Department, Musgrove Park Hospital, Taunton, UK

15 Navi Mumbai Institute of Research in Mental and Neurological Handicap, Navi Mumbai, India

16 Department of Paediatrics, Medical Faculty of Masaryk University and University Hospital Brno, Brno, Czech Republic

17 Department of Paediatrics and Adolescent Medicine, First Faculty of Medicine, Charles University in Prague and General University Hospital in Prague, Prague, Czech Republic

18 Hayward Genetics Centre at Tulane University, New Orleans, USA

Correspondence to: Dr. Dirk J. Lefeber,
Department of Neurology, Laboratory for Genetic,
Endocrine and Metabolic Diseases,
Radboud University Medical Centre,
Geert Grooteplein 10, 6525 GA Nijmegen,
The Netherlands
E-mail: Dirk.Lefeber@radboudumc.nl

Congenital disorders of glycosylation comprise a group of genetic defects with a high frequency of intellectual disability, caused by deficient glycosylation of proteins and lipids. The molecular basis of the majority of the congenital disorders of glycosylation type I subtypes, localized in the cytosol and endoplasmic reticulum, has been solved. However, elucidation of causative genes

Received September 10, 2013. Revised December 6, 2013. Accepted December 15, 2013.

© The Author (2014). Published by Oxford University Press on behalf of the Guarantors of Brain. All rights reserved.

For Permissions, please email: journals.permissions@oup.com

for defective Golgi glycosylation (congenital disorders of glycosylation type II) remains challenging because of a lack of sufficiently specific diagnostic serum methods. In a single patient with intellectual disability, whole-exome sequencing revealed *MAN1B1* as congenital disorder of glycosylation type II candidate gene. A novel mass spectrometry method was applied for high-resolution glycoprofiling of intact plasma transferrin. A highly characteristic glycosylation signature was observed with hybrid type *N*-glycans, in agreement with deficient mannosidase activity. The speed and robustness of the method allowed subsequent screening in a cohort of 100 patients with congenital disorder of glycosylation type II, which revealed the characteristic glycosylation profile of *MAN1B1*-congenital disorder of glycosylation in 11 additional patients. Abnormal hybrid type *N*-glycans were also observed in the glycoprofiles of total serum proteins, of enriched immunoglobulins and of alpha1-antitrypsin in variable amounts. Sanger sequencing revealed *MAN1B1* mutations in all patients, including severe truncating mutations and amino acid substitutions in the alpha-mannosidase catalytic site. Clinically, this group of patients was characterized by intellectual disability and delayed motor and speech development. In addition, variable dysmorphic features were noted, with truncal obesity and macrocephaly in ~65% of patients. In summary, *MAN1B1* deficiency appeared to be a frequent cause in our cohort of patients with unsolved congenital disorder of glycosylation type II. Our method for analysis of intact transferrin provides a rapid test to detect *MAN1B1*-deficient patients within congenital disorder of glycosylation type II cohorts and can be used as efficient diagnostic method to identify *MAN1B1*-deficient patients in intellectual disability cohorts. In addition, it provides a functional confirmation of *MAN1B1* mutations as identified by next-generation sequencing in individuals with intellectual disability.

Keywords: *MAN1B1* (EC 3.2.1.113); intellectual disability; congenital disorders of glycosylation; glycomics; biomarker

Abbreviation: CDG = congenital disorder of glycosylation

Introduction

Protein glycosylation is important for human brain development and function. Genetic deficiencies in this process lead to the congenital disorders of glycosylation (CDG). The majority of the >70 known subtypes presents with intellectual disability (Wolfe and Krasnewich, 2013). Patients with protein *N*-glycosylation defects can be identified through screening by serum transferrin isoelectric focusing. Defects in the assembly of the lipid-linked oligosaccharide and glycan transfer to nascent proteins in the endoplasmic reticulum typically lead to a multisystem disorder. The majority of patients in this group, CDG type I (CDG-I), can be diagnosed with currently >20 subtypes reported (Timal *et al.*, 2012; Freeze, 2013). Isolated intellectual disability is rare in CDG-I type glycosylation defects. Although some adult patients with PMM2-CDG have been described with intellectual disability and ataxia, without systemic abnormalities (Krasnewich *et al.*, 2007), and a few patients with DPAGT1-CDG, ALG2-CDG and ALG14-CDG were observed with global developmental delay with variable degree of myasthenia and subtle dysmorphism (Belaya *et al.*, 2012; Cossins *et al.*, 2013; Iqbal *et al.*, 2013), so far only two type I defects (MAGT1-CDG and TUSC3-CDG) have been reported with non-syndromic intellectual disability (Garshasbi *et al.*, 2008; Molinari *et al.*, 2008). Elucidation of CDG-II defects, showing deficient glycan processing in the Golgi apparatus, is more complicated. The clinical spectrum is highly heterogeneous (Mohamed *et al.*, 2011) and lacks clear clinical clues towards a diagnosis. For a limited number of Golgi defects, such as SLC35A1-CDG with intellectual disability and epilepsy (Mohamed *et al.*, 2013), glycan analysis of total serum proteins directly lead to a diagnosis. In contrast, non-syndromic autosomal recessive intellectual disability caused by *ST3GAL3* mutations, a brain-specific glycosylation disorder, presents with normal serum transferrin glycosylation profiles (Hu *et al.*, 2011). Intellectual disability can be caused by a large number of genetic

disorders (Ellison *et al.*, 2013). Novel causative genes are regularly identified through massive next-generation sequencing efforts (Najmabadi *et al.*, 2011; Veltman and Brunner, 2012). An example includes *MAN1B1* deficiency, an autosomal-recessive intellectual disability (Rafiq *et al.*, 2011). The next challenge is to unravel the functional relevance of the plethora of new genetic variants by fast and highly specific diagnostic tests.

In this study, we apply a novel high resolution mass spectrometry method for direct glycoprofiling of intact plasma transferrin. This allowed the identification of 12 patients with *MAN1B1*-CDG, aged 1–35 years and presenting with an intellectual disability syndrome.

Materials and methods

Patient information and congenital disorder of glycosylation screening

Blood and fibroblasts of patients (clinical information in Table 2) were obtained for diagnostics of inborn errors of metabolism and used after informed consent from parents and treating physicians. Isoelectric focusing of serum transferrin for analysis of protein *N*-glycosylation defects and of serum apolipoprotein CIII for analysis of mucin type *O*-glycosylation defects were carried out as described before (Wopereis *et al.*, 2007). A transferrin polymorphism was excluded by neuraminidase digestion of the sample before transferrin isoelectric focusing.

Whole exome sequencing

Genomic DNA was extracted from fibroblast pellets of Patient 1 according to the manufacturer's protocol using a Qiagen Mini kit, and was checked for DNA degradation on agarose gels. Next generation sequencing and analysis was performed as described (Stránecký *et al.*, 2013). In brief, exome enrichment was performed using the SureSelect

Human All Exon 50 Mb Kit (Agilent), covering ~21 000 genes. The exome library was sequenced on a SOLiD 5500xl sequencer (Life Technologies). Colour space reads were iteratively mapped to the hg19 reference genome with the SOLiD LifeScope software version 2.1. Called variants and indels were annotated using an in-house annotation pipeline (Visser *et al.*, 2010) and common variants were filtered out based on a frequency of >0.5% in dbSNP and a frequency of >0.3% in our in-house database of >1300 exomes. Quality criteria were applied to filter out variants with less than five variant reads and <20% variation. Furthermore, synonymous variants, deep intronic, intergenic and untranslated region variants were excluded.

Sanger sequencing

Genomic DNA was extracted from fibroblast pellets or white blood cells from 12 patients and available family members. Primers (available on demand) were designed to amplify the different exons of the *MAN1B1* gene (GenBank accession number NM_016219.4), including at least 50 bp of the flanking intronic regions. Standard PCR reactions were based on 1 µl DNA and 0.2 µl Platinum[®] Taq polymerase (Invitrogen) in a total volume of 25 µl. Standard reaction conditions were 3 min at 95°C, then 10 cycles of 30 s at 95°C, 30 s at 65°C (–1°C each cycle) and 1 min at 72°C, followed by 25 cycles of 30 s at 95°C, 30 s at 55°C and 1 min at 72°C. The reaction was completed with a final elongation of 5 min at 72°C. For the sequencing of the resulting PCR product, the BigDye[®] Terminator Ready reaction cycle sequencing kit v.3.1 (Applied Biosystems) was used. Analysis of the results was performed on an ABI3100 Avant (Applied Biosystems).

Mass spectrometry of total plasma protein N-glycans and affinity-enriched plasma proteins

Plasma *N*-glycan profiling of Patient 8.1 was performed by MALDI (Matrix-assisted laser desorption/ionization) linear ion trap mass spectrometry as described (Guillard *et al.*, 2009), using 10 µl of plasma.

For high-resolution mass spectrometry of transferrin, a 10 µl plasma sample was incubated with anti-transferrin beads as described (Lacey *et al.*, 2001). The eluate was analysed on a microfluidic 6540 LC-chip-QTOF instrument (Agilent Technologies) using a C8 protein chip. Data analysis was performed using Agilent Mass Hunter Qualitative Analysis Software B.04.00. The Agilent BioConfirm Software was used to deconvolute the charge distribution raw data to reconstructed mass data.

Immunoglobulin G (IgG) and alpha1-antitrypsin (AAT) were affinity-enriched from plasma using protein G and anti-AAT beads (CaptureSelect[™]; Life Technologies), respectively (Ruhaak *et al.*, 2013). *N*-glycans were enzymatically released, derivatized by methyl ester formation and lacton formation (Wheeler *et al.*, 2009), subsequently purified by hydrophilic interaction liquid chromatography-solid phase extraction (HILIC-SPE) and registered as sodium adducts by MALDI-TOF-MS (Selman *et al.*, 2011).

Results

Identification of *MAN1B1* gene mutations

In our previous studies in patients with CDG-II, no clear clinical signs could be detected for further subgrouping of the patients.

In addition, biochemical analyses, including *N*-glycan profiling of total serum proteins, showed a general disturbance of the glycosylation process, not suggestive for a specific genetic defect (Mohamed *et al.*, 2011). To identify disease causing genes, DNA of several cases was submitted for whole exome sequencing.

After exome sequencing in Patient 1 (Table 2), we ordered the genetic variants using a prioritization scheme as described earlier to identify the pathogenic mutation (Timal *et al.*, 2012). To this end, we excluded variants known in dbSNPv137 as well as variants from our in-house database, consisting of >1300 exomes from healthy individuals and patients with other rare diseases. This analysis reduced the number of candidate DNA variants to 238. Based on a recessive inheritance model, we identified 21 candidate genes (Supplementary Table 1), 19 with potential homozygous inheritance (determined by >80% variant reads), and two genes with compound heterozygous inheritance (determined by >20% variant reads). Of the nine variants, not previously annotated as single nucleotide polymorphisms (SNP), the c.1000C>T variant in *MAN1B1* showed the highest level of conservation (PhyloP 5.938) with a sequencing depth of 102 reads and 100% variant reads. Moreover, *MAN1B1*, encoding mannosyl-oligosaccharide 1,2- α -mannosidase (EC 3.2.1.113) involved in the processing of *N*-glycans, was the only gene in the list that is correlated with protein *N*-glycosylation. Therefore, we considered this as the most likely disease-causing gene.

MAN1B1-congenital disorder of glycosylation shows specific glycosylation abnormalities

To identify more specific serum glycosylation markers for CDG-II diagnosis, we developed a high resolution mass spectrometry method to analyse the glycoprofile of an individual protein, by direct analysis of intact plasma transferrin. Ten microlitres of serum was used to immunopurify transferrin from patient samples, which could directly be analysed by nanochip-QTOF mass spectrometry using a C8 protein nanochip with a total analysis time of <2 h. In controls, a major peak is observed at 79 556 Da, corresponding with the molecular weight of the transferrin protein and two completely synthesized *N*-glycans (Fig. 1A). In serum of Patient 1, a major glycosylated variant was found with a molecular mass of 79 224 Da with >50% abundance, corresponding with one hybrid type *N*-glycan and one normal glycan structure. In addition, a mass of 79 062 Da was observed, also corresponding with a hybrid type *N*-glycan (Fig. 1A). The high-mass resolution allowed as to clearly discriminate these glycans from 79 260 Da indicating the loss of one sialic acid, which is present in similar amounts as in controls. The presence of both hybrid type *N*-glycans with one and two additional mannoses, respectively, is in agreement with deficient processing of protein linked glycans by the α -mannosidase *MAN1B1*.

The short sample preparation and analysis time of <2 h subsequently allowed us to screen our previous CDG-II cohort as well as newly included patients with severe and mild type II glycosylation abnormalities, 100 patients in total. In 11 additional patients, we could identify the presence of the same two hybrid type *N*-glycans

at average mass of 79 224 Da and 79 062 Da, respectively (Fig. 1A and Supplementary Fig. 1). Inspection of the glycoprofile of total serum proteins in the previously analysed Patient 8.1 (Supplementary Fig. 2B) showed the presence of a hybrid type *N*-glycan at mass to charge ratio (*m/z*) 2394 Da at an abundance of ~10% relative to the main bi-antennary *N*-glycan at *m/z* 2796 Da. Other hybrid type *N*-glycans could be observed at *m/z* 2190, 2364, and 2568 as minor compounds. In total, the percentage of hybrid type glycans was 4.8% of the total plasma *N*-glycan pool (Supplementary Table 2). The presence of hybrid type *N*-glycans and high-mannose *N*-glycans was also detected in total serum glycoprofiles of a few other patients with unsolved CDG-II (Supplementary Fig. 2C) without the recognizable profile of intact transferrin. Additionally, increased fucosylation and the presence of truncated glycans lacking galactose and sialic acid were observed in those patients. Subsequently, we analysed *N*-glycans released from IgG (Supplementary Fig. 3A) and alpha1-antitrypsin (AAT, Supplementary Fig. 3B), enriched from sera of five patients. Hybrid type *N*-glycans were clearly detectable for both proteins in all patients. The relative amount of hybrid type *N*-glycans compared with the total amount of *N*-glycans was 16.1% for IgG and 8% for AAT (Supplementary Table 2).

All 12 patients showed a recognizable profile in routine CDG screening by transferrin isoelectric focusing with an isolated increase of trisialotransferrin (28–38%, reference: 4.9–10.6%, Fig. 1B). An identical profile is observed for a known polymorphism in the transferrin protein that can readily be recognized after treatment with neuraminidase (Fig. 1B). An isolated increase of trisialotransferrin was observed more often in our cohort. However, the abundance was in general lower and no glycosylation abnormalities suggestive for MAN1B1-CDG could be observed by mass spectrometry of intact transferrin. Isoelectric focusing of APOC3 did not show abnormalities.

Sanger sequencing confirmed the presence of MAN1B1 mutations

Sanger sequencing of the *MAN1B1* gene was performed in DNA of all affected individuals with a characteristic glycosylation signature, and of available family members (Table 2 and Supplementary Fig. 4). Five homozygous and four compound heterozygous mutations were identified. *MAN1B1* belongs to the glycosyl hydrolase 47 family and consists of 699 amino acids with the catalytic pocket facing the organelle lumen as in a type II protein (Fig. 1C). A crystal structure of the protein in complex with a disaccharide substrate (Karaveg *et al.*, 2005) has indicated the specific amino acids that are required for enzymatic function and substrate binding. Missense mutations leading to amino acid substitutions (p.R334P, p.R334C, p.S409P, p.R597W, p.F659C, and p.E689K) were observed in highly conserved amino acid residues (Supplementary Fig. 5). Arg334 is close to the active site and is suggested to influence the ionization state of the catalytic residue Glu330. Arg597 and Glu689 are involved in hydrogen bonding to the sugar substrate. Phe659 is also important for binding of the substrate by hydrophobic stacking. Four mutations leading to a premature stop codon were identified; p.W75X leads to a

large truncation of the protein, whereas p.Q617X, p.W621X and p.E689X lead to a loss of the N-terminal 83, 79 and 11 amino acids, respectively. These include important amino acids for substrate and calcium binding such as Phe659, Glu663, Thr688, and Glu689. In Patient 6, apart from the p.S409P substitution, a heterozygous frameshift mutation was identified leading to a premature stop codon. Finally, in the two brothers of Family 8, a splice variant was identified at position –2 of intron 4 at the paternal allele and a deletion of 13 bp in exon 4 at the maternal allele leading to a frameshift and a premature stop.

The identification of mutations in all patients with characteristic glycosylation abnormalities confirmed the efficiency of our novel mass spectrometric assay in the diagnosis of MAN1B1 deficiency.

Clinical presentation

The patient group (Table 2) showed a predominant neurological presentation with a wide range of mild to severe global developmental delay in all 12 patients. Intellectual disability was present in all patients >5 years. The degree of intellectual disability ranged from an IQ of 33 to 55, however, most patients were in the moderate disability range. All patients had speech delay. Muscle hypotonia was present in the majority of patients, leading to delayed motor skills. All patients showed delay in both gross and fine motor skills. Motor skills gradually improved in older patients, while abnormal speech remained a significant problem, even in adult age. Seizures were present in three patients. Brain MRI was performed in all patients except Patients 5.1 and 9. Mild abnormalities were reported for Patient 2 with a mildly delayed myelination, and for Patient 7, showing mild cerebellar hypoplasia. Compared with previously reported cases only a few patients in our cohort had psychological/behavioural symptoms including aggressivity, autistic features or tics. In the current patient group, we found recognizable features like macrocephaly, truncal obesity and characteristic dysmorphism, including a flat oval face, low frontal hairline, curved eyebrows with lateral thinning, strabismus, prominent, bulbous nose tip and thin upper lip (Fig. 2). Compared to patients with 'classic' CDG, only one-third of the patients had abnormal fat distribution or inverted nipples, and ataxia was also rare. None of the patients showed cutis laxa or wrinkled skin as observed in several CDG-II defects. No internal organ anomalies were noted. Laboratory abnormalities were found in a few patients, including mild coagulation abnormalities (slight elevation of partial thromboplastin and activated partial thromboplastin time in 1 of 9 and 1 of 10 patients, respectively) and mild liver function test elevations in 2 of 10 patients.

There was a striking variability in the phenotypic presentation of MAN1B1-deficient patients. In Family 4, Patient 4.1 shows features that are commonly present in other types of CDGs, including hypotonia, strabismus and inverted nipples, whereas the other sibling has a syndromal intellectual disability phenotype with macrocephaly, aggressivity and behavioural abnormalities. This intra-familial difference can be partially explained by the age difference. However, significant variability was reported in the two other sibling pairs (Patients 5.1 and 5.2, and Patients 8.1 and 8.2) as well, who had a more similar age. In Family 5, the older boy

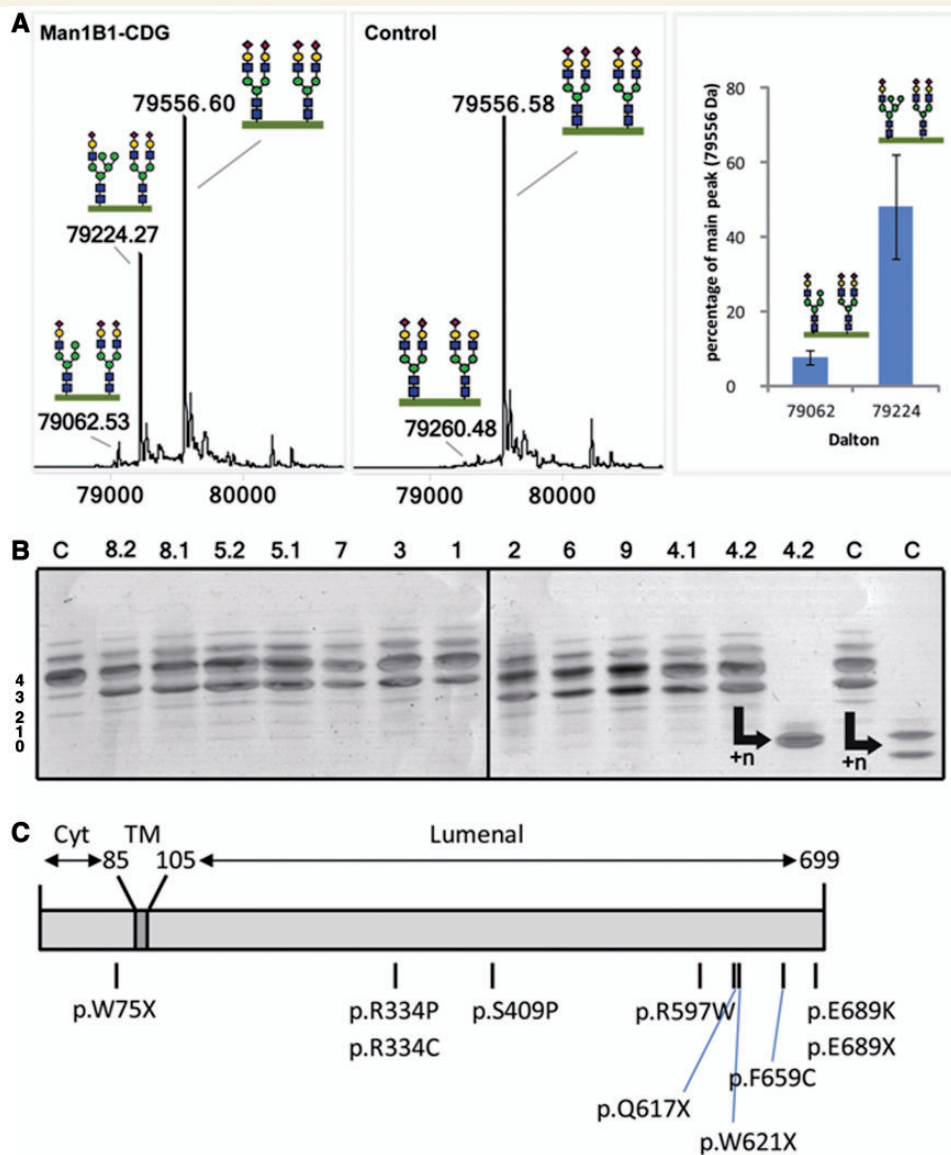


Figure 1 Glycosylation abnormalities in MAN1B1-CDG. (A) A representative mass spectrometry profile of intact transferrin is shown for Patient 5.1, as analysed by nanochip-C8-QTOF-MS. Glycan structure annotations are based on the consortium for functional genomics (CFG). The bar graph indicates the average percentage of the two abnormal transferrin peaks for all 12 patients (Supplementary Table 1). (B) Routine CDG screening by isoelectric focusing of serum transferrin showed an isolated increase of trisialotransferrin for all patients. The presence of a known polymorphism in the transferrin protein can complicate interpretation of the abnormal glycosylation. By treatment with neuraminidase (+n), a single band is observed for MAN1B1-CDG, whereas a polymorphism is indicated by two bands after treatment with neuraminidase. (C) Schematic presentation of the MAN1B1 protein, indicating the cytosolic (Cyt), transmembrane (TM), and luminal parts. The amino acid substitutions identified in our patient cohort (Table 1) are shown.

Table 1 Identified mutations in MAN1B1

Patient	1 (Female)	2 (Male)	3 (Male)	4.1 (Female)	4.2 (Female)	5.1 (Male)	5.2 (Female)	6 (Female)	7 (Female)	8.1 (Male)	8.2 (Male)	9 (Male)
Complementary DNA	c.1000C > T	c.2065G > T	c.1001G > C c.1849C > T	c.1863G > A	M: c.1789C > T P: c.2065G > A	M: c.1282delA P: c.1225T > C	c.1976T > G	M: c.530_542del P: c.621-2A > G	c.224G > A			
Protein	p.R334C	p.E689X	p.R334P p.Q617X	p.W621X	M: p.R597W P: p.E689K	M: p.I428fs*43 P: p.S409P	p.F659C	M: p.L177Pfs*32 P: splice	p.W75X			

M = maternal allele; P = paternal allele.

Table 2 Clinical symptoms and laboratory parameters in 12 patients with MAN1B1-CDG

Patient (sex, age in years)	1 (M, 15)	2 (M, 1)	3 (M, 14)	4.1 (F, 3)	4.2 (F, 19)	5.1 (M, 5)	5.2 (F, 3)	6 (F, 3)	7 (F, 17)	8.1 (F, 34)	8.2 (M, 35)	9 (M, 13)	Total
Neurological													
Intellectual disability (mean IQ)	+ (55)	(NA)	+ (35)	NA	+ (N/A)	+ (40)	NA	+ (50)	+ (50)	+ (<35)	+ (55)	+ (33)	9/9
Global developmental delay	+ (mild-mod)	+	+ (severe)	+	+ (mod)	+ (mod-sev)	+	+ (mod)	+ (mod)	+ (severe)	+ (mild-mod)	+ (severe)	12/12
Speech delay	++	+	++	+	++	++	+	++	++	++	++	++	12/12
Motor developmental delay*	+	+	+	+	+	+	+	transient	+	+	+	+	12/12
Decreased muscle tone	-	+	+	+	-	+	+	+	+	+	-	-	8/12
Strabismus	-	-	+	+	-	+	-	+	-	-	+	-	5/12
Autism/anxiety/tics	+	-	+	-	-	-	-	-	-	-	+	+	4/12
Seizures	-	-	-	-	-	-	-	+	+	+	+	-	3/12
Aggressivity	-	-	+	-	+	-	-	-	-	+	-	-	3/12
Ataxia	-	-	-	-	-	-	-	+	+	-	-	+	2/12
Dysmorphic features													
Thin lateral eyebrows	+	+	+	-	+	-	-	+	+	-	+	-	7/12
Bulbous nose tip	+	-	+	-	-	-	-	+	+	+	+	+	7/12
Thin upper lip	+	+	+	-	-	-	-	+	+	+	+	-	6/12
Inverted nipples	-	+	+	+	-	+	-	+	-	-	-	-	5/12
Abnormal fat distribution	-	+	+	+	-	+	-	+	-	-	-	-	5/12
Skeletal and joint involvement													
Macrocephaly	+	+	+	-	-	+	+	+	-	+	+	Transient	8/12
Dolichocephaly	-	+	-	-	-	-	-	-	-	+	+	-	3/12
Short stature	-	-	-	-	+	-	-	-	+	+	-	-	3/12
Joint laxity	+	+	-	-	-	-	-	-	+	-	-	-	3/12
Contractures	-	-	-	-	-	-	-	-	+	-	-	-	1/12
Overweight/obesity													
Truncal obesity	+	-	+	-	-	+	-	+	+	+	+	+	8/12
Overweight (BMI)	+ (27)	-	- (24.8)	-	-	- (22.1)	-	+ (25)	+ (26.7)	+ (49.3)	+ (35.1)	- (22)	5/12
Laboratory abnormalities													
Antithrombin-III	N	N/A	D	N/A	N/A	N	N	N	D	N	N	N/A	2/8
APTT	N	N/A	N	N	N	N	N	N	E	N	N	N/A	1/10
PT	N/A	N/A	E	N	N	N	N	N	N	N	N	N/A	1/9
ASAT/ALAT	N	N	E	N	N/A	N	N	E	N	N	N	N/A	2/10
Serum albumin	N/A	N	N	N	N	N	N	N/A	N	N	N	N/A	0/9

ASAT/ALAT = aspartate amino transferase/alanine amino transferase; N/A = not available; D = Decreased; E = elevated; N = normal; NA = not applicable; BMI = body mass index; M = male; F = female; PT = partial thromboplastin; APTT = activated partial thromboplastin time.

*Motor developmental delay in gross motor and fine motor skill.



Figure 2 Characteristic facial features in MAN1B1-CDG. Pictures of five patients [Patient 6 (A), Patient 1 (B), Patient 8.1 (C), Patient 3 (D), and Patient 8.2 (E)], showing oval, flat face, low frontal hair line, curved eyebrows with lateral thinning, prominent nose tip, large ears and variable degree of strabismus (A–E) and thin upper lips (B–E). Note obesity (C).

(Patient 5.1) was more severely affected than the younger girl (Patient 5.2) with more severe mental retardation and obesity. In the two adult patients of Family 8, the younger brother was more severely affected.

Discussion

In this paper, we describe a novel serum glycoprofiling method for functional diagnostic studies in MAN1B1 deficiency, an autosomal recessive intellectual disability syndrome.

Defects in genes involved in the process of protein glycosylation contribute significantly to intellectual disability. The vast majority of the >70 known subtypes of CDG present with intellectual disability (Wolfe and Krasnewich, 2013). In CDG-II, with defects in the processing steps in the Golgi apparatus, intellectual disability is present in the majority of subtypes as part of a multisystem presentation as well. B4GALT1-CDG is an exception without neurological symptoms (Guillard *et al.*, 2011). This is explained by the presence of a brain-specific isoform (B4GALT2) for this step in the glycosylation pathway. Especially the presence of fucose and sialic acid on protein glycans is important for proper

functioning of glycoproteins in the brain, as exemplified by the presence of intellectual disability in SLC35C1-CDG (GDP-fucose transporter deficiency) and SLC35A1- and ST3GAL3-CDG (CMP-sialic acid transporter and sialyltransferase deficiencies, respectively). MAN1B1 deficiency has been described as an intellectual disability syndrome, without significant associated findings, except facial dysmorphism (prominent nose and ear abnormalities and pointed chin in the three originally reported families; Rafiq *et al.*, 2011). Here, we report on 12 new patients with MAN1B1 deficiency and a neurological phenotype including global developmental delay, motor and speech delay, and hypotonia. As in the originally reported patients, our cohort shows associated dysmorphic features including truncal obesity and macrocephaly in ~65% of the patients and abnormal fat distribution with inverted nipples in 5 of 12 patients. Variable facial dysmorphism was noted with thin lateral eyebrows, bulbous nose tip and thin upper lip as most common symptoms in about half of the patients. Mild liver involvement and coagulation factor deficiencies were found in a few patients. Very recently, a presentation of syndromic intellectual disability was also reported in a group of seven patients with MAN1B1-CDG (Rymen *et al.*, 2013). Based on the frequent presence of macrocephaly, subtle dysmorphic

features and truncal obesity, MAN1B1-CDG should be indeed considered as a syndromic intellectual disability. As macrocephaly and obesity are also frequently present in healthy individuals, making a targeted, early diagnosis in the MAN1B1 cases could be difficult without screening for the suggestive glycosylation pattern abnormalities.

Interestingly, although the MAN1B1 enzyme is expressed in the whole body, the clinical features mainly involve the CNS. MAN1B1 deficiency prevents further removal of mannose residues during processing of protein linked *N*-glycans, which is required for the extension of the second antenna and subsequent synthesis of further branches on *N*-glycans. These branches typically contain poly-lactosamine extensions that can be decorated with specific sugar residues such as fucose that form essential glycan epitopes for cellular recognition. Our mass spectrometry experiments have shown that hybrid type *N*-glycans in MAN1B1-CDG are present on different proteins in variable amounts. Further glycoproteomic studies in model systems are required to identify the abnormally glycosylated brain proteins in MAN1B1-CDG that are particularly dependent on their glycans for normal function to identify a possible mechanism of disease. Another hint for disease pathology in MAN1B1-CDG originates from recent work showing altered Golgi morphology in patient fibroblasts, which could be related to the role of MAN1B1 in endoplasmic reticulum-associated degradation (Rymen *et al.*, 2013).

Analysis of intact transferrin more clearly highlights MAN1B1-specific abnormalities with accumulation of hybrid type *N*-glycans. In combination with the speed and robustness, this method is currently applied as a first step after CDG screening in our diagnostics of patients with unsolved CDG-II. With the emerging number of new patients with *MAN1B1* mutations, MAN1B1-CDG seems to be a relatively common intellectual disability syndrome. Patients can be recognized based on the association of speech and learning disability with truncal obesity and a recognizable dysmorphic appearance. In such cases, direct application of our mass spectrometry method will quickly lead to a diagnosis. Several patients presented with intellectual disability without recognizable dysmorphic features or significant associated organ involvement, complicating a direct clinical diagnosis. Screening for CDG in patients with global developmental delay or intellectual disability with dysmorphic features is indicated even in the absence of associated liver function and coagulation abnormalities. The specific glycosylation pattern found in patients with the clinical trials of intellectual disability, macrocephaly and truncal obesity in MAN1B1-CDG is diagnostic. With the advent of next-generation sequencing, our method will prove highly valuable to confirm the functional relevance of genetic variants in *MAN1B1* and to identify additional patients by analysis of CDG-II patient cohorts.

Acknowledgements

We thank the CDG patients and their families for their participation. We thank the genomic disorders group Nijmegen for the technical support in exome sequencing.

Funding

This work was financially supported by the Institute of Genetic and Metabolic Disease (IGMD) [Grant to D.L., R.R. and J.V.] and by grants from the Dutch Organisation for Scientific Research, NWO (Medium Investment Grant 40-00506-98-9001 and VIDI Grant 91713359 to D.L.), and by the grant IGA MZ NT 12166-5/2011 to H.H. and O.N.. This research was funded by grants from the Research Foundation (FWO) Flanders (G.0553.08 and G.0505.12), by grant ERARE11-135 of the ERA-Net for Research Programs on Rare Diseases Joint Transnational Call 2011 (EURO-CDG), and by the HighGlycan grant (#278535) of the European Commission. Daisy Rymen and Romain Peanne are respectively research assistant and postdoctoral researcher (FWO Pegasus Marie Curie Fellow) of the FWO. We thank L. Keldermans (Centre for Human Genetics, Leuven) for technical support.

Supplementary material

Supplementary material is available at *Brain* online.

References

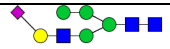
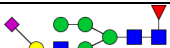
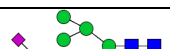
- Belaya K, Finlayson S, Slater CR, Cossins J, Liu WW, Maxwell S, et al. Mutations in DPAGT1 cause a limb-girdle congenital myasthenic syndrome with tubular aggregates. *Am J Hum Genet* 2012; 91: 193–201.
- Cossins J, Belaya K, Hicks D, Salihi MA, Finlayson S, Carboni N, et al. Congenital myasthenic syndromes due to mutations in ALG2 and ALG14. *Brain* 2013; 136: 944–56.
- Ellison JW, Rosenfeld JA, Shaffer LG. Genetic basis of intellectual disability. *Annu Rev Med* 2013; 64: 441–50.
- Freeze HH. Understanding human glycosylation disorders: biochemistry leads the charge. *J Biol Chem* 2013; 288: 6936–45.
- Garshasbi M, Hadavi V, Habibi H, Kahrizi K, Kariminejad R, Behjati F, et al. A defect in the TUSC3 gene is associated with autosomal recessive mental retardation. *Am J Hum Genet* 2008; 82: 1158–64.
- Guillard M, Gloerich J, Wessels HJ, Morava E, Wevers RA, Lefeber DJ. Automated measurement of permethylated serum N-glycans by MALDI-linear ion trap mass spectrometry. *Carbohydr Res* 2009; 344: 1550–7.
- Guillard M, Morava E, de Ruijter J, Roscioli T, Penzien J, van den Heuvel L, et al. B4GALT1-congenital disorders of glycosylation presents as a non-neurologic glycosylation disorder with hepatointestinal involvement. *J Pediatr* 2011; 159: 1041–3.e2.
- Hu H, Eggers K, Chen W, Garshasbi M, Motazacker MM, Wrogemann K, et al. ST3GAL3 mutations impair the development of higher cognitive functions. *Am J Hum Genet* 2011; 89: 407–14.
- Iqbal Z, Shahzad M, Vissers LE, van Scherpenzeel M, Gilissen C, Razaq A, et al. A compound heterozygous mutation in DPAGT1 results in a congenital disorder of glycosylation with a relatively mild phenotype. *Eur J Hum Genet* 2013; 21: 844–9.
- Karaveg K, Siriwardena A, Tempel W, Liu ZJ, Glushka J, Wang BC, et al. Mechanism of class 1 (glycosylhydrolase family 47) alpha-mannosidases involved in N-glycan processing and endoplasmic reticulum quality control. *J Biol Chem* 2005; 280: 16197–207.
- Krasnewich D, O'Brien K, Sparks S. Clinical features in adults with congenital disorders of glycosylation type Ia (CDG-Ia). *Am J Med Genet C Semin Med Genet* 2007; 145C: 302–6.
- Lacey JM, Bergen HR, Magera MJ, Naylor S, O'Brien JF. Rapid determination of transferrin isoforms by immunoaffinity liquid

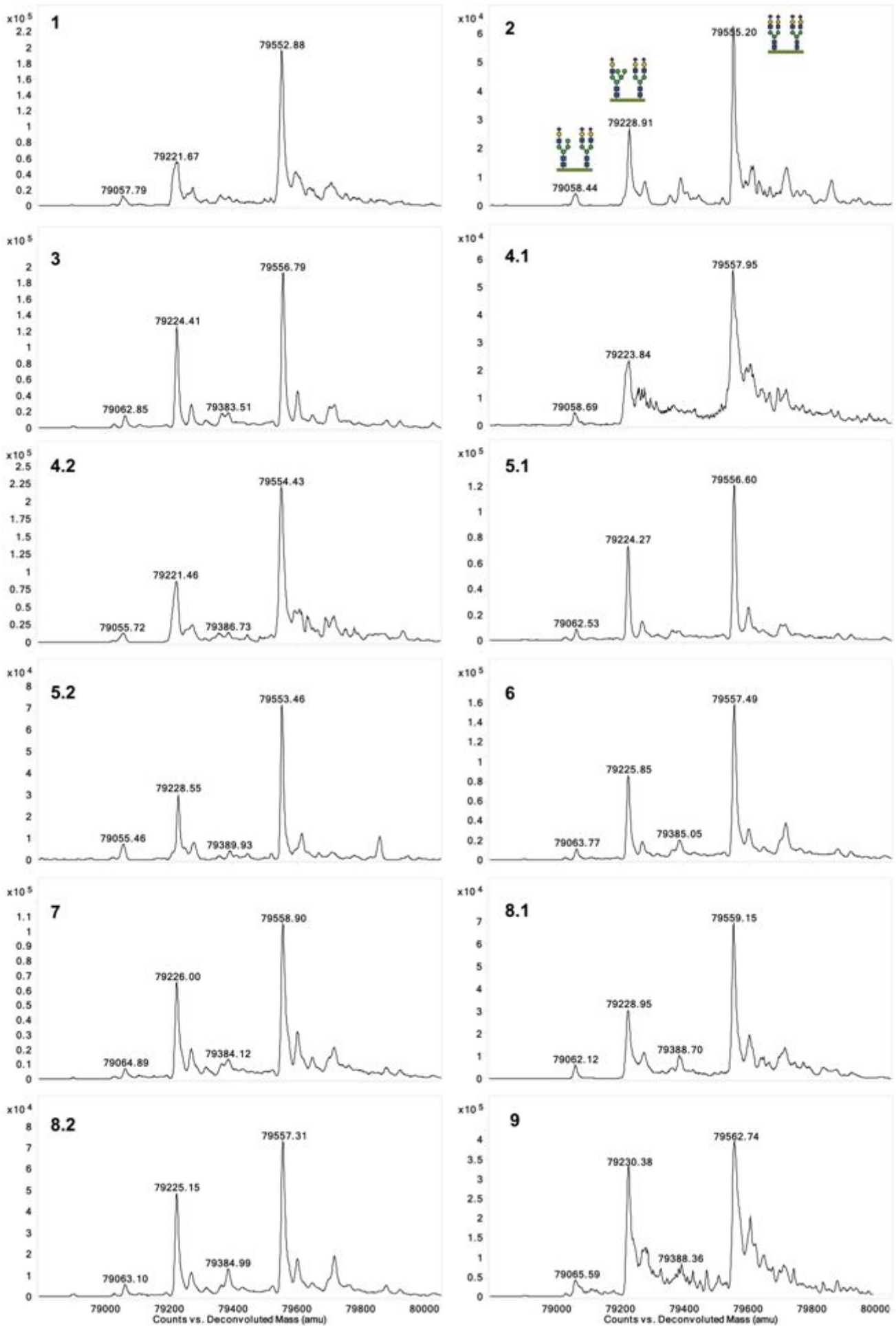
- chromatography and electrospray mass spectrometry. *Clin Chem* 2001; 47: 513–8.
- Mohamed M, Guillard M, Wortmann SB, Cirak S, Marklova E, Michelakakis H, et al. Clinical and diagnostic approach in unsolved CDG patients with a type 2 transferrin pattern. *Biochim Biophys Acta* 2011; 1812: 691–8.
- Mohamed M, Ashikov A, Guillard M, Robben JH, Schmidt S, van den Heuvel B, et al. Intellectual disability and bleeding diathesis due to deficient CMP-sialic acid transport. *Neurology* 2013; 81: 681–7.
- Molinari F, Foulquier F, Tarpey PS, Morelle W, Boissel S, Teague J, et al. Oligosaccharyltransferase-subunit mutations in nonsyndromic mental retardation. *Am J Hum Genet* 2008; 82: 1150–7.
- Najmabadi H, Hu H, Garshasbi M, Zemojtel T, Abedini SS, Chen W, et al. Deep sequencing reveals 50 novel genes for recessive cognitive disorders. *Nature* 2011; 478: 57–63.
- Rafiq MA, Kuss AW, Puettmann L, Noor A, Ramiah A, Ali G, et al. Mutations in the alpha 1,2-mannosidase gene, MAN1B1, cause autosomal-recessive intellectual disability. *Am J Hum Genet* 2011; 89: 176–82.
- Ruhaak LR, Koeleman CA, Uh HW, Stam JC, van Heemst D, Maier AB, et al. Targeted biomarker discovery by high throughput glycosylation profiling of human plasma alpha1-antitrypsin and immunoglobulin A. *PLoS One* 2013; 8: e73082.
- Rymen D, Peanne R, Millón MB, Race V, Sturiale L, Garozzo D, et al. MAN1B1 Deficiency: an Unexpected CDG-II. *PLoS Genet* 2013; 9: e1003989.
- Selman MH, Hemayatkar M, Deelder AM, Wuhrer M. Cotton HILIC SPE microtips for microscale purification and enrichment of glycans and glycopeptides. *Anal Chem* 2011; 83: 2492–9.
- Stránecký V, Hoischen A, Hartmannová H, Zaki MS, Chaudhary A, Zudaire E, et al. Mutations in ANTXR1 cause GAPO syndrome. *Am J Hum Genet* 2013; 92: 792–9.
- Timal S, Hoischen A, Lehle L, Adamowicz M, Huijben K, Sykut-Cegielska J, et al. Gene identification in the congenital disorders of glycosylation type I by whole-exome sequencing. *Hum Mol Genet* 2012; 21: 4151–61.
- Veltman JA, Brunner HG. De novo mutations in human genetic disease. *Nat Rev Genet* 2012; 13: 565–75.
- Vissers LE, de Ligt J, Gilissen C, Janssen I, Steehouwer M, de Vries P, et al. A de novo paradigm for mental retardation. *Nat Genet* 2010; 42: 1109–1112.
- Wheeler SF, Domann P, Harvey DJ. Derivatization of sialic acids for stabilization in matrix-assisted laser desorption/ionization mass spectrometry and concomitant differentiation of alpha(2->3)- and alpha(2->6)-isomers. *Rapid Commun Mass Spectrom* 2009; 23: 303–12.
- Wolfe LA, Krasnewich D. Congenital disorders of glycosylation and intellectual disability. *Dev Disabil Res Rev* 2013; 17: 211–25.
- Wopereis S, Grünewald S, Huijben KM, Morava E, Mollicone R, van Engelen BG, et al. Transferrin and apolipoprotein C-III isofocusing are complementary in the diagnosis of N- and O-glycan biosynthesis defects. *Clin Chem* 2007; 53: 180–7.

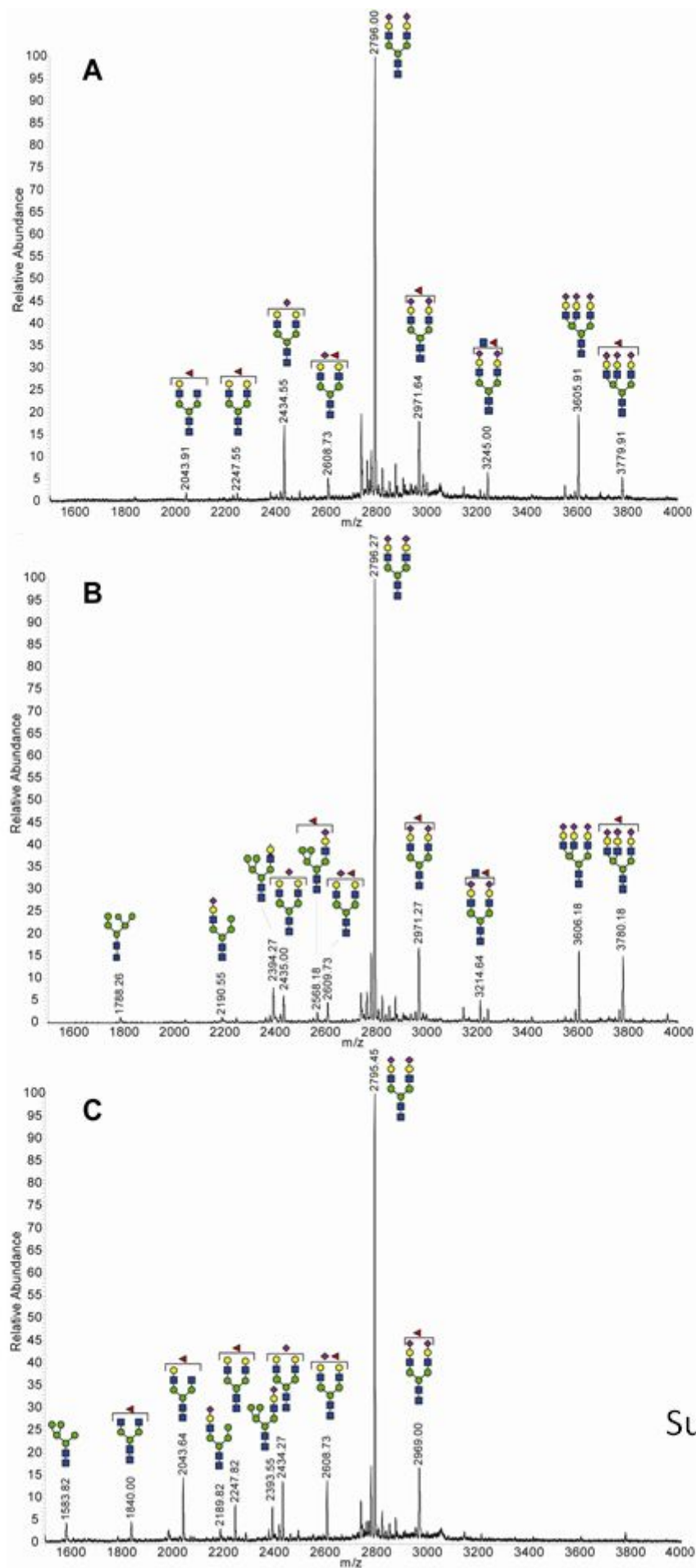
Supplemental Table 1. Quantification of the transferrin mass spectra. The intensities are shown of the three main peaks in the transferrin mass spectra of all MAN1B1 patients (Supplemental Fig.1), as well as the ratio of the two hybrid type N-glycan peaks compared to the main transferrin peak at 79556 Da. The data are presented in the bar graph in Fig. 1A.

patient	Average intensity of			Percentage relative to 79556	
	79058 Da	79228 Da	79556 Da	of 79058	of 79228
1	11514.8	54772.2	194967.2	5.9	28.1
2	4083.6	26619.4	62536.4	6.5	42.6
3	16610	125680.8	209381.7	7.9	60.0
4.1	2023.4	13436	35464.8	5.7	37.9
4.2	12554.6	86166.9	219748.7	5.7	39.2
5.1	14476.5	82950.4	182747.8	7.9	45.4
5.2	7075.8	30015.7	71258.6	9.9	42.1
6	21129.3	109917.2	206405.1	10.2	53.3
7	8439	74257.9	157260.3	5.4	47.2
8.1	5907.4	30369.8	68786.9	8.6	44.2
8.2	7643.9	63836.2	119734.7	6.4	53.3
9	41011.1	327673.4	391466.2	10.5	83.7
			average	7.558	48.078
			stdev	1.910	13.044

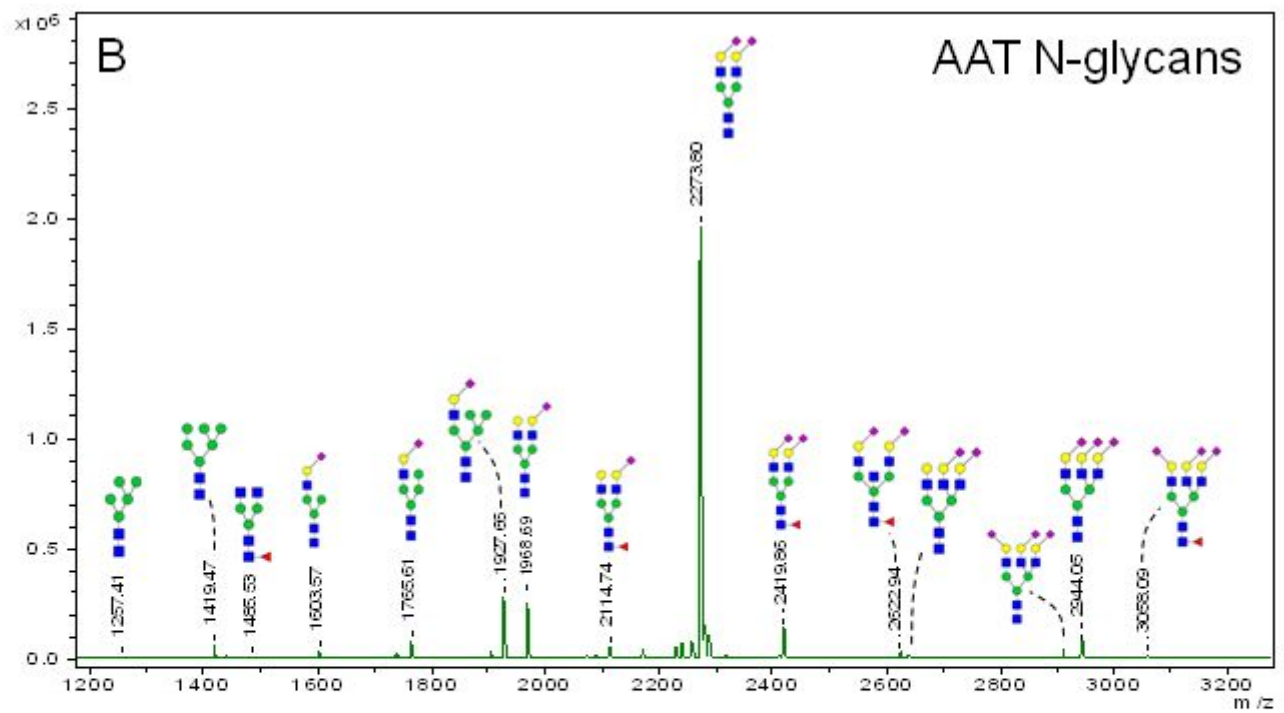
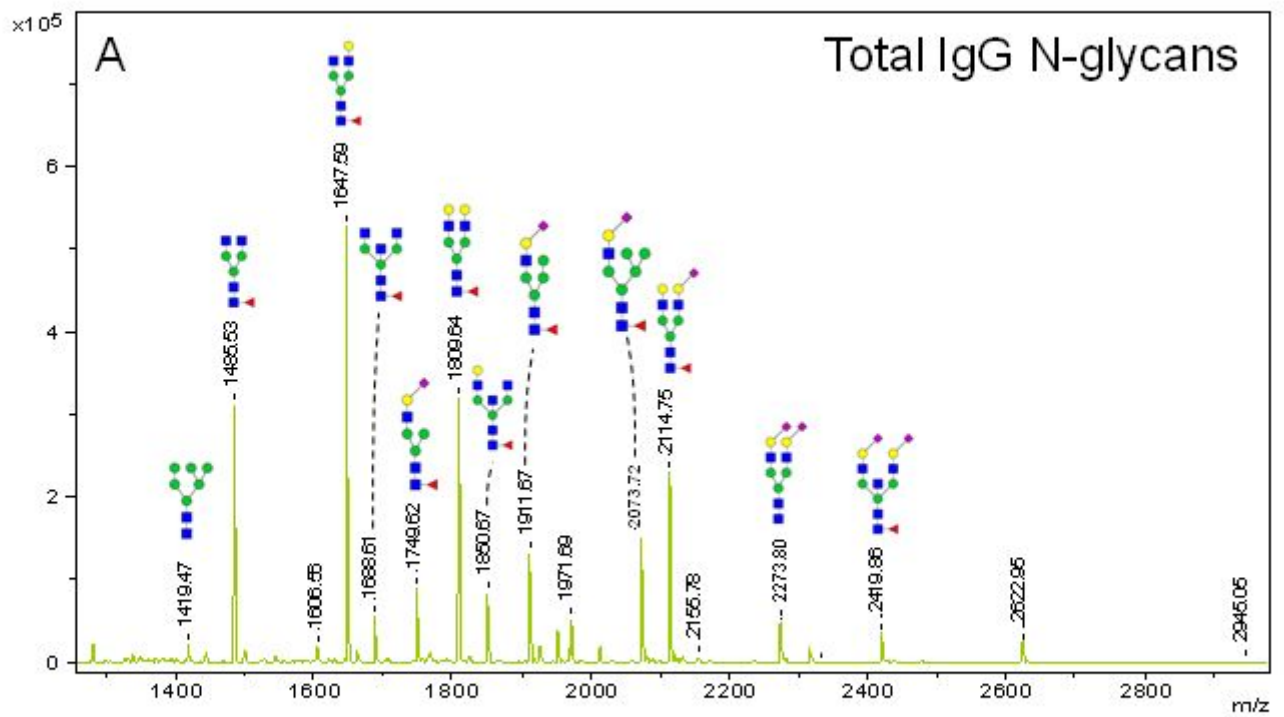
Supplemental Table 2. Percentages of hybrid N-glycans for total serum proteins, enriched IgG and alpha-1-antitrypsin (AAT). Relative abundances are expressed as percentage of the total amount of N-glycans. Four hybrid type N-glycans were observed in each sample, and compared with the abundance of these glycans in a control sample. For IgG and AAT analysis, sera of patients 1, 3, 4.1, 5.2, and 6 were used and the average values are shown.

Proposed glycan structure	Total serum proteins			IgG			AAT		
	m/z	patient 8.1	Control	m/z	patients (n=5)	Control	m/z	patients (n=5)	Control
	2190.55	0.7	0.4	1765.613	0.5	0.1	1765.613	1.9	0.2
	2364.27	0.7	0.3	1911.671	7.2	0.1	1911.671	0.2	0.1
	2394.27	2.6	0.7	1927.666	1.2	0.0	1927.666	5.5	0.3
	2568.18	0.8	0.4	2073.724	7.2	0.1	2073.724	0.4	0.1
Total	Total	4.8	1.8	Total	16.1	0.3	Total	8.0	0.7

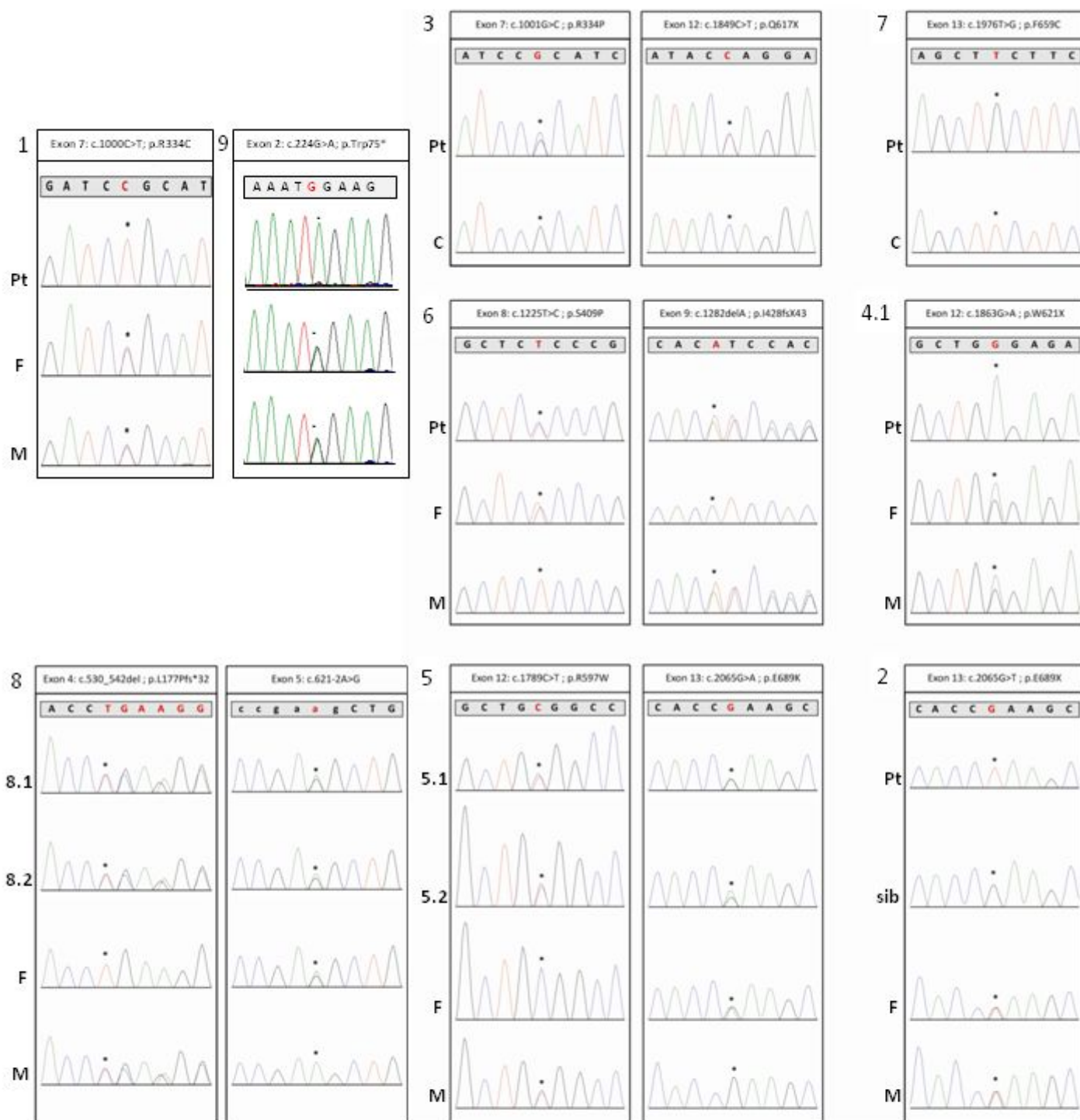




Suppl Figure 2



Supplemental Figure 3



Suppl Figure 4

R334
↓

<i>H. sapiens</i>	V	D	V	N	L	F	E	S	T	I	R	I	L	G	G	L	L	S	A	Y	H
<i>P. troglodytes</i>	V	D	V	N	L	F	E	S	T	I	R	I	L	G	G	L	L	S	A	Y	H
<i>C. familiaris</i>	V	D	V	N	L	F	E	S	T	I	R	I	L	G	G	L	L	S	A	Y	H
<i>M. musculus</i>	V	D	V	N	L	F	E	S	T	I	R	I	L	G	G	L	L	S	T	Y	H
<i>R. norvegicus</i>	V	D	V	N	L	F	E	S	T	I	R	I	L	G	G	L	L	S	A	Y	H
<i>C. elegans</i>	S	T	L	S	V	F	E	T	T	I	R	F	L	G	G	L	L	S	L	Y	A
<i>D. melanogaster</i>	A	E	L	S	V	F	E	T	N	I	R	F	V	G	G	M	L	T	L	Y	A
<i>S. cerevisiae</i>	A	E	V	N	V	F	E	T	T	I	R	M	L	G	G	L	L	S	A	Y	H

S409
↓

<i>H. sapiens</i>	T	S	I	Q	L	E	F	R	E	L	S	R	L	T	G	D	K	K	F	Q	E
<i>P. troglodytes</i>	T	S	I	Q	L	E	F	R	E	L	S	R	L	T	G	D	K	K	F	Q	E
<i>C. familiaris</i>	T	S	I	Q	L	E	F	R	E	L	S	R	L	T	G	S	K	K	F	Q	E
<i>M. musculus</i>	T	S	I	Q	L	E	F	R	E	L	S	R	L	T	G	I	K	K	F	Q	E
<i>R. norvegicus</i>	T	S	I	Q	L	E	F	R	E	L	S	R	L	T	G	I	K	K	F	Q	E
<i>C. elegans</i>	G	S	L	H	L	E	F	L	Y	L	S	R	I	S	N	A	P	I	F	E	K
<i>D. melanogaster</i>	G	T	L	H	L	E	F	A	Y	L	S	D	I	T	G	N	P	L	Y	R	E
<i>S. cerevisiae</i>	T	T	L	Q	M	E	F	K	Y	L	A	Y	L	T	G	N	R	T	Y	W	E

F659
↓

<i>H. sapiens</i>	G	E	T	L	K	Y	L	F	L	L	F	S	D	D	P	N	L	L	S	L	D
<i>P. troglodytes</i>	G	E	T	L	K	Y	L	F	L	L	F	S	D	D	P	N	L	L	S	L	D
<i>C. familiaris</i>	G	E	T	L	K	Y	L	Y	L	L	F	S	D	D	P	D	L	L	S	L	D
<i>M. musculus</i>	G	E	T	L	K	Y	L	Y	L	L	F	S	D	D	L	E	L	L	S	L	D
<i>R. norvegicus</i>	G	E	T	L	K	Y	L	Y	L	L	F	S	D	D	L	E	L	L	G	L	D
<i>C. elegans</i>	A	E	F	L	K	Y	A	Y	L	T	F	A	D	E	-	S	L	I	S	L	D
<i>D. melanogaster</i>	A	E	T	L	K	Y	L	Y	L	L	F	S	D	D	-	S	V	L	P	L	D
<i>S. cerevisiae</i>	A	E	T	L	K	Y	L	Y	I	L	F	L	D	E	F	-	-	-	D	L	T

R597
↓

<i>H. sapiens</i>	V	K	P	A	D	R	H	N	L	L	R	P	E	T	V	E	S	L	F	Y	L
<i>P. troglodytes</i>	V	K	P	A	D	R	H	N	L	L	R	P	E	T	V	E	S	L	F	Y	L
<i>C. familiaris</i>	V	K	P	A	D	R	H	N	L	L	R	P	E	T	V	E	S	L	F	Y	L
<i>M. musculus</i>	V	K	P	A	D	R	H	N	L	L	R	P	E	T	V	E	S	L	F	Y	L
<i>R. norvegicus</i>	V	K	P	A	D	R	H	N	L	L	R	P	E	T	V	E	S	L	F	Y	L
<i>C. elegans</i>	K	-	H	S	E	N	G	Y	I	Q	R	P	E	V	I	E	G	W	F	Y	L
<i>D. melanogaster</i>	L	R	S	Q	E	K	Y	Y	I	L	R	P	E	T	F	E	S	Y	F	V	L
<i>S. cerevisiae</i>	V	K	P	L	D	R	H	N	L	Q	R	P	E	T	V	E	S	I	M	F	M

E689
↓

<i>H. sapiens</i>	L	S	L	D	A	Y	V	F	N	T	E	A	H	P	L	P	I	W	T	P	A
<i>P. troglodytes</i>	L	S	L	D	A	Y	V	F	N	T	E	A	H	P	L	P	I	W	T	P	A
<i>C. familiaris</i>	L	S	L	D	T	Y	V	F	N	T	E	A	H	P	L	P	I	W	A	P	P
<i>M. musculus</i>	L	S	L	D	S	C	V	F	N	T	E	A	H	P	L	P	I	W	A	P	A
<i>R. norvegicus</i>	L	G	L	D	T	C	V	F	N	T	E	A	H	P	L	P	I	W	S	P	A
<i>C. elegans</i>	I	S	L	D	K	W	V	F	N	T	E	A	H	P	V	P	V	L	T	N	-
<i>D. melanogaster</i>	L	P	L	D	E	W	V	F	N	T	E	A	H	P	L	P	I	K	G	A	N
<i>S. cerevisiae</i>	-	D	L	T	K	V	V	F	N	T	E	A	H	P	F	P	V	L	D	E	E

Suppl Figure 5

Supplemental Figure 1. Nanochip-QTOF profiles of all MAN1B1-CDG patients

A zoom-in is shown of the nanochip-C8-QTOF-MS spectra of immunopurified transferrin from all patients. Indicated are the diagnostic hybrid type N-glycans and the normal glycosylated transferrin.

Supplemental Figure 2. Serum N-glycan profile by MALDI-LTQ mass spectrometry

MALDI-LTQ spectra are shown of a control (A), MAN1B1-CDG patient 8.1 (B), and a patient with uncharacterized CDG-II (C). Structures were annotated on basis of known masses for N-glycans and MS-MS fragmentation spectra as reported previously (Guillard *et al.*, 2009).

Supplemental Figure 3. IgG and AAT N-glycosylation profiles by MALDI-TOF mass spectrometry

N-glycan profiles of affinity-enriched immunoglobulin G (IgG, panel A) and alpha-1-antitrypsin (AAT, panel B) of patient 6 were registered by MALDI-TOF-MS. Sialic acids are depicted in a linkage-specific manner, with 2-6-linked sialic acids subjected to methyl esterification (tilted right) and 2-3-linked sialic acids undergoing lactone formation (tilted left), resulting in a 32 Dalton mass difference between the linkage isomers.

Supplemental Figure 4. Base-pair chromatograms of the MAN1B1 mutations

Chromatograms are shown of the families identified by Sanger sequencing. If parental DNA was available, heterozygous mutations were detected in DNA of the father (F) or mother (M).

A healthy sibling (sib) of patient 2 was homozygous wild-type. DNA of 4.2, sibling of 4.1, was not available.

Supplemental Figure 5. Conservation of the substitution mutations

For the amino acid substitutions, conservation is shown across the species indicated. p.R334C (pt 1), p.R334P (pt 3), p.S409P (pt 6), p.F659C (pt 7), p.R597W and p.E689K (pt 5.1&5.2).

Mutation of Nogo-B Receptor, a Subunit of *cis*-Prenyltransferase, Causes a Congenital Disorder of Glycosylation

Eon Joo Park,^{1,6} Kariona A. Grabińska,^{1,6} Ziqiang Guan,² Viktor Stránecký,³ Hana Hartmannová,³ Kateřina Hodaňová,³ Veronika Barešová,³ Jana Sovová,³ Levente Jozsef,¹ Nina Ondrušková,⁴ Hana Hansíková,⁴ Tomáš Honzík,⁴ Jirí Zeman,⁴ Helena Hůlková,³ Rong Wen,⁵ Stanislav Kmoch,^{3,*} and William C. Sessa^{1,*}

¹Department of Pharmacology and Vascular Biology and Therapeutics Program, Yale University School of Medicine, 10 Amistad Street, New Haven, CT 06520, USA

²Department of Biochemistry, Duke University Medical Center, DUMC 2927, Durham, NC 27710, USA

³Institute for Inherited Metabolic Disorders, First Faculty of Medicine, Charles University and General University Hospital, Ke Karlovu 2, Prague 2, 128 08 Czech Republic

⁴Department of Pediatrics, First Faculty of Medicine, Charles University and General University Hospital, Ke Karlovu 2, Prague 2, 128 08 Czech Republic

⁵Bascom Palmer Eye Institute, University of Miami, Miller School of Medicine, 900 NW 17th Street, Miami, FL 33136, USA

⁶Co-first author

*Correspondence: skmoch@lf1.cuni.cz (S.K.), william.sessa@yale.edu (W.C.S.)

<http://dx.doi.org/10.1016/j.cmet.2014.06.016>

SUMMARY

Dolichol is an obligate carrier of glycans for N-linked protein glycosylation, O-mannosylation, and GPI anchor biosynthesis. *cis*-prenyltransferase (*cis*-PTase) is the first enzyme committed to the synthesis of dolichol. However, the proteins responsible for mammalian *cis*-PTase activity have not been delineated. Here we show that Nogo-B receptor (NgBR) is a subunit required for dolichol synthesis in yeast, mice, and man. Moreover, we describe a family with a congenital disorder of glycosylation caused by a loss of function mutation in the conserved C terminus of NgBR-R290H and show that fibroblasts isolated from patients exhibit reduced dolichol profiles and enhanced accumulation of free cholesterol identically to fibroblasts from mice lacking NgBR. Mutation of NgBR-R290H in man and orthologs in yeast proves the importance of this evolutionarily conserved residue for mammalian *cis*-PTase activity and function. Thus, these data provide a genetic basis for the essential role of NgBR in dolichol synthesis and protein glycosylation.

INTRODUCTION

Nogo-B receptor (NgBR) was identified via expression cloning as a protein that interacts with the N terminus of Nogo-B, also called reticulon-4b (Miao et al., 2006). NgBR is a polytypic membrane protein, and its C-terminal domain shares significant homology with two gene products: (1) NUS1, a gene in yeast required for survival and N-glycosylation (Harrison et al., 2011; Yu et al., 2006) and (2) *cis*-prenyltransferases (*cis*-PTase), including genes in yeast (*RER22* and *SRT1*), a human ortholog, (*hCIT*, also called

dehydrodolichol diphosphate synthase [*DHDDS*]), and bacterial undecaprenyl pyrophosphate synthase (*uppS*) (Sato et al., 1999; Schenk et al., 2001; Surmacz and Swiezewska, 2011). In lower organisms, single subunit *cis*-PTases such as UPPS catalyze the condensation reactions of isopentenyl pyrophosphate (IPP) with farnesyl pyrophosphate (FPP) to synthesize linear polyprenyl pyrophosphate with specific chain lengths. Polyprenyl pyrophosphate is dephosphorylated into polyprenol and then reduced by a polyprenol reductase to produce dolichol (Cantagrel et al., 2010). In mammals, the relative contribution of Nus1/NgBR versus Rer2/Srt1/hCIT to *cis*-PTase activity and dolichol synthesis is unknown since loss of function of each grouping of genes results in reduced glycosylation.

Congenital disorders of glycosylation (CDG) are genetic diseases that represent an extremely broad spectrum of clinical presentations due to defects in several steps of protein glycosylation. Recently, there have been several reports of genetic defects in the dolichol biosynthetic pathway, such as mutations in *DHDDS/hCIT* and *SRD5A3* (Cantagrel et al., 2010; Kasapkara et al., 2012; Zelinger et al., 2011; Züchner et al., 2011). *DHDDS*-CDG is associated with inherited retinitis pigmentosa, a disorder causing retinal degeneration, and *DHDDS*-CDG patients did not show the other typical CDG symptoms. *SRD5A3*-CDG affects the final step in dolichol synthesis. Its clinical features are typical for CDG type 1 glycosylation disorders, including psychomotor retardation, ocular malformations, cerebellar hypoplasia, skin lesions, and facial dysmorphism.

Here, we characterize the dolichol biosynthesis pathway in mice and yeast and demonstrate the necessity of both hCIT and NgBR for dolichol biosynthesis. In addition, we describe a unique congenital disorder of glycosylation caused by a mutation in NgBR, a conserved subunit of *cis*-PTase. Patients harboring a R290H mutation of NgBR have congenital scoliosis, profound psychomotor retardation, refractory epilepsy, and macular lesions showing retinitis pigmentosa. Thus, hCIT/NgBR heteromers are essential, conserved components of the machinery necessary for glycosylation reactions in mammals.

RESULTS AND DISCUSSION

Targeted Disruption of *NgBR* Causes Early Embryonic Lethality In Vivo and Defective *cis*-PTase Activity and Cholesterol Levels in Isolated Fibroblasts

To examine the physiological significance of NgBR, we generated a conditional knockout mouse (Figures S1A–S1C available online). The *NgBR* knockout allele (*NgBR*^d) was generated by crossing *NgBR* conditional allele (*NgBR*^f) with a protamine Cre driver expressed in the male germline (O’Gorman et al., 1997). Heterozygous *NgBR* mice (*NgBR*^{d/+}) appeared normal, and intercrosses with *NgBR*^{d/+} showed no viable homozygous mice (*NgBR*^{d/d}) (Figure 1A). To determine when lethality occurred, timed pregnancies of *NgBR*^{d/+} breeding were examined at embryonic day 6.5 (E6.5) and E7.5. No *NgBR*^{d/d} embryos were identified at these time points indicating postimplantation embryonic lethality before E6.5 (Figures 1B and 1C). Next, we established mouse embryonic fibroblasts (MEFs) cultured from *NgBR*^{fl/fl} mice using an inducible Cre-loxP system. Reduced expression of NgBR in the tamoxifen inducible *NgBR* knockout (*NgBR* iKO) MEF cells was confirmed by PCR and western blotting for mRNA and protein levels, respectively (Figure S1D). *NgBR* iKO MEFs showed accumulation of free cholesterol as determined by filipin staining (Figure 1D), decreased *cis*-PTase activity in isolated membranes (Figure 1E), and mannose incorporation into protein (Figure 1F). Transduction of cells with lentiviral human *NgBR* rescues the increase in free cholesterol (Harrison et al., 2009) and the decrease in mannose incorporation (Figures 1E and 1F). Furthermore, we exposed cells to lovastatin, an inhibitor of 3-hydroxy-3-methylglutaryl-coenzyme A (HMG-CoA) reductase, the rate-limiting enzyme in the synthesis of isoprenoids, and measured cell viability using an MTT assay. *NgBR* iKO MEF cells were significantly more sensitive to lovastatin than control MEF cells (Figure 1G). Since defects in protein glycosylation can induce the unfolded protein response (UPR), activation of the UPR pathway in wild-type (WT) and *NgBR* iKO MEF cells was examined by RT-PCR for marker genes of the pathway, including *Bip*, *Chop*, and *Chac* (Figure 1H). All three genes were markedly increased in *NgBR* iKO MEFs, implying that defects in dolichol synthesis and protein glycosylation were activating the UPR pathway of ER stress. Thus, *NgBR* is essential for early development and *cis*-PTase activity in vivo.

Heteromeric Organization of *cis*-Prenyltransferase Is Conserved between Fungi and Mammals

The eukaryotic *cis*-PTase was initially presumed to be a homodimer based on studies of UPPS of *E. coli* and *M. luteus* (Fujihashi et al., 2001; Guo et al., 2005). Our previous work demonstrated that hCIT or NgBR were necessary for *cis*-PTase activity (Harrison et al., 2011). However, we did not provide unequivocal evidence that NgBR is indispensable for enzymatic complex formation and activity. To definitively dissect the roles of NgBR and hCIT as components of *cis*-PTase activity, we characterized the yeast orthologs (in *S. cerevisiae* and *S. pombe*) of NgBR and hCIT using genetic and biochemical approaches. We hypothesized that baker’s yeast may have two heteromeric *cis*-PTase complexes: Nus1-Rer2 and Nus1-Srt1. To test this, we generated a triple deletion strain, *nus1Δ, rer2Δ, srt1Δ*, expressing the homomeric *cis*-PTase from *Giardia lamblia*

(GlcisPT) to support growth (Grabińska et al., 2010). Indeed, we were able to isolate yeast cells lacking chromosomal copies of *NUS1*, *RER2*, and *SRT1* genes but bearing instead GlcisPT on a plasmid with a *URA3* marker (Figure 2A). To examine conservation of the heteromeric structure of *cis*-PTases, the triple deletion strain was transformed with *MET15* and *LEU2* plasmids bearing the cDNAs indicated in Figure 2A. As expected, viable strains were obtained after expressing *NUS1/RER2* or *NUS1/SRT1* as positive controls (Figure 2A). In addition, *NUS1* is also compatible with *Sprer2* or *hCIT*, *Spnus1* with *Sprer2*, *Spnus1* with *hCIT*, and *NgBR* with *hCIT* only. Reverse-phase thin-layer chromatography (TLC) of polyprenols generated from membranes isolated from wild-type BY4742 or transformed mutant cells revealed that human and *S. pombe* enzymes synthesize polyprenols similarly to that in their parental organisms (Figure 2B). However, the size of the dominant polyprenol pyrophosphate synthesized by the hybrid enzymes varied, implying that the different gene products (*NgBR/Nus1* and *hCIT/Rer2/Srt1*) determined polyprenol chain length.

To examine the enzymatic activities of the gene products, we used in vitro translation (IVT) followed by *cis*-PTase assays on the above combinations of the *cis*-PTase components. Enzymes present in the IVT mixture were able to incorporate ¹⁴C-IPP into short prenols up to 6 units (Figure 2C, first column) but were unable to synthesize longer chain polyprenyl pyrophosphates. Expression of Nus1, Rer2, or mixtures of IVT Nus1 with Rer2 products in equal amounts (as shown by western blotting in the bottom panel) did not catalyze formation of polyprenols. Interestingly, only cotranslation of Nus1 with Rer2 and its orthologs in *S. pombe* or humans formed an active *cis*-PTase complex producing prenols of expected lengths (Figures 2C–2F, lane 5), indicating that both proteins are required for a functional enzyme (Figures 2D–2F). Collectively, the data support the heteromeric structure of mammalian and yeast *cis*-PTase and suggest that eukaryotic *cis*-PTase is assembled during translation since only cotranslation, but not mixing of the proteins, yields active enzyme. Taken together, these data provide a clear rationale for the role of *RER2/NUS1* and related genes in dolichol biosynthesis and advance our understanding of this important pathway.

A Mutation on *NgBR* Causes Congenital Scoliosis, Severe Neurological Impairment, Refractory Epilepsy, Hearing Deficit, and Visual Impairment

Recently, exome sequencing of individual families with symptoms of a congenital disorder of glycosylation (CDG) has led to the discovery of mutations in DHDDS (hCIT) and SRD5A3, genes involved in the early steps of polyprenol synthesis (Cantagrel et al., 2010; Kasapkara et al., 2012; Zelinger et al., 2011; Züchner et al., 2011). DHDDS-CDG is associated with inherited retinitis pigmentosa, a disorder causing retinal degeneration, and SRD5A3-CDG patients exhibit psychomotor retardation, ocular malformations, cerebellar hypoplasia, skin lesions, and facial dysmorphism. In our clinic, a family of Roma origin (Figure 3A) composed of healthy, unrelated parents and four siblings was examined, and two siblings presented with congenital scoliosis, severe neurological impairment, refractory epilepsy, hearing deficit, and visual impairment with discrete bilateral macular lesions.

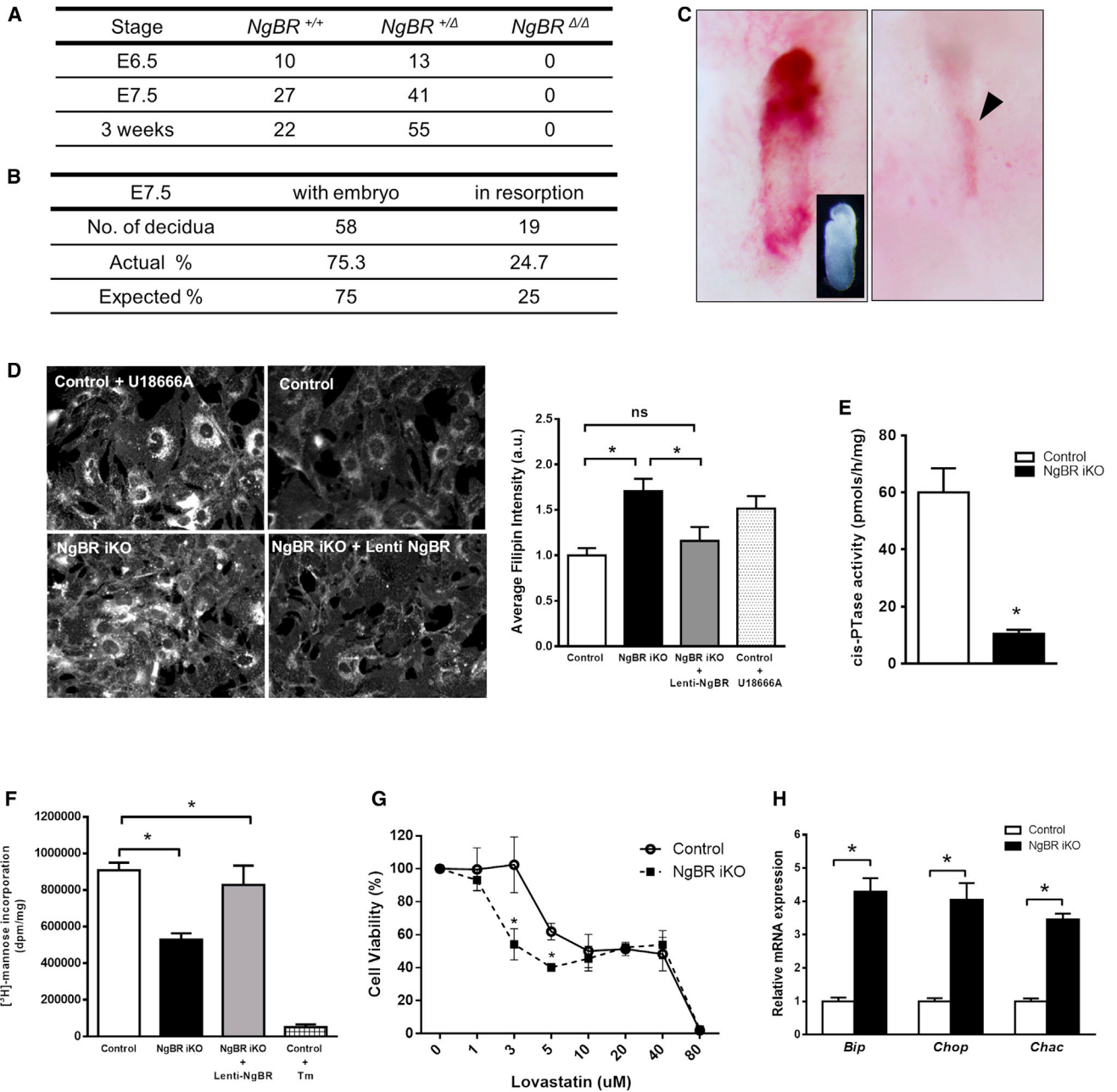


Figure 1. Characterization of NgBR Knockout Mouse Embryos and Fibroblasts

(A) Genotype obtained from the progeny of heterozygous mating. No *NgBR* ^{Δ/Δ} embryo was detected.
 (B) Embryo resorption frequencies during postimplantation development. Resorption sites were apparent at E7.5 among ~25% decida.
 (C) Representative decida of E7.5 embryo resorption sites analyzed. Decida were obtained from *NgBR* ^{$\Delta/+$} × *NgBR* ^{$\Delta/+$} breeding. Decida with embryo contained normally developed E7.5 embryo (insert). Presumptive *NgBR* ^{Δ/Δ} decida exhibit implanted site for embryo without evident embryonic material (arrowhead).
 (D) Filipin staining and quantitative representation for MEF. Filipin staining was performed 48 hr after Lenti-*NgBR* transduction into *NgBR* iKO MEF cells. U18666A was used as a positive control for inhibition of cholesterol trafficking.
 (E) Microsomal *cis*-PTase activity assay for *NgBR* iKO MEF. Enzyme activity was reduced by 83% in *NgBR* iKO MEF compare to control.
 (F) [³H]-mannose labeling of proteins in mouse embryonic fibroblasts. Tunicamycin (Tm) treatment was used as a control.
 (G) Statin sensitivity measured by MTT assay. Cell viability was determined by MTT assay after 16 hr exposure with various concentrations of lovastatin (1–80 μ M). Cell viability was calculated by the following equation: MTT optical density value of treated sample / MTT OD value of nontreated sample.
 (H) RT-PCR for UPR pathway genes. Relative mRNA expression to control show increased expression.
 Data are representative of at least three experiments. **p* < 0.05. Data are mean \pm SE. See also [Figure S1](#).

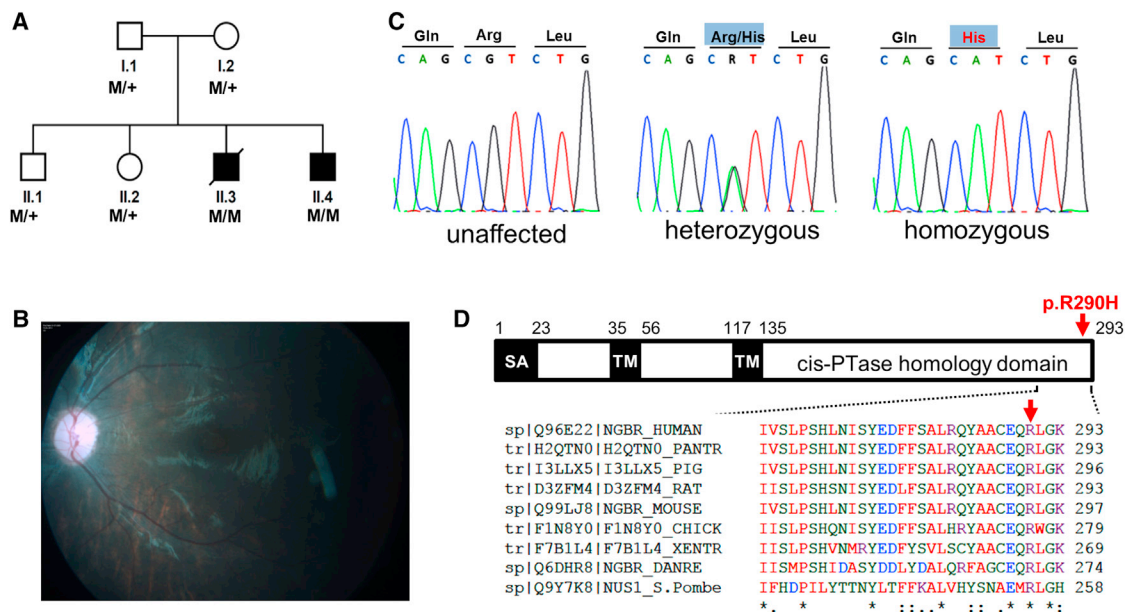


Figure 3. Identification of a Conserved Mutation in the NgBR Gene in Patients with a Constellation of Symptoms Consistent with a Glycosylation Disorder

(A) Pedigree of the Czech family. Black symbols denote affected individuals, open symbols denote unaffected parents and siblings. M/+ denotes presence (M) or absence (+) of the mutation as defined by Sanger sequencing.

(B) Dilated fundus photograph in proband II.4 reveals a granular yellow-white lesion in the fovea, pale optic nerve, and retinal vessels with signs of attenuation.

(C) Chromatograms of *NgBR* genomic DNA sequences showing identified mutations in the family. Left: sequence of the unaffected individual. Middle: sequence showing heterozygous mutation c.G869 > A in the heterozygous carrier. Right: sequence showing homozygous mutation c.G869 > A in one of the probands.

(D) Schematic representation of NgBR showing the protein primary structure, location of the p.R290H mutation, and amino acid sequence alignment of the C-terminal part of the protein. SA, putative signal anchor; TM, putative transmembrane domain. The amino acid residues are color coded: small amino acids are red, acidic in blue, basic in magenta, and hydroxyl with amine in green. See also Table S1.

c.869G > A mutation was confirmed by Sanger sequencing, and the affected probands are homozygous for this mutation, whereas their parents and healthy siblings are heterozygous (Figure 3C). The mutation encodes for amino acid exchange p.Arg290His (R290H), which is located in the evolutionarily conserved C-terminal domain of NgBR (Figure 3D) and is predicted to affect protein function with a score of 0.00 according to SIFT and to be damaging using Polyphen. This mutation was not reported in dbSNP, 1000 Genomes, or the Exome variant server and was not listed in our internal exome database (>250 exomes). Targeted genotyping of genomic DNA from 255 individuals of Roma origin identified two additional heterozygous carriers of the c.869G > A mutation. Even though the identity and relation status of these two carriers is unknown, this finding suggests that the congenital disorder of glycosylation caused by a loss-of-function mutation of NgBR may be relatively frequent among the European Roma population.

NgBR R290H Mutation Triggers Defects in Cellular Cholesterol Trafficking and Dolichol Biosynthesis

To characterize the NgBR R290H mutation, fibroblasts were isolated from control and NgBR R290H patients and we examined the levels of NgBR mRNA, protein, and interaction of NgBR with hCIT (Figures S3A–S3C). We did not observe any significant differences in the migration of NgBR on SDS-PAGE or the levels of NgBR protein compared to WT (Figure S1B). This suggests that the translation and the subsequent processing of mutant

NgBR protein were not altered by the presence of the mutation. NgBR was isolated as a protein that interacted with reticulum 4B, also called Nogo-B (Miao et al., 2006). Therefore, we examined whether Nogo-B levels and its interaction with NgBR were altered in carriers of the NgBR mutation. The levels of Nogo-B, its interaction with NgBR, and the localization of Nogo-B were not different (Figures S3D–S3F). Next, we assessed three aspects of NgBR function, free cholesterol levels, *cis*-PTase activity, and glycosylation. WT cells had little filipin-positive free cholesterol, whereas treatment with U18666A to induce a Niemann-Pick C (NPC) disease phenotype (Cenedella, 2009) increased free cholesterol (Figure 4A, quantified in the right panel). In contrast, NgBR R290H mutant cells exhibited increased accumulation of free cholesterol similar to cells where NgBR was silenced (Harrison et al., 2009). Additionally, *cis*-PTase activity (Figure 4B) and mannose incorporation into proteins (Figure 4C) was markedly lower in NgBR R290H fibroblasts compared to control. We also examined defective glycosylation of proteins in patient fibroblasts by western blotting for two known glycoproteins, LAMP-1 and ICAM-1 (He et al., 2012; Xiang et al., 2013). Both LAMP-1 and ICAM-1 were hypoglycosylated in the patient fibroblasts (Figure 4D). Thus, the NgBR R290H mutant is a loss-of-function mutation that affects *cis*-PTase function of NgBR without disrupting complex formation with hCIT or Nogo-B. The reduced *cis*-PTase activity in fibroblasts was manifested as altered dolichol profiles in the urine or serum as assessed by mass spectrometry of all carriers of

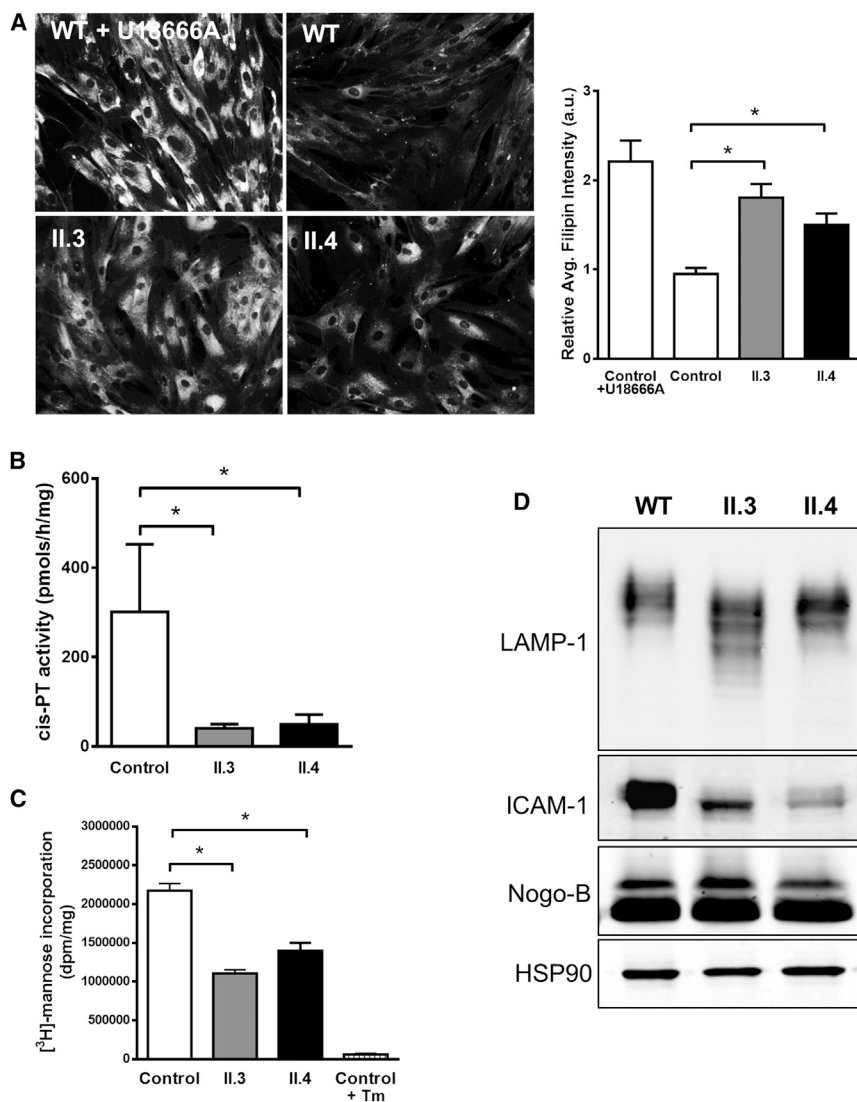


Figure 4. NgBR R290H Mutation Causes Defects in Cellular Cholesterol Trafficking and the Dolichol Biosynthesis Pathway

(A) Filipin staining and quantitative representation for human dermal fibroblast cells from patients (II.3 and II.4). U18666A was used as a positive control for inhibition of cholesterol trafficking.

(B) Microsomal *cis*-PTase activity using isolated membrane from fibroblasts. Compared to wild-type, less than 20% of activity was detected in the patient cells.

(C) [³H]-mannose labeling of proteins. Cells were incubated with [³H]-mannose for 4 hr, and TCA precipitated proteins were counted by scintillation. Tunicamycin (Tm) treatment was used as a control for loss of [³H]-mannose incorporation into newly synthesized proteins. **p* < 0.05. Data are mean ± SE, with *n* = 4 from three independent experiments.

(D) Western blot analysis of LAMP-1 and ICAM-1 levels in patient fibroblasts. Total lysates were analyzed, and the loading controls Nogo-B and Hsp90 are shown. See also Figure S2.

the R290H mutation (Figure S4), as recently described for patients harboring loss-of-function mutations in DHDDS (Wen et al., 2013).

Amino Acid at the Fourth Position from the C Terminus of NgBR Is a Functionally and Evolutionarily Conserved Residue

Alignment of NgBR orthologs from distantly related eukaryotic organisms reveals a high degree of conservation at the C terminus, with arginine or asparagine present at the fourth position from the C terminus (Figure 5A). To test the evolutionary conservation of this position, hCIT was expressed with NgBR or NgBR R290H in the *nus1Δ*, *rer2Δ*, *srt1Δ* triple knockout strain. Cells expressing the NgBR R290H allele have lower *cis*-PTase activity (Figure 5B), overall polyprenols (Figure 5C), and dolichol levels as measured by MS (Figure 5D). In addition, we analyzed *S. cerevisiae* and *S. pombe* Nus1 mutants to determine the importance of the amino acid conservation at the fourth position from the C terminus in NgBR orthologs. *S. cerevisiae* Nus1 belongs to group of fungi and plants NgBR orthologs bearing

asparagine instead of arginine, while *S. pombe* Nus1 encodes arginine at position 255 corresponding to the R290 in human NgBR. Therefore, we compared *cis*-PTase activity of the *S. cerevisiae nus1Δ* strain expressing wild-type Nus1, Nus1-N372H (mimicking NgBR R290H mutation), as well as Nus1-N372R. Also, we expressed wild-type SpNus1 or SpNus1-R255H in the *nus1Δ* fission yeast strain. Mutation of the same position in Nus1 in *S. cerevisiae* (Figures 5E and 5F) and *S. pombe* (Figures 5G and 5H) resulted in a similar loss of function. Interestingly, the N372R allele of Nus1 from *S. cerevisiae* affects only the chain length of the product (Figures 5F) but not the rate of incorporation of IPP (Figures 5E).

Recently, altered ratios of plasma and urinary dolichols were observed in retinitis pigmentosa patients carrying the K42E mutation in DHDDS/hCIT (Wen et al., 2013). To compare the influence of NgBR R290H and hCIT K42E mutations on *cis*-PTase activity, we expressed hCIT or hCIT K42E with NgBR or NgBR R290H in the *S. cerevisiae* triple knockout strain and measured enzyme activity. Introduction of this mutant into the triple knockout strain expressing WT NgBR reduced steady-state *cis*-PTase activity to an extent similar to that of NgBR R290H expressed with WT hCIT (Figure 5I), and combining the mutations reduced activity, further demonstrating epistasis of the gene products.

NgBR and its orthologs are essential genes, and NgBR/hCIT heteromers are responsible for dolichol synthesis in mammalian cells (Figures 6A and 6B). Based on previous work, NgBR can interact with hCIT, NPC2, and Nogo-B (Figure 6B; numbered 1–3). The interaction with NPC2 was identified by an independent broad-based screening strategy (Harrison et al., 2009).

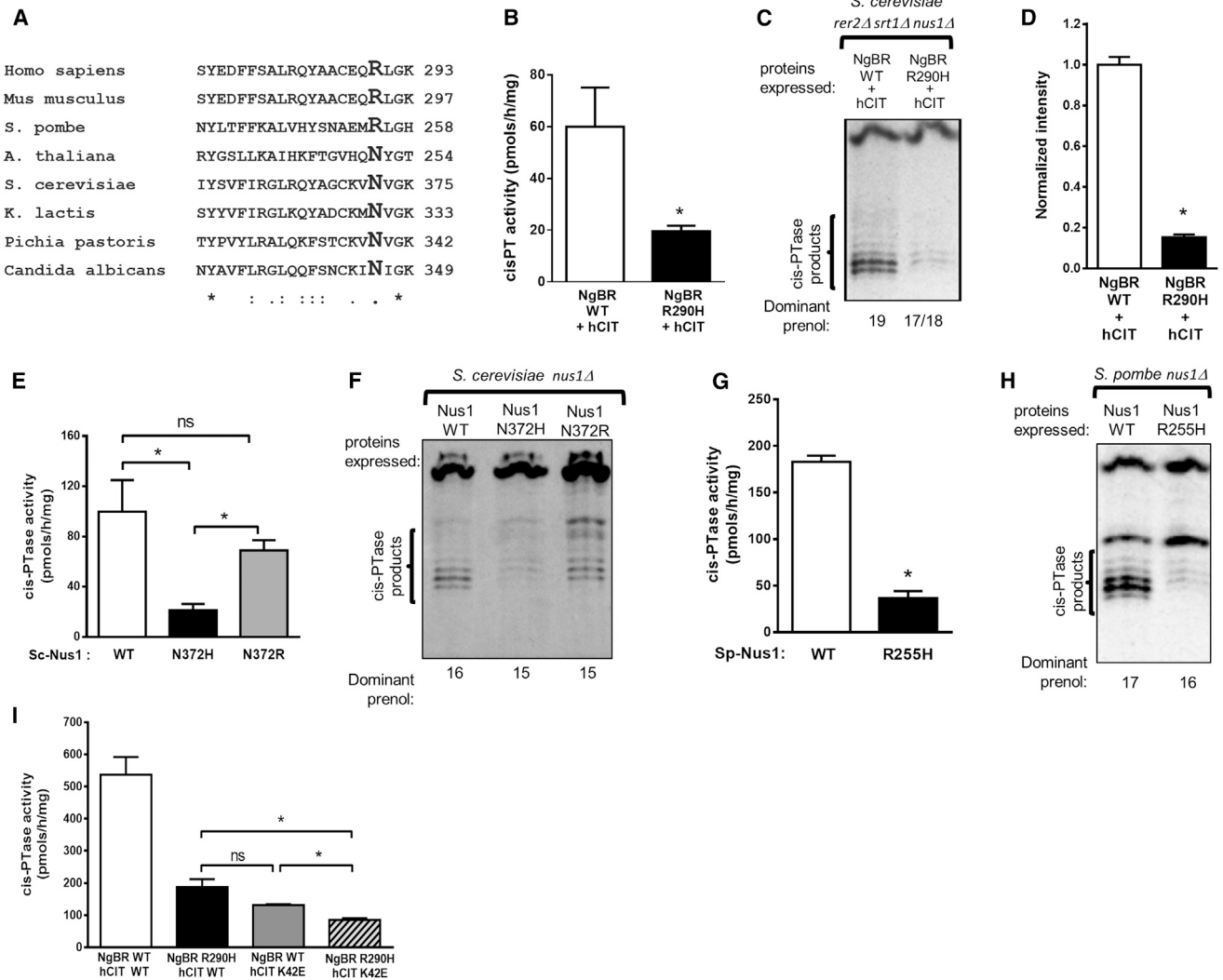


Figure 5. Characterization of NgBR/NUS1 Mutation in *S. cerevisiae* and *S. pombe*

(A) Amino acid alignment of the C terminus of NgBR orthologs. Arginine or asparagine is present at the fourth position from the C terminus.
 (B and D) Shown are the *cis*-PTase activity measurements (B) and total dolichol level (D) measured from *rer2Δ, srt1Δ, nus1Δ* *S. cerevisiae* strain expressing hCIT and NgBR or NgBR-R290H by mass spectrometry.
 (C) Reverse-phase TLC separation of *cis*-PTase products from *rer2Δ, srt1Δ, nus1Δ* triple deletion *S. cerevisiae* strain expressing the indicated constructs. About 15% of dolichol was detected in the NgBR mutant-expressing cells compared to wild-type NgBR.
 (E and F) Shown are *cis*-PTase activity (E) and reverse-phase TLC separation (F) in *S. cerevisiae nus1Δ* strain expressing the indicated constructs.
 (G and H) Shown are *cis*-PTase activity (G) and TLC separation of the products (H) in *S. pombe nus1Δ* strain expressing the indicated constructs. Mutated form of NgBR or Nus1-expressing cells show reduced *cis*-PTase activity. Not only reduced *cis*-PTase product, but also shortened chain length was detected in the mutated form of protein-expressed cells.
 (I) *cis*-PTase activity in *rer2Δ, srt1Δ, nus1Δ* *S. cerevisiae* strain expressing NgBR and hCIT indicated constructs. Samples were not dephosphorylated prior to TLC analysis. Data are \pm SE. * $p < 0.05$. See also Figure S3.

Genetic evidence for the importance of this interaction stems from data showing that NgBR knockout MEFs and patient fibroblasts harboring the R290H mutation exhibit increased free cholesterol levels. Since NPC2 is a soluble glycoprotein (Naurackiene et al., 2000) and glycosylation of NPC2 is important for its function (Chikh et al., 2004), it is feasible that in addition to a direct stabilizing effect of NgBR on NPC2, mutant NgBR can influence NPC2 glycosylation due to reduced *cis*-PTase activity contributing to this phenotype (Figure 6B). The interaction of

NgBR with Nogo-B does not impact *cis*-PTase activity or cellular cholesterol content and may influence intracellular signaling pathways.

Little is known about the function of dolichol species in vivo besides its role as a glycan carrier, although in vitro evidence suggests that dolichol can modulate biophysical properties of membranes and serve as a cellular antioxidant (Surmacz and Swiezewska, 2011). Patients carrying a mutation in NgBR demonstrated altered ratios of dolichol in urine and in blood.

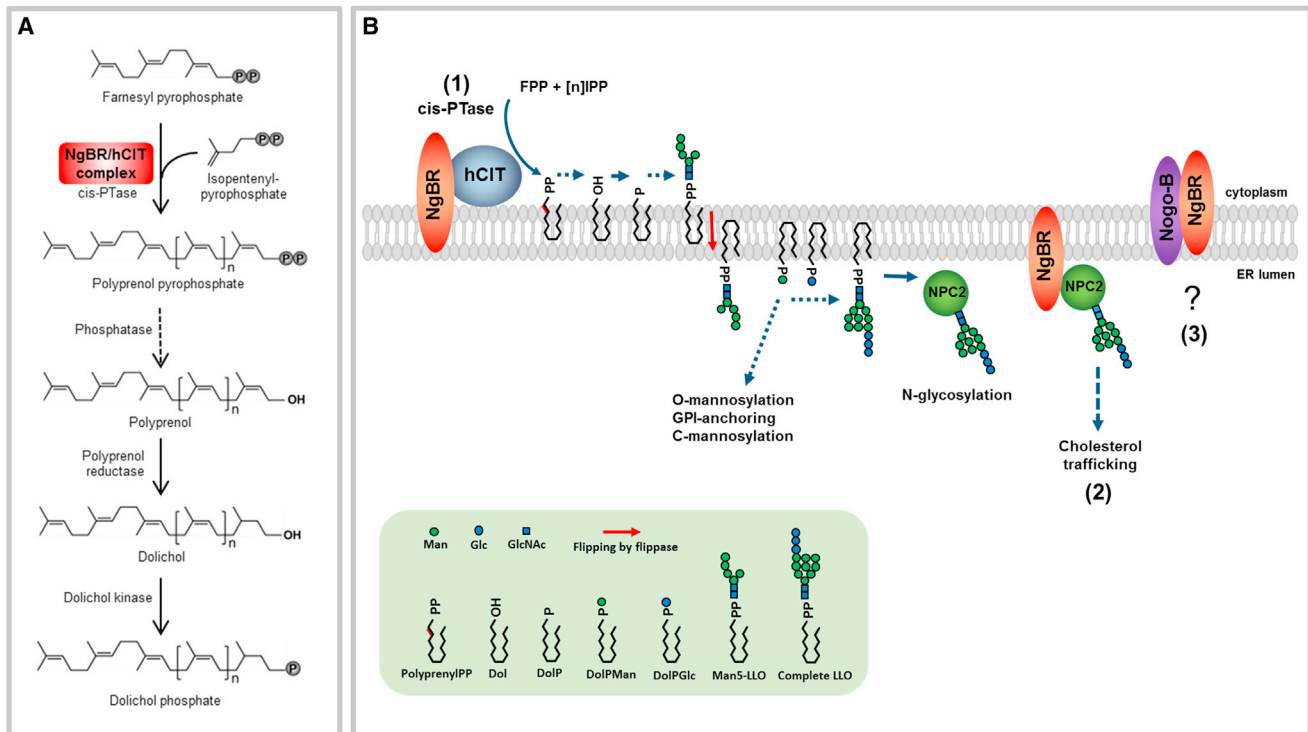


Figure 6. Functions of the NgBR/hCIT Complex in Cellular Metabolism

(A) The NgBR and hCIT complex promotes *cis*-PTase activity. NgBR/hCIT catalyzes the condensation of isopentenyl pyrophosphate with farnesyl pyrophosphate to generate a polyprenyl pyrophosphate. Polyprenyl pyrophosphate is dephosphorylated by unidentified phosphatase (SRD5A3) to form dolichol. Finally, dolichol is phosphorylated by dolichol kinase prior to the synthesis of dolichol-linked sugars required for glycosylation pathways.

(B) (1) NgBR and hCIT assembly is essential for *cis*-PTase activity generating polyprenyl pyrophosphate on the cytoplasmic leaflet of the ER membrane. Polyprenyl pyrophosphate serves as an intermediate in synthesis of dolichol-linked saccharides. Dolichol-pyrophosphate tetradecasaccharide (LLO) is indispensable for protein N-glycosylation reactions. Dolichol-phosphate mannose (DoIPMan) is also involved in O-mannosylation, GPI-anchor synthesis, and C-mannosylation. (2) NgBR influences cholesterol trafficking by directly interacting with NPC2 and indirectly via modifying NPC2 N-glycosylation. (3) The interaction between Nogo-B and NgBR does not influence glycosylation or cholesterol trafficking, and the function of this interaction remains to be clarified.

Although altered dolichol chain length ratios are important biomarkers in patients with mutations in hCIT/DHDDS and NgBR, alterations in dolichol chain length are unlikely to exert a dominant effect since lipid-linked oligosaccharides built on as few as 11 dolichol units seem to be efficient substrates in N-glycosylation reactions (Grabińska et al., 2010; Rush et al., 2010). However, the overall lower dolichol content of cell membranes not only directly affects glycosylation but can impair membrane structure and, in turn, affect multiple cellular processes including sterol biosynthesis. In summary, the development of a knockout strain of mice, the establishment of a NgBR/hCIT reconstitution system in yeast, and the discovery of a highly conserved mutation in the NgBR mutation in humans will assist in the further characterization of the cellular functions of this essential polyisoprene lipid.

EXPERIMENTAL PROCEDURES

Generation of NgBR Mouse Embryonic Fibroblasts

NgBR^{fl/fl} was crossed with NgBR^{+Δ}; R26CreER (Badea et al., 2003), and primary MEFs were prepared from E13.5 embryos. Each MEF line was derived from an individual embryo. Isolated MEFs were immortalized using an SV40-large-T-expressing retrovirus obtained from Genecoepeia (LP-SV40T-

LV105-0205) according to the manufacturer's protocol. Immortalized cells were maintained in Dulbecco's modified Eagle's medium (DMEM) with 1% penicillin/streptomycin containing 10% FBS. The genotypes of control MEFs and NgBR iKO MEFs used in this study are NgBR^{fl/+} and NgBR^{+Δ}; R26CreER. Both cell lines were treated with 1 μM 4-hydroxytamoxifen (Sigma) for more than 5 days to induce Cre recombination. mRNA or protein expression level was confirmed for each experiment. All experiments with NgBR^{fl/fl} mice were approved by the Institutional Animal Care Use Committee at Yale School of Medicine.

Filipin Staining

Filipin staining was performed as previously described (Harrison et al., 2009). In brief, cells were fixed in 4% paraformaldehyde for 10 min and permeabilized in 0.1% Triton X-100 for 5 min. Cells were then incubated with a 50 μg/ml concentration of filipin (Sigma, F4767) for 1 hr. As a positive control for induction of cholesterol accumulation, cells were treated for 8 hr with 1 μM U18666A (EMD Biosciences). Relative intensity of filipin staining was quantified by calculating average pixel intensity using Adobe Photoshop according to the following equation: average filipin intensity = total intensity above low threshold / number of pixels above low threshold (Pipalia et al., 2006).

Microsomal *cis*-PTase Activity Assay

For mammalian cells, crude microsomes were prepared as described before (Rush et al., 2010) with minor modification. *cis*-PTase activity in mammalian

cells was assayed as described before (Harrison et al., 2011) with minor modification. For *S. cerevisiae* and *S. pombe*, membrane fraction was prepared as described before (Szkopińska et al., 1997). *cis*-PTase assay using yeast membranes was performed as described (Szkopińska et al., 1997) with minor modifications. For a detailed description, please see the [Supplemental Experimental Procedures](#).

[2-³H]-Mannose Incorporation

D-[2-³H]-mannose (15–30 Ci/mmol) was purchased from PerkinElmer. Cells were grown in 6-well dishes until 80%–90% confluent. Growth medium was replaced and incubated for 1 hr with glucose-free DMEM supplemented with 0.1 mg/ml glucose and 5% dialyzed fetal calf serum. Next, 5 μg/ml of tunicamycin was added to media as a control for inhibition of N-glycosylation. After 1 hr, 20 uCi/ml [2-³H]-mannose was added and incubated for 4 hr at 37°C. Then, cells were washed with PBS and lysed in RIPA buffer. Cell lysates were then subjected to precipitation of proteins with 10% trichloroacetic acid (TCA) for 1 hr on ice. Precipitates were resuspended in 6 M Urea/SDS buffer and counted by scintillation.

Coimmunoprecipitation and Western Blot Analysis

Cos7 cells were transfected using Lipofectamine 2000 (Invitrogen) according to the manufacturer's protocol and harvested 48 hr after transfection. Cells were collected and lysed in IP buffer (IP buffer: 50 mM HEPES, 150 mM NaCl, 1 mM EDTA, 1% Triton X-100, 1.5 mg/ml protease inhibitor cocktail). Lysates were cleared at 12,000 rpm, and 20 μl of anti-HA agarose (Pierce) was used to pull down the HA-tagged protein from 1 mg of cell lysate. After incubation for 2 hr at 4°C, agarose beads were washed with IP buffer, resuspended in SDS loading buffer, and boiled for 5 min before western blotting.

Quantitative RT-PCR

Cells were collected in RLT buffer (QIAGEN). Total RNA were extracted using the RNeasy mini kit (QIAGEN), and 500 ng of total RNA was transcribed using superscript First-Strand Synthesis System with oligo dT primers (Invitrogen). Quantitative RT-PCR was performed using iQ SYBR Green Supermix (Bio-Rad) for the detection of fluorescence during amplification. Gapdh was used as an internal control. Expression of target genes was normalized to that of Gapdh using the comparative ΔCT method. Data are presented in relative expression to control ± SEM.

Human Subjects and DNA Analysis

The family of Roma origin was ascertained at the Department of Pediatrics of the First Faculty of Medicine, Charles University in Prague. Investigations were approved by the Institutional Review Board and conducted according to the Declaration of Helsinki principles. Written, informed consent was obtained from all subjects. Participants provided urine and venous blood. Skin biopsy was obtained from both affected individuals, and skin fibroblasts were cultured according to standard protocols. Autopsy material has been collected from deceased proband II.3. Genomic DNA was isolated from blood using standard technology and analyzed as described in the [Supplemental Experimental Procedures](#).

Yeast Strains, Plasmids, and Culture Methods

S. cerevisiae strains used in these studies include: KG404-16B (*nus1Δ/pNEV-GlcISPT*), KG405 (*rer2Δ, srt1Δ, nus1Δ/pNEV-GlcISPT*), and BY4742 and their derivatives. The *S. pombe* strain used was KGSP16 (*Spnus1Δ REP42GW-GlcISPT*). For yeast culture methods and detailed information about the strains, please see the [Supplemental Experimental Procedures](#).

Analysis of Dolichols by LC-MS

Serum and urine from family members and healthy unrelated controls were collected according to standard protocols. The samples were frozen at –80°C until the lipid extraction and the analysis. The lipid fraction was isolated from membranes isolated of *S. cerevisiae* (2 mg of proteins) or fibroblast (0.5 mg of proteins) as described before (Grabińska et al., 2005), and dolichol content was analyzed by liquid chromatography and mass spectrometry (LC-MS) (Guan and Eichler, 2011; Wen et al., 2013). For a detailed description, please see the [Supplemental Experimental Procedures](#).

SUPPLEMENTAL INFORMATION

Supplemental Information includes Supplemental Experimental Procedures, three figures, and one table and can be found with this article online at <http://dx.doi.org/10.1016/j.cmet.2014.06.016>.

AUTHOR CONTRIBUTIONS

E.J.P. and K.A.G. contributed equally to all aspects of this paper: E.J.P. characterized NgBR deficient mice and performed all mammalian cell based studies and cloning/plasmid construction, and K.A.G. developed yeast strains and *cis*-PTase characterization in vivo and in vitro. Both authors contributed to the writing and editing of the manuscript. Z.G. and R.W. contributed to MS analysis of urinary and serum dolichol levels and the writing of the manuscript. V.S., H. Hartmannová, and K.H. performed genotyping, linkage analysis, homozygosity mapping, and exome sequencing. V.B., J.S., N.O., H. Hansíková, and H. Hůlková contributed to acquisition of clinical specimens and phenotypic characterization of patients. T.H. and J.Z. were responsible for clinical and diagnostic assessment of affected patients. L.J. performed high-resolution imaging of Nogo-B in patient cells. W.C.S., E.J.P., K.A.G., and S.K. were responsible for concept development and preparation of the manuscript. S.K. was responsible for overseeing the genetic aspects of the study, and W.C.S. was responsible for overall integration and execution of the scientific approaches.

ACKNOWLEDGMENTS

We would like to thank Dr. Patrick Lusk (Department of Cell Biology, Yale School of Medicine) for giving us access to a dissection microscope for yeast tetrad separation and Marcela Michalíková (General Faculty Hospital Prague) for ophthalmologic investigations. This work was supported by grants R01 HL64793, R01 HL61371, R01 HL081190, R01 HL096670, and P01 HL70295 from the National Institutes of Health to W.C.S. Z.G. and the mass spectrometry facility in the Department of Biochemistry, Duke University Medical Center were supported by a LIPID MAPS glue grant (GM-069338) from the National Institutes of Health. V.S., H. Hartmannová, K.H., V.B., J.S., N.O., H. Hansíková, T.H., J.Z., H. Hůlková, and S.K. were supported by the Charles University institutional programs PRVOUK-P24/LF1/3, UNCE 204011, and SVV2014/260 022 and by BIOCEV – Biotechnology and Biomedicine Centre of the Academy of Sciences and Charles University (CZ.1.05/1.1.00/02.0109) from the European Regional Development Fund. Specific support was provided by grants NT13116-4/2012 and NT12166-5/2011 from the Ministry of Health of the Czech Republic.

Received: March 11, 2014

Revised: May 28, 2014

Accepted: June 14, 2014

Published: July 24, 2014

REFERENCES

- Badea, T.C., Wang, Y., and Nathans, J. (2003). A noninvasive genetic/pharmacologic strategy for visualizing cell morphology and clonal relationships in the mouse. *J. Neurosci.* 23, 2314–2322.
- Cantagrel, V., Lefebvre, D.J., Ng, B.G., Guan, Z., Silhavy, J.L., Bielas, S.L., Lehle, L., Hombauer, H., Adamowicz, M., Swiezewska, E., et al. (2010). SRD5A3 is required for converting polyprenol to dolichol and is mutated in a congenital glycosylation disorder. *Cell* 142, 203–217.
- Cenedella, R.J. (2009). Cholesterol synthesis inhibitor U18666A and the role of sterol metabolism and trafficking in numerous pathophysiological processes. *Lipids* 44, 477–487.
- Chikh, K., Vey, S., Simonot, C., Vanier, M.T., and Millat, G. (2004). Niemann-Pick type C disease: importance of N-glycosylation sites for function and cellular location of the NPC2 protein. *Mol. Genet. Metab.* 83, 220–230.
- Fujihashi, M., Zhang, Y.W., Higuchi, Y., Li, X.Y., Koyama, T., and Miki, K. (2001). Crystal structure of *cis*-prenyl chain elongating enzyme, undecaprenyl diphosphate synthase. *Proc. Natl. Acad. Sci. USA* 98, 4337–4342.

- Grabińska, K., Sosińska, G., Orłowski, J., Swieżewska, E., Berges, T., Karst, F., and Palamarczyk, G. (2005). Functional relationships between the *Saccharomyces cerevisiae* cis-prenyltransferases required for dolichol biosynthesis. *Acta Biochim. Pol.* *52*, 221–232.
- Grabińska, K.A., Cui, J., Chatterjee, A., Guan, Z., Raetz, C.R., Robbins, P.W., and Samuelson, J. (2010). Molecular characterization of the cis-prenyltransferase of *Giardia lamblia*. *Glycobiology* *20*, 824–832.
- Guan, Z., and Eichler, J. (2011). Liquid chromatography/tandem mass spectrometry of dolichols and polyprenols, lipid sugar carriers across evolution. *Biochim. Biophys. Acta* *1811*, 800–806.
- Guo, R.T., Ko, T.P., Chen, A.P., Kuo, C.J., Wang, A.H., and Liang, P.H. (2005). Crystal structures of undecaprenyl pyrophosphate synthase in complex with magnesium, isopentenyl pyrophosphate, and farnesyl thiopyrophosphate: roles of the metal ion and conserved residues in catalysis. *J. Biol. Chem.* *280*, 20762–20774.
- Harrison, K.D., Miao, R.Q., Fernandez-Hernández, C., Suárez, Y., Dávalos, A., and Sessa, W.C. (2009). Nogo-B receptor stabilizes Niemann-Pick type C2 protein and regulates intracellular cholesterol trafficking. *Cell Metab.* *10*, 208–218.
- Harrison, K.D., Park, E.J., Gao, N., Kuo, A., Rush, J.S., Waechter, C.J., Lehrman, M.A., and Sessa, W.C. (2011). Nogo-B receptor is necessary for cellular dolichol biosynthesis and protein N-glycosylation. *EMBO J.* *30*, 2490–2500.
- He, P., Ng, B.G., Losfeld, M.E., Zhu, W., and Freeze, H.H. (2012). Identification of intercellular cell adhesion molecule 1 (ICAM-1) as a hypoglycosylation marker in congenital disorders of glycosylation cells. *J. Biol. Chem.* *287*, 18210–18217.
- Kasapkar, C.S., Tümer, L., Ezgü, F.S., Hasanoğlu, A., Race, V., Matthijs, G., and Jaeken, J. (2012). SRD5A3-CDG: a patient with a novel mutation. *Eur. J. Paediatr. Neurol.* *16*, 554–556.
- Miao, R.Q., Gao, Y., Harrison, K.D., Prendergast, J., Acevedo, L.M., Yu, J., Hu, F., Strittmatter, S.M., and Sessa, W.C. (2006). Identification of a receptor necessary for Nogo-B stimulated chemotaxis and morphogenesis of endothelial cells. *Proc. Natl. Acad. Sci. USA* *103*, 10997–11002.
- Naureckiene, S., Sleat, D.E., Lackland, H., Fensom, A., Vanier, M.T., Wattiaux, R., Jadot, M., and Lobel, P. (2000). Identification of HE1 as the second gene of Niemann-Pick C disease. *Science* *290*, 2298–2301.
- O’Gorman, S., Dagenais, N.A., Qian, M., and Marchuk, Y. (1997). Protamine-Cre recombinase transgenes efficiently recombine target sequences in the male germ line of mice, but not in embryonic stem cells. *Proc. Natl. Acad. Sci. USA* *94*, 14602–14607.
- Pipalia, N.H., Huang, A., Ralph, H., Rujoi, M., and Maxfield, F.R. (2006). Automated microscopy screening for compounds that partially revert cholesterol accumulation in Niemann-Pick C cells. *J. Lipid Res.* *47*, 284–301.
- Rush, J.S., Matveev, S., Guan, Z., Raetz, C.R., and Waechter, C.J. (2010). Expression of functional bacterial undecaprenyl pyrophosphate synthase in the yeast *rer2Delta* mutant and CHO cells. *Glycobiology* *20*, 1585–1593.
- Sato, M., Sato, K., Nishikawa, S., Hirata, A., Kato, J., and Nakano, A. (1999). The yeast *RER2* gene, identified by endoplasmic reticulum protein localization mutations, encodes cis-prenyltransferase, a key enzyme in dolichol synthesis. *Mol. Cell. Biol.* *19*, 471–483.
- Schenk, B., Rush, J.S., Waechter, C.J., and Aebi, M. (2001). An alternative cis-isoprenyltransferase activity in yeast that produces polyisoprenols with chain lengths similar to mammalian dolichols. *Glycobiology* *11*, 89–98.
- Surmacz, L., and Swieżewska, E. (2011). Polyisoprenoids - Secondary metabolites or physiologically important superlipids? *Biochem. Biophys. Res. Commun.* *407*, 627–632.
- Szkopińska, A., Grabińska, K., Delourme, D., Karst, F., Rytka, J., and Palamarczyk, G. (1997). Polyprenol formation in the yeast *Saccharomyces cerevisiae*: effect of farnesyl diphosphate synthase overexpression. *J. Lipid Res.* *38*, 962–968.
- Wen, R., Lam, B.L., and Guan, Z. (2013). Aberrant dolichol chain lengths as biomarkers for retinitis pigmentosa caused by impaired dolichol biosynthesis. *J. Lipid Res.* *54*, 3516–3522.
- Xiang, Y., Zhang, X., Nix, D.B., Katoh, T., Aoki, K., Tiemeyer, M., and Wang, Y. (2013). Regulation of protein glycosylation and sorting by the Golgi matrix proteins GRASP55/65. *Nat Commun* *4*, 1659.
- Yu, L., Peña Castillo, L., Mnaimneh, S., Hughes, T.R., and Brown, G.W. (2006). A survey of essential gene function in the yeast cell division cycle. *Mol. Biol. Cell* *17*, 4736–4747.
- Zelinger, L., Banin, E., Obolensky, A., Mizrahi-Meissonnier, L., Beryozkin, A., Bandah-Rozenfeld, D., Frenkel, S., Ben-Yosef, T., Merin, S., Schwartz, S.B., et al. (2011). A missense mutation in *DHDDS*, encoding dehydrolipichyl diphosphate synthase, is associated with autosomal-recessive retinitis pigmentosa in Ashkenazi Jews. *Am. J. Hum. Genet.* *88*, 207–215.
- Züchner, S., Dallman, J., Wen, R., Beecham, G., Naj, A., Farooq, A., Kohli, M.A., Whitehead, P.L., Hulme, W., Konidari, I., et al. (2011). Whole-exome sequencing links a variant in *DHDDS* to retinitis pigmentosa. *Am. J. Hum. Genet.* *88*, 201–206.

Cell Metabolism, Volume 20

Supplemental Information

Mutation of Nogo-B Receptor, a Subunit of *cis*-Prenyltransferase, Causes a Congenital Disorder of Glycosylation

Eon Joo Park, Kariona A. Grabińska, Ziqiang Guan, Viktor Stránecký, Hana Hartmannová, Kateřina Hodaňová, Veronika Barešová, Jana Sovová, Levente Jozsef, Nina Ondrušková, Hana Hansíková, Tomáš Honzík, Jiří Zeman, Helena Hůlková, Rong Wen, Stanislav Kmoch, and William C. Sessa

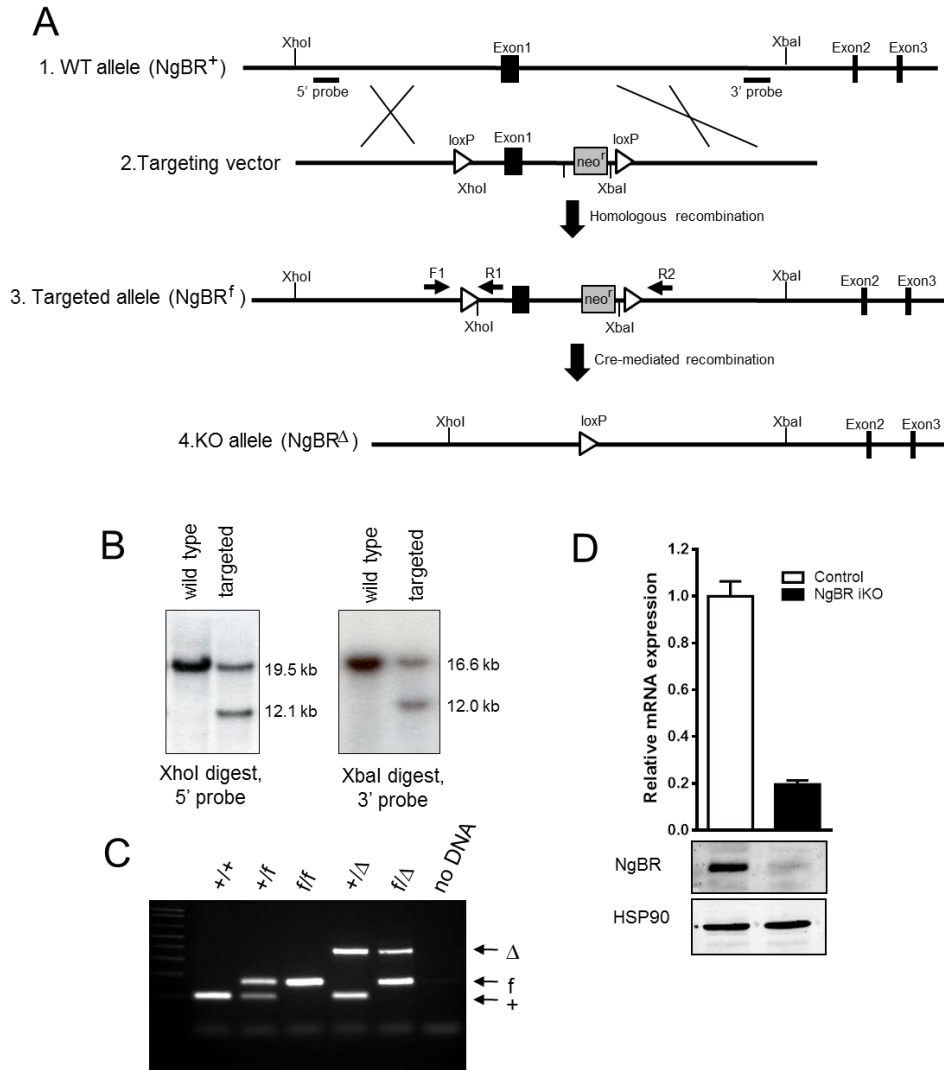


Figure S1. Generation of conditional NgBR knockout mice and mouse embryonic fibroblast, Related to Figure 1 (A) Schematic representation of the knockout strategy for NgBR gene. Panel 1. Genomic DNA fragment of NgBR gene containing exon 1-3. Panel 2. Schematic structure of the NgBR targeting vector. Panel 3. Genomic structure of NgBR allele after homologous recombination. Panel 4. Genomic structure of NgBR allele after Cre-mediated recombination. (B) Southern blot analysis of genomic DNA extracted from targeted ES clones. The 19.5 and 12.1kb of XhoI fragments represent WT and modified alleles, respectively. The 16.6 and 12kb of XbaI fragments represent WT and modified allele, respectively. The location of 5'probe and 3'probe was shown in (A), panel 1. (C) Mouse genotyping by PCR. Tail DNA was used for genotyping. The top band represents the null allele, the middle band shows the conditional allele, and the bottom band is the wild type allele. The primers used for genotyping are depicted by black arrow on (A), panel 3. (D) NgBR mRNA and protein expression in NgBR MEF cells. MEF cells were incubated with 4-hydroxytamoxifen for 7-10 days. mRNA expression level by qRT-PCR (upper panel) and protein expression level by Western blotting (lower panel) show reduced NgBR levels in NgBR iKO MEF cells.

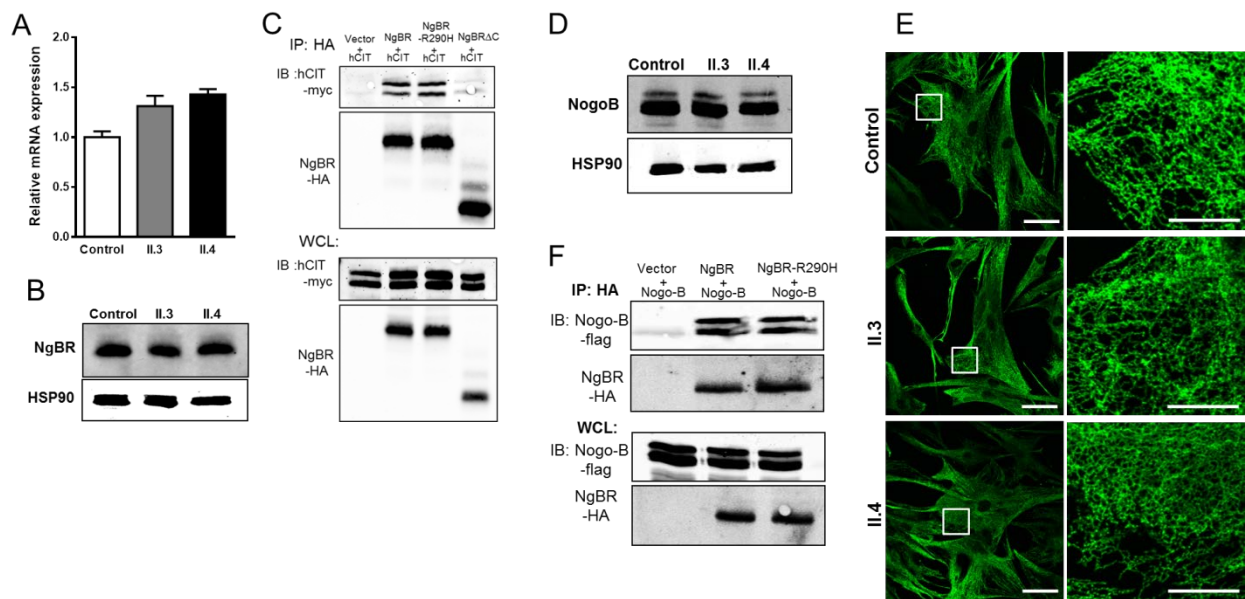


Figure S2. Characterization of NgBR-R290H mutation, Related to Figure 4. (A) NgBR mRNA expression levels in human fibroblasts by qRT-PCR. (B) Detection of NgBR protein by Western blotting in fibroblasts from patients. (C) Interaction between hCIT and NgBR/NgBR-R290H. Co-immunoprecipitation was performed using COS7 cell expressing the indicated constructs. The co-association between hCIT and NgBR was similar with WT or mutant NgBR. (D) Nogo-B expression in human fibroblasts by Western blotting. The levels of Nogo-B protein were not altered in the NgBR patient fibroblasts. (E) Subcellular localization of Nogo-B in human fibroblasts. Wild type (left panel) and NgBR mutant (right panels) fibroblasts were fixed and immunostained for Nogo-B to reveal its cellular distribution by confocal imaging. Lower panels show boxed regions at high magnification. Note that RTN4b localizes to tubular ER in both wild type and NgBR mutant fibroblasts. Scale bar, 50 μ m. (F) Interaction between Nogo-B and NgBR/NgBR-R290H. Co-immunoprecipitation was performed using COS7 cell expressing the indicated constructs. Both WT and NgBR-R290H co-associated with Nogo-B. IP, immunoprecipitate; WCL, whole cell lysate

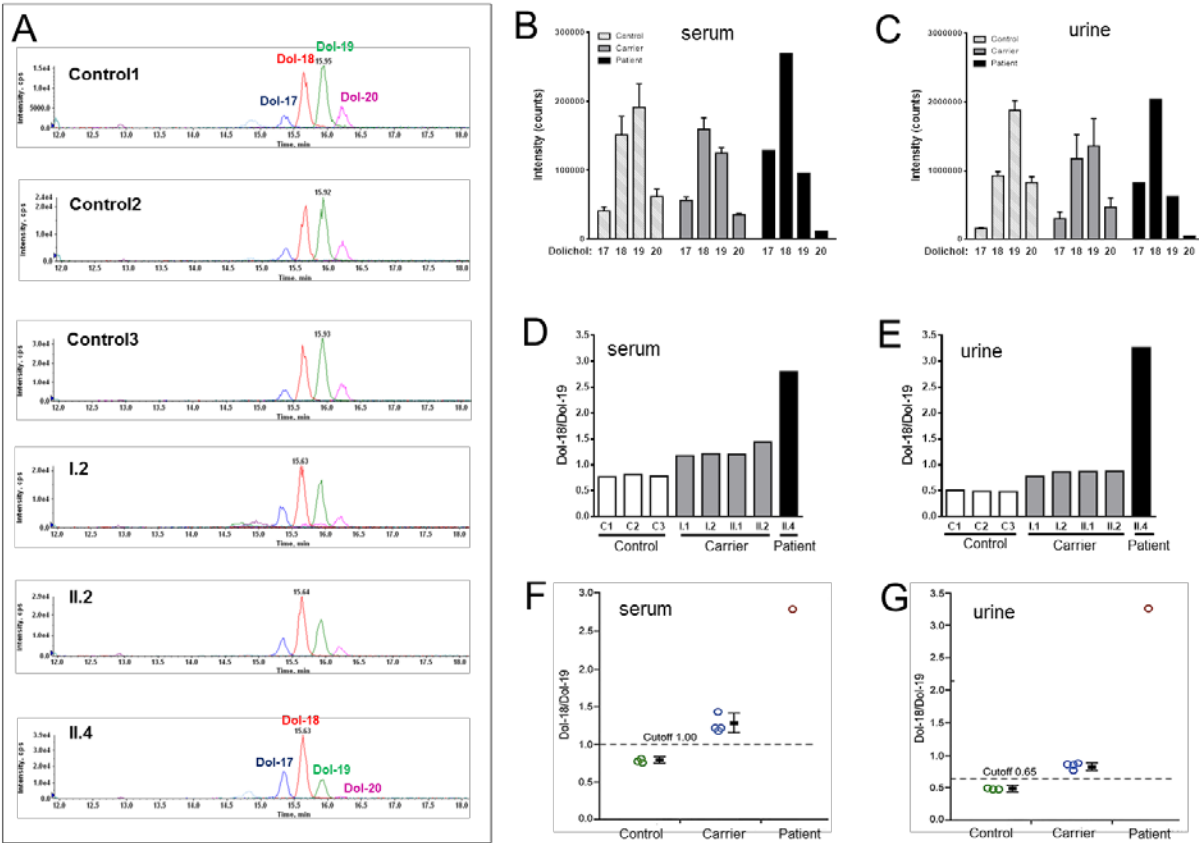


Figure S3. Mutation of NgBR changes ratio of dolichol chain lengths in humans as revealed by liquid chromatography-mass spectrometry, Related to Figure 5. (A) LC-multiple reaction monitoring (MRM) chromatograms of Dolichol-17, 18, 19 and 20 in serum samples from healthy controls (I-3), unaffected heterozygous carrier (I.2 and II.2) and affected homozygous patient (II.4). Distribution of dolichol in serum (B) and urine (C) from control (healthy control, N=3), Carrier (parents and two unaffected heterozygous siblings, N=4) and an affected patient (II.4). Error bar represent the mean \pm standard error. Dolicho-18/Dolichol-19 ratio in serum (D) and urine (E) collected from individuals. The ratio in each sample is plotted as a color-coded circle (green for normal individuals, blue for R290H NgBR carriers, and red for R290H NgBR homozygous patient). A bar representing the mean Dol-18/Dol-19 ratio (\pm SD) of each group is placed next to the plotted data from serum (F) and urine (G). The cutoff values to identify carriers from normal individuals are present in each graph.

Table S1. Candidate homozygous variants identified by exome sequencing in probands, Related to Figure 2

Chromosome	Position	Reference	Observed	Gene	Accession	cDNA Nucleotide change	Amino Acid change	SIFT	PolyPhen2
6	112496575	G	A	LAMA4	NM_001105206	c.C1297T	p.R433C	0	1
6	117127956	A	C	GPRC6A	NM_148963	c.T912G	p.N304K	0.15	0.547
6	118028165	G	A	NUS1	NM_138459	c.G869A	p.R290H	0	1
21	14982797	C	A	POTED	NM_174981	c.C248A	p.S83Y	0	0.981

All coordinates refer to hg19.

SUPPLEMENTAL EXPERIMENTAL PROCEDURES

Microsomal cis-PTase activity assay

For mammalian cells, crude microsomes were prepared as described (Rush et al., 2010) with minor modifications. cis-PTase activity in mammalian cells was assayed as described (Harrison et al., 2011) with minor modifications. For *S. cerevisiae* and *S. pombe*, membrane fraction was prepared as described before (Szkopinska et al., 1997). cis-PTase assay using yeast membranes was performed as described (Szkopinska et al., 1997) with minor modifications.

For mammalian cells, cells were collected into PBS containing 1 mM EDTA, collected with a 500-g spin, and resuspended in hypotonic buffer (10 mM Tris-HCl, pH 7.4, 1 mM EDTA, 250 mM sucrose). Cells were disrupted by sonication on ice. Unbroken material was cleared with a 1000-g centrifugation, and the supernatant from this spin was re-centrifuged at 100 000 g for 35 min at 4°C. Post-100 000 g pellets were washed twice with cis-PTase reaction buffer (25 mM Tris-HCl, pH 7.4, 5 mM MgCl₂, 1.25 mM DTT, 2.5 mM sodium orthovanadate), then resuspended in reaction buffer. cis-PTase activity in mammalian cells was assayed as described. Reaction mixture contained 100 µg microsomal protein, 45 µM FPP, 50 µM [1-¹⁴C]-isopentenyl pyrophosphate (IPP) (55 mCi/mmol), 25 mM Tris-HCl, pH 7.4, 5 mM MgCl₂, 1.25 mM DTT, 2.5 mM sodium orthovanadate, 10 µM Zaragozic acid A and 0.35% Triton X-100 in a total volume of 0.1 ml. Reactions were performed at 37°C for 1 hr and stopped by the addition 4 ml of chloroform:methanol (3:2 ratio). The protein pellet was removed by centrifugation and supernatant was washed three times with 1/5 volume of 10 mM EDTA in 0.9% NaCl. The incorporation of radioactive IPP into organic fraction containing polyprenyl pyrophosphate was measured by scintillation counting.

For *S. cerevisiae* and *S. pombe*, membrane fractions were prepared as described (Szkopinska et al., 1997) and cis-PTase activity measured (Szkopinska et al., 1997) with minor modifications. Briefly the incubation mixture contained, in a final volume of 250 µl, 45 µM FPP, 50 µM [1-¹⁴C]-IPP (55 mCi/mmol) 25 mM Tris-HCl pH 7.4, 5 mM MgCl₂, 20 mM β-mercaptoethanol, 10 mM KF, 10 µM Zaragozic acid A and 500 µg of membranes protein. hCIT/NgBR cisPTase activity was stimulated by the presence of 0.34% of Triton X-100. After 90 min incubation at 30°C, the reaction was terminated by the addition of 4 ml of chloroform-methanol 3:2. The protein pellet was removed by centrifugation and the supernatant was washed three times with 1/5 volume of 10 mM EDTA in 0.9% NaCl. The organic phase was concentrated under a stream of nitrogen and polyprenol pyrophosphates were dephosphorylated (Fujii et al., 1982). Dephosphorylated lipids were loaded onto HPTLC RP-18 pre-coated plates with a concentrating zone and run in acetone containing 50 mM H₃P₀₄. Plates were exposed to a phosphor screen and radiolabelled products were detected by phosphoimaging. To measure incorporation of radioactive IPP into polyprenol fraction, the gel from the zone containing radiolabeled polyprenols was scraped and subjected to liquid scintillation counting.

Immunofluorescent staining of Nogo-B.

For the detection of endogenous Nogo-B, cells were grown on 35 mm glass-bottom dishes (MatTek), fixed and permeabilized in 100% methanol at -20°C for 10min and blocked with 1% BSA (Sigma). Samples were incubated with anti-RTN4b antibody (1:500 dilution; Santa Cruz Biotech) overnight at 4°C , and then with the secondary AlexaFluor488 conjugated donkey anti-goat antibody (1:5,000 dilution; Invitrogen) for 1 h at room temperature. Washes were performed using PBS. Samples were kept in PBS and images were acquired using a Leica TCS SP5 confocal laser-scanning microscope with a $\times 63/1.49$ NA oil-immersion objective. Image analysis was performed with ImageJ software (NIH).

DNA analysis of human patient.

Genomic DNA was isolated from blood using standard technology. DNA samples from parents and both affected probands were genotyped using Affymetrix GeneChip Mapping 6.0 Array (Affymetrix, Santa Clara, CA) at the microarray core facility of the Institute of Molecular Genetics in Prague according to the manufacturer's protocol. Raw feature intensities were extracted from the Affymetrix GeneChip Scanner 3000 7G images using the GeneChip Command Console Software 2.1. Individual SNP calls were generated using Affymetrix Genotyping Console Software 4.1. Copy number changes were identified in Affymetrix Genotyping Console Software (GTC version 4.1). Data from both SNP and copy number probes were used to identify copy number aberrations compared to built-in reference. Only regions larger than 10 Kb containing at least 5 probes were reported. Regions of homozygosity (ROHs) were identified in Affymetrix Genotyping Console Software version 4.1 using the algorithm comparing values from the user's sample set and SNP-specific distributions derived from a reference set of two hundred ethnically diverse individuals. Only regions larger than 3Mb were reported.

Multipoint parametric linkage analysis along with determination of the most likely haplotypes was performed with version 1.1.2 of Merlin software.(Abecasis et al., 2002). The analysis was carried out assuming a recessive mode of inheritance with a 1.00 constant, age independent penetrance, 0.00 phenocopy rate, and 0.05 frequency of disease allele. The results were visualized in the version 1.043 of the HaploPainter software(Thiele and Nurnberg, 2005) and in version 2.9.2 of R-project statistical software (<http://www.r-project.org/>).

Exome sequencing was performed using 2 μg of DNA from parents and both affected probands. For DNA enrichment, individually bar-coded DNA libraries and SureSelect All Exome Kit V4 (Agilent, Santa Clara, USA) were used according to the manufacturer's protocol. DNA sequencing was performed on the captured barcoded DNA library using SOLiD™ 4 System (Applied Biosystems, Carlsbad, USA) at the Institute for Inherited Metabolic Disorders (Prague, Czech Republic). Reads were aligned in color space to the reference genome (hg19) using NovoalignCS version 1.08 (Novocraft, Malaysia) with default parameters. Sequence variants in analyzed samples were identified using SAMtools package (version 0.1.8). The high confidence variants list was annotated using ANNOVAR Annotation tool (hg19). Only the sequence variants present in both affected individuals and having frequency lower than 0.05 in the dbSNP, 1000 Genomes, Exome Variant Server (<http://evs.gs.washington.edu/EVS/>) and internal exome database were prioritized for further analysis. Identified genetic variants were filtered according to expected genetic model of the disease and evaluated according to biological relevance of corresponding genes. Candidate variants were visualized in Integrative Genomics Viewer (IGV)

- version 1.5.65.

The mutation-bearing fragment of NGBR (NM_138459) was PCR amplified from genomic DNA of all individuals from the family and sequenced using version 3.1 Dye Terminator cycle sequencing kit (Applied Biosystems, Foster City, CA) with electrophoresis on an ABI 3500XL Avant Genetic Analyzer (Applied Biosystems). Data were analyzed using Sequencing Analysis software, and the segregation of the candidate NGBR mutation with the phenotype was assessed. Targeted genotyping of the c.869G>A mutation was performed using PCR-RFLP based assay employing SfaNI (NEB) recognition and restriction at the mutation site.

Analysis of dolichols by LC-MS.

LC was operated at a flow rate of 200 μ l/min with a linear gradient as follows: 100% of mobile phase A was held isocratically for 2 min and then linearly increased to 100% mobile phase B over 14 min and held at 100% B for 4 min. Mobile phase A consisted of methanol/acetonitrile/aqueous 1 mM ammonium acetate (60/20/20, v/v/v). Mobile phase B consisted of 100% ethanol containing 1 mM ammonium acetate. A Zorbax SB-C8 reversed-phase column (5 μ m, 2.1 \times 50mm) was obtained from Agilent. MRM was performed in the negative ion mode with MS settings as follows: CUR=20 psi, GS1=20 psi, GS2=30 psi, Ion spray (IS)=-4500 V, TEM=350°C, Interface Heater=ON, DP=-40V, EP=-10V and CXP=-5V. The voltage used for collision-induced dissociation was -40V. For the MRM pairs, the precursor ions are the [M+acetate]⁻ adduct ions, and the product ions are the acetate ions (m/z 59). Dolichols are detected as their acetate adduct ions, [M+Ac]⁻, by ESI/MS in the negative ion mode.

Yeast strains and culture methods

S. cerevisiae and *S. pombe* strains used in this study are listed below.

Cultures were grown at 30°C in YPD. Synthetic minimal media were made of 0.67% (wt/vol) yeast nitrogen base and 2% (wt/vol) glucose supplemented with auxotrophic requirements. For solid media, agar (BD, Sparks MD) was added at a 2% (wt/vol) final concentration. Transformations, sporulation of the diploid cells, tetrad dissection and plasmid swapping experiments on 5-fluoroorotic synthetic complete medium were performed by standard yeast genetic methods. Yeast cells were harvested at medium logarithmic growth phase (~3 OD units/mL).

In order to obtain KG404-16 (*nus1* Δ) strain, deletion of *NUS1* gene was accomplished by the method described by Gueldener et al. The deletion cassette was amplified with primers atgccacgatgatcaaaaaggatgataaagcaatggagccccctaatgacagctgaagctctgtagcgc and cttgtaaatccaacgaaggcccgaagtataacagtaaatctggttcgggtgcataggccactagtgatctg from the pUG27 plasmid used as a template and then transformed into BY4743 yeast cells. Transformants able to grow on medium lacking histidine were isolated, and correct insertion of the cassette was verified by PCR. Finally, the diploid strain was transformed with pNEV-GlcisPT plasmid, subjected to sporulation and haploid colonies growing on synthetic medium lacking histidine were isolated. Triple deletion *nus1* Δ , *rer2* Δ , *srt1* Δ strain KG405 was obtain by mating of KG404-16 and KG119 following sporulation of diploid cells and colonies were identified by PCR. *Spnus1*/ Δ GlcisPT fission yeast strain is derivative of the heterozygous deletion h+/ h+ strains

with exchanged one copy of SPBC2A9.06c ORFs for kanMX4 cassette (Genome-wide Deletion Mutant Library (Bioneer). The diploid cells were transformed with REP41-GW empty vector or REP41-GW-GlcisPT expressing *G. lamblia* cis-PTase from a thiamine repressible promoter. Colonies able to grow on the synthetic EMM medium lacking leucine were subjected for random sporulation. The colonies able to grow on synthetic medium supplemented with G418 were obtained only when they were transformed with REP41-GW-GlcisPT KGSP16 is a derivative of *Spnus1*/ΔGlcisPT and CHP429 fission yeast strain obtained by crossing, transformation with REP42GW-GlcisPT plasmid, sporulation and isolation of haploid cells lacking chromosomal copy of *Spnus1* gene. REP42GW-GlcisPT plasmid was exchanged for pSP-GW1-*Spnus1* or pSP-GW1-*Spnus1R255* in KGSP16 using FOA plasmid swapping method.

S. pombe cells were cultured in Edinburgh minimal medium (EMM) supplemented with auxotrophic requirements or yeast extract with supplements (YES) medium (Forsburg and Rhind, 2006). Pombe Glutamate medium (PMG) was used for selection of spores resistant to G418. Transformation and random sporulation of the diploid cells were performed by standard fission yeast genetic methods (Forsburg and Rhind, 2006).

S. cerevisiae and *S. pombe* strains used in this study

Source	<i>S. cerevisiae</i> strain name	Genotype/description
Euroscarf	BY4741	<i>Mat a his3Δ1 leu2Δ1 met15Δ01 ura3Δ1</i>
Euroscarf	BY4743	MATa/MATα <i>his3Δ1/his3Δ1 leu2Δ0/leu2Δ0 met15Δ0/MET15 LYS2/lys2Δ0 ura3Δ0/ura3Δ0</i>
Euroscarf	BY4742	<i>Mat alfa his3Δ1 leu2Δ1 lys2D0Δ01 ura3Δ1</i>
Euroscarf	<i>alg5Δ</i>	As for BY471, <i>alg52::kanMX6</i>
(Grabinska et al., 2010)	KG119	As for BY471, <i>rer2::kanMX6 srt1::his3MX6loxP/pNEV-GlcisPT</i>
This study	KG404-16	<i>Mat alfa his3Δ 0; leu2Δ ; met15Δ 0; lys2Δ 0; ura3Δ 0 nus1::his3MX6loxP/p NEV-GlcisPT</i>
This study	KG405	<i>Mat a his3Δ 0; leu2Δ ; met15Δ 0; lys2Δ 0; ura3Δ 0, rer2::kanMX4, srt1:: nus1::his3MX6loxP, his3MX6loxP/pNEV-GlcisPT</i>
Source	<i>S. pombe</i> strain name	Genotype/description
BIONEER	SPBC2A9.06c	<i>h+/h+, ade6-M10/ade6-M216, ura4-D18/ura4-D18 leu1-32/leu-32 SPBC2A9.06c(nus1)/SPBC2A9.06c::kanMX4</i>
This study	KGSP16	<i>h⁻ SPBC2A9.06c kanMX4(Spnus1Δ)::, his7⁻, ade6⁻, ura4⁻, leu1⁻, REP42GW-GlcisPT</i>
(Forsburg, 1993), (ATCC# 201400)	CHP429	<i>h+ his7⁻, ade6⁻, ura4⁻, leu1⁻,</i>
This study	<i>Spnus1ΔGlcisPT</i>	<i>h+ ade6⁻, ura4-D18, leu1-32, SPBC2A9.06c::kanMX4(Spnus1Δ) REP41GW-GlcisPT</i>

Plasmids used for Yeast studies

Invitrogen Gateway Cloning strategy was used to insert cDNA into yeast expression vectors. pCR8/GW/TOPO plasmid was used as an entry vector. To express proteins in *S. pombe* three new plasmids were constructed: REP42-GW, REP41-GW and pSP1-GW vectors (derivative of REP42X, REP41X or pSLF101 respectively made by introducing Gateway Cassette A into Sma I site). To express proteins in baker's yeast under control of *TDH3* promoter and terminator using leucine selection, pKG-GW1 Gateway cloning vector was made (derivative of Yep351 (Hill et al 1986). In order to use methionine selection, *LEU2* marker of pKG-GW1 was exchange for *MET15* marker to obtain pKG-GW2 vector. Baker's yeast ORFs were amplified from genomic

DNA, fission yeast were amplified from cDNA obtained from RNA of WT *S. pombe* cells, NgBR and *GlcisPT* ORFs were amplified from previously described plasmids (Grabinska et al., 2010; Harrison et al., 2011) and hCIT isoform 1 variant MET-253 was amplified using cDNA clone 3532466 from Open Biosystems. In order to obtain mutated variants of *NgBR*, *NUS1*, and *Spnus1*, mutations were introduced into reverse primers. R290H mutated allele of NgBR was amplified with primer: GCGGCCGCCTACTTTCCAGATGCTGTTAC, N372H mutated allele of *NUS1* was amplified with primer: GCGGCCGCTCATTTACCAACATGCACTTTACA, N372R mutated allele of *NUS1* was amplified with primer: GCGGCCGCTCATTTACCAACACGCACTTTACA, and R255H mutated allele of *Spnus1* was amplified with primer: GCGGCCGCTCAGTGCCCTAAATGCATTTCTG. hCIT K42E (c.124A>G substitution) mutant was obtained using TagMaster *Site-Directed. Mutagenesis Kit* (GM Biosciences). Plasmids used in this study are listed below.

Plasmids used for *S. cerevisiae* strains in this study

Source	<i>S. cerevisiae</i>	Description
Grabinska et al 2010	pNEV-GlcisPT	<i>URA3</i> marker, 2 μ origin of replication, express <i>GlcisPT</i> gene under <i>PMA1</i> promoter,
This study	pKG-GW1	<i>LEU2</i> marker, 2 μ origin of replication, gateway cloning (GW) vector, derivative of Yep351
This study	pKG-GW2	Derivative of pKG-GW2 with <i>MET15</i> marker
This study	pKG-GW1-GlcisPT	Derivative of pKG-GW1, express <i>GlcisPT</i> gene
This study	pKG-GW2-GlcisPT	Derivative of pKG-GW2, express <i>GlcisPT</i> gene
This study	pKG-GW2-NgBR	Derivative of pKG-GW2, express <i>NgBR</i> gene
This study	pKG-GW2-NgBR R290H	Derivative of pKG-GW2, express <i>NgBR</i> R290H allele
This study	pKG-GW2-NUS1	Derivative of pKG-GW2, express <i>NUS1</i> gene
This study	pKG-GW2-NUS1 N374H	Derivative of pKG-GW2, express <i>nus1</i> N372H allele
This study	pKG-GW2-NUS1 N374R	Derivative of pKG-GW2, express <i>nus1</i> N372R allele
This study	pKG-GW2-Spnus1	Derivative of pKG-GW2, express <i>Spnus1</i> gene
This study	pKG-GW1-hCIT	Derivative of pKG-GW1, express <i>hCIT</i> gene
This study	pKG-GW1-hCIT K42E	Derivative of pKG-GW1, express <i>hCIT</i> K42E allele
This study	pKG-GW1-RER2	Derivative of pKG-GW1, express <i>RER2</i> gene
This study	pKG-GW1-SRT1	Derivative of pKG-GW1, express <i>SRT1</i> gene
This study	pKG-GW1-Sprer2	Derivative of pKG-GW1, express <i>Sprer2</i> gene

Plasmids used for *S. pombe* strains in this study

Source	<i>S. pombe</i>	Description
Forsburg 1993, (ATCC# 87605)	REP41X	<i>LEU2</i> marker, ars origin of replication, nmt thiamine repressible promoter
This study	REP41GW	Derivative of REP41X , gateway cloning vector
This study	REP41GW-GlcisPT	Derivative of REP41GW, express <i>GlcisPT</i> gene
Forsburg 1993, ATCC# 87607)	REP42X	<i>URA3</i> marker, ars origin of replication, nmt thiamine repressible promoter
This study	REP42GW	Derivative of REP42X , gateway cloning vector
This study	REP42GW-GlcisPT	Derivative of REP42GW, express <i>GlcisPT</i> gene
Forsburg 1993, (ATCC#87619)	pSLF101	<i>LEU2</i> marker, ars origin of replication, CaMV with tet operator
This study	pSP-GW1	Derivative of pSLF101 , gateway cloning vector
This study	pSP-GW1-Spnus1	Derivative of pSP1GWGW, express <i>Spnus1</i> gene
This study	pSP-GW1-Spnus1R255H	Derivative of REP41GW, express <i>Spnus1</i> R255H allele

Plasmids used for *in vitro* translation in this study

Source	<i>In vitro</i> translation	Description
Pierce	pT7CFE1-NMyc	N-terminal c-Myc tag
Pierce	pT7CFE1-NHA	N-terminal HA tag
This study	pT7-HA-RER2	Express HA tagged Rer2
This study	pT7-HA-SRT1	Express HA tagged Srt1
This study	pT7-HA-NUS1	Express HA tagged Nus1
This study	pT7-HA-Spnus1	Express HA tagged SpNus1
This study	pT7-HA-Sprer2	Express HA tagged SpRer2
This study	pT7-HA-NgBR	Express HA tagged NgBR
This study	pT7-myc-hCIT	Express c-Myc tagged hCIT

SUPPLEMENTAL REFERENCES

Abecasis, G.R., Cherny, S.S., Cookson, W.O., and Cardon, L.R. (2002). Merlin--rapid analysis of dense genetic maps using sparse gene flow trees. *Nat Genet* 30, 97-101.

Forsburg, S.L. (1993). Comparison of *Schizosaccharomyces pombe* expression systems. *Nucleic acids research* 21, 2955-2956.

Forsburg, S.L., and Rhind, N. (2006). Basic methods for fission yeast. *Yeast* 23, 173-183.

Fujii, H., Koyama, T., and Ogura, K. (1982). Efficient enzymatic hydrolysis of polyprenyl pyrophosphates. *Biochimica et biophysica acta* 712, 716-718.

Grabinska, K.A., Cui, J., Chatterjee, A., Guan, Z., Raetz, C.R., Robbins, P.W., and Samuelson, J. (2010). Molecular characterization of the cis-prenyltransferase of *Giardia lamblia*. *Glycobiology* 20, 824-832.

Harrison, K.D., Park, E.J., Gao, N., Kuo, A., Rush, J.S., Waechter, C.J., Lehrman, M.A., and Sessa, W.C. (2011). Nogo-B receptor is necessary for cellular dolichol biosynthesis and protein N-glycosylation. *The EMBO journal* 30, 2490-2500.

Rush, J.S., Matveev, S., Guan, Z., Raetz, C.R., and Waechter, C.J. (2010). Expression of functional bacterial undecaprenyl pyrophosphate synthase in the yeast *rer2*{Delta} mutant and CHO cells. *Glycobiology* 20, 1585-1593.

Szkopinska, A., Grabinska, K., Delourme, D., Karst, F., Rytka, J., and Palamarczyk, G. (1997). Polyrenol formation in the yeast *Saccharomyces cerevisiae*: effect of farnesyl diphosphate synthase overexpression. *Journal of lipid research* 38, 962-968.

Thiele, H., and Nurnberg, P. (2005). HaploPainter: a tool for drawing pedigrees with complex haplotypes. *Bioinformatics* 21, 1730-1732.

Isoelectric Focusing of Serum Apolipoprotein C-III as a Sensitive Screening Method for the Detection of O-glycosylation Disturbances

**Nina Ondrušková¹, Tomáš Honzík¹, Jitka Kytnarová¹,
Martin Matoulek², Jiří Zeman¹, Hana Hansíková¹**

¹Department of Pediatrics and Adolescent Medicine, First Faculty of Medicine, Charles University in Prague and General University Hospital in Prague, Prague, Czech Republic;

²3rd Department of Medicine – Department of Endocrinology and Metabolism, First Faculty of Medicine, Charles University in Prague and General University Hospital in Prague, Prague, Czech Republic

Received January 23, 2015; Accepted June 1, 2015.

Key words: Apolipoprotein C-III – O-glycosylation – Screening – Inherited disorders – Prader-Willi

Abstract: Apolipoprotein C-III (ApoC-III) is a glycoprotein carrying the most common O-linked glycan structure and is abundantly present in serum, what renders it a suitable marker for analysis of O-glycosylation abnormalities. Isoelectric focusing followed by a Western blot of ApoC-III, using PhastSystem™ Electrophoresis System (GE Healthcare), was introduced as a rather simple and rapid method for screening of certain subtypes of inherited glycosylation disorders. The study's aim was to establish this method in our laboratory, what included performing the analysis in a group of 170 healthy individuals to set the reference range of detected relative amounts of sialylated ApoC-III isoforms and to evaluate the gender- and age-dependent differences. A significant relative increase of asialo-ApoC-III with growing age was found. Secondly, we examined serum from patients with selected metabolic disorders and detected minor O-glycosylation changes

This study was supported by the grants GAUK 638512 (Charles University in Prague), IGA MZ NT/12166-5/2011, ExAM-CZ.1.05./2.1.00/03.0124 and RVO-VFN64165.

Mailing Address: RNDr. Hana Hansíková, PhD., Department of Pediatrics and Adolescent Medicine, First Faculty of Medicine, Charles University in Prague and General University Hospital in Prague, Ke Karlovu 2, 128 08 Prague 2, Czech Republic; Phone: +420 224 967 748; e-mail: hana.hansikova@lf1.cuni.cz

in diseases such as Prader-Willi syndrome, PGM1 (phosphoglucomutase 1) or MAN1B (class 1B alpha-1,2-mannosidase) deficiency. Our results show that this method allows for a sensitive detection of ApoC-III O-glycosylation status, however this might be modulated by several factors (i.e. nutrition, medication) whose exact role remains to be determined.

Introduction

Glycosylation is a functionally important and common posttranslational modification, with more than half of all human proteins estimated to be glycosylated (Christiansen et al., 2014). Congenital disorders of glycosylation (CDG) comprise a rapidly expanding family of metabolic diseases resulting from defects in glycosylation-related genes. Depending on which glycoprotein biosynthesis pathway is affected, more than 100 of N- and/or O-glycosylation disorders can be distinguished with a broad spectrum of clinical features (Freeze et al., 2014). In the more common group of N-glycosylation disorders, psychomotor retardation is often present along with hypotonia, cerebellar hypoplasia, dysmorphism, strabismus, atypical fat distribution and coagulopathy; however, various other manifestations such as recurrent infections, gastrointestinal symptoms or deafness may occur. Combined N- and O-glycosylation defects have a similar multi-systemic clinical picture, frequently including skeletal and skin anomalies. In contrast, isolated O-glycosylation disorders usually have a distinct phenotype defined by pronounced involvement of a single organ (brain, muscle) due to tissue-specific character of the enzymes involved in O-glycosylation (Wopereis et al., 2006b). As clinical report and basic laboratory tests are not sufficient for diagnosing CDG, selective screening methods are required to detect and categorize the glycosylation defect. Accordingly, additional experiments are performed (enzyme measurements, glycan structure analysis, immunocytochemical studies, etc.), before diagnosis is confirmed.

For CDG screening, serum N-glycoprotein transferrin (TRF) and O-glycoprotein apolipoprotein C-III (ApoC-III) are used as markers. ApoC-III is a core 1 mucin type plasma protein synthesized predominantly in liver, acting as an inhibitor

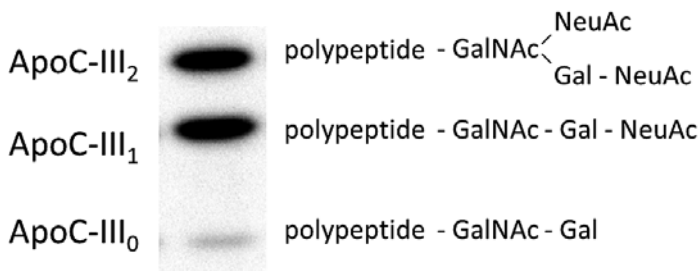


Figure 1 – Structure of ApoC-III O-glycosylated isoforms. Sialylated ApoC-III isoforms separated by isoelectric focusing (left) and the schematic structure of their corresponding glycan chains (right).

of lipoprotein and hepatic lipases, i.e. VLDL or LDL clearance. It contains one branched oligosaccharide chain (glycan) attached via a hydroxy group to its polypeptide chain (threonine), and three isoforms with different sialic acid content can be detected: ApoC-III₂, ApoC-III₁ and ApoC-III₀ (di-, mono- and asialoform, respectively; Figure 1). In CDG types with impaired mucin O-glycosylation, which occurs exclusively in Golgi as opposed to N-glycosylation localized both in ER (glycan assembly) and Golgi (further glycan modification), a pathological ApoC-III profile is observed characterized by decreased ApoC-III₂ and increased ApoC-III₁ or ApoC-III₀ (relative to total ApoC-III). To this date, aberrant ApoC-III sialylation has been described in glycosylation disorders including the deficiency of SLC35A1 (Wopereis et al., 2007), Conserved Oligomeric Golgi (COG) complex subunits 1, 2, 5, 6, 7 and 8 (Spaapen et al., 2005; Foulquier et al., 2006, 2007; Paesold-Burda et al., 2009; Lübbehusen et al., 2010; Kodera et al., 2015), ATP6V0A2 (Huchtagowder et al., 2009), ATP6V1A (Gardeitchik et al., 2014) and TMEM165 (Zeevaert et al., 2013). Recently, a new type of CDG due to phosphoglucomutase 1 (PGM1) deficiency was identified with an unusual TRF pattern in the CDG screening test, not clearly distinguishing which part of the glycosylation pathway is affected. No hypoglycosylation of ApoC-III was detected in the PGM1-CDG patient described by Pérez et al. (2013). Defect in the class 1B alpha-1,2-mannosidase (*MAN1B1*) gene manifests with a so called type 2 TRF pattern suggesting a disturbance in Golgi glycan modification, however no changes in ApoC-III glycosylation were reported (Van Scherpenzeel et al., 2014). The exact role of *MAN1B1*, originally thought of as an ER-resident mannosidase, has just lately been re-evaluated and it is currently presumed that the protein participates in Golgi-based protein biosynthesis quality control (Pan et al., 2013). Aside from the inborn defects in the glycosylation machinery, there are some pathophysiological factors that can influence the extent of serum ApoC-III sialylation. Documented secondary causes for ApoC-III hypoglycosylation include the acute phase of hemolytic uremic syndrome (HUS), where an enzyme cleaving sialic acid residues (neuraminidase) is released to circulation by *Streptococcus pneumoniae*, and Hutchinson Gilford progeria syndrome (HGSP) due to mutation in *LMNA* gene, possibly altering the biosynthesis of CMP-NeuAc (Wopereis et al., 2007). Other examples are metabolic syndrome (Savinova et al., 2014) and Prader-Willi syndrome (Munce et al., 2010). On the other hand, excess ApoC-III sialylation resulting from CMP-NeuAc overproduction was demonstrated in sialuria, which is caused by defective *GNE* gene (Wopereis et al., 2006a). Increased ApoC-III₂ to ApoC-III₁ ratio was also detected in individuals with chronic renal dysfunction (Holdsworth et al., 1982).

The study's aim was to determine the distribution of ApoC-III sialylated isoforms separated by isoelectric focusing (IEF) in sera from healthy individuals (a reference range) and to evaluate the gender- and age-dependent differences. The second aim was then to use the determined reference range for analysis of potential O-glycosylation abnormalities in patients with selected metabolic disorders.

Material and Methods

Material

The control group consisted of 170 healthy individuals (age interval 1 day–42 years), 89 males and 81 females. To examine O-glycosylation abnormalities possibly arising secondarily to non-CDG etiologies, we analyzed 10 patients with Prader-Willi syndrome (s.), two patients with Rett s. and one individual each from Silver-Russell s., DiGeorge s., Gapo s., Schnitzler s., Marfan s., Stickler s., dyschondrosteosis and unexplained chronic renal dysfunction. The second tested group included 5 selected deficiencies of glycosylation enzymes or proteins (CDG) not directly involved in mucin O-glycosylation due to mutations in *PMM2*

Table 1 – Overview of selected clinical and laboratory parameters in the analyzed group of patients

	Gender	Age	BMI	Sleep apnoea	Triacylglycerols in serum (mmol/l)	Metformin therapy
PWS, Patient 1	F	23 y	49.7	Y	3.50	N
PWS, Patient 2	F	27 y	59.1	Y	1.07	Y
PWS, Patient 3	F	20 y	45.8	N	1.69	N
PWS, Patient 4	M	21 y	43.4	N	1.07	Y
PWS, Patient 5	F	33 y	38.1	N	1.05	Y
PWS, Patient 6	M	17 y	41.3	N	0.62	Y
PWS, Patient 7	F	21 y	51.9	N	1.40	N
PWS, Patient 8	F	18 y	27.0	N	1.02	N
PWS, Patient 9	M	27 y	56.1	Y	1.32	N
PWS, Patient 10	M	5 m	14.5	N	NA	N
Chronic renal dysfunction	M	2 y	12.7	N	NA	N
Rett syndrome, Patient 1	F	2 y	13.7	N	1.10	N
Rett syndrome, Patient 2	M	7 y	12.5	N	2.22	N
Silver-Russell syndrome	M	18 y	12.8	N	1.05	N
DiGeorge syndrome	F	12 y	16.5	N	0.46	N
Gapo syndrome	M	18 y	NA	NA	NA	NA
Schnitzler syndrome	M	46 y	NA	NA	NA	NA
Marfan syndrome	M	27 y	NA	N	NA	N
Stickler syndrome	F	32 y	23.1	N	0.80	N
Dyschondrosteosis	F	32 y	32.5	N	0.77	N
PMM2-CDG	F	24 y	23.7	N	1.20	N
EXT1-CDG	F	3 y	NA	N	NA	N
NGBR deficiency	M	11 m	14.7	N	NA	N
PGM1-CDG	M	7 y	21.7	N	0.47	N
MAN1B1-CDG	M	10 y	NA	NA	NA	NA

PWS – Prader-Willi syndrome; F – female; M – male; y – years; m – months; BMI – body mass index; NA – not analyzed/no information

(phosphomannomutase 2), *PGM1*, *EXT1* (exostosin glycosyltransferase 1), *MAN1B1* and *NGBR* (Nogo-B receptor) genes, one patient from each group. Selected clinical and laboratory data of the analyzed patients are shown in Table 1. Serum was separated by centrifugation (630 g, 10 min) and stored at -20°C until tested. Analyses were performed with informed consent from each participant or their parents.

Isoelectric focusing (IEF) and Western blot of ApoC-III

IEF of ApoC-III was carried out as described by Wopereis et al. (2003), with minor modifications. Dry IEF gels (17-0677-01, GE Healthcare) were incubated in a rehydrating solution (8.3 M urea, 4% (V/V) Pharmalyte pH 4.2–4.9 (17-0562-01, GE Healthcare), 2% (V/V) Ampholine pH 3.5–5 (80-1125-89, GE Healthcare)) for 1.5 h. Serum was centrifuged at 6600 g for 2 min and the clear middle fraction (non-diluted) was used as a sample. The separation of samples (approx. 0.5 μl each) by isoelectric focusing was performed on PhastSystem™ Electrophoresis System (GE Healthcare). After the run was completed, gels were briefly washed in transfer buffer (25 mM Tris, 192 mM glycine, 20% methanol) and proteins were blotted onto nitrocellulose membranes (pre-equilibrated in transfer buffer) by diffusion at 60°C for 1 h. The membranes were then blocked in milk solution (5% (w/V) in PBST: PBS with 0.5% (V/V) Tween 20), labelled with primary ApoC-III antibody (0650-1707, Biotrend) diluted 1:1000 in BSA solution (2% (w/V) in PBST) and anti-rabbit secondary antibody conjugated to horseradish peroxidase (A-0545, Sigma; 1:5000 in 2% (w/V) milk in PBST). Each incubation was carried out for 1 h, with 3×10 min washes (PBS with 0.05% (V/V) Tween 20) in between. After the final washing in PBS (2×5 min), blots were visualized by chemiluminescence (SuperSignal West Femto Substrate, Thermo Scientific) using GBOX Imaging System (Syngene). The profiles of ApoC-III isoforms were quantified densitometrically with Quantity One software (Bio-Rad). Examples of both normal and hypoglycosylated ApoC-III profiles are shown in Figure 2. The coefficient of variation for intra-run variability (CV_1) was determined by evaluating 8 profiles of serum from one healthy control analyzed

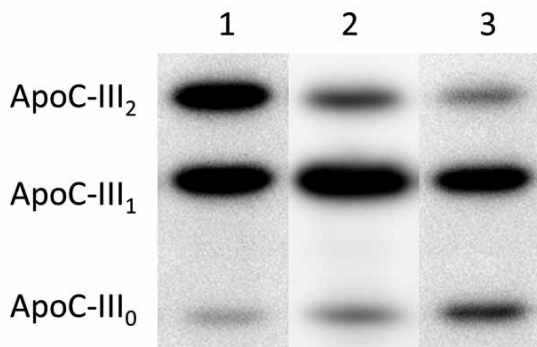


Figure 2 – Comparison of normal vs. hypoglycosylated ApoC-III IEF profiles. The picture shows an example of a physiological ApoC-III profile (1) and pathological profiles characterized by a relative decrease of ApoC-III₂ with relatively increased ApoC-III₁ (2) or ApoC-III₀ (3). The ratios vary in different syndromes and patients.

within one gel/run, and the same control sample was analyzed in 35 different gels/runs for the calculation of the coefficient of variation for inter-run variability (CV_2). CV_1 : 8.4, 6.8, 22.1; CV_2 : 6.7, 4.9, 23.5 (for ApoC-III₂, ApoC-III₁ and ApoC-III₀, respectively).

Statistical analysis

Because of the non-normal distribution of the data, the reference range was calculated using 2.5% and 97.5% sample quantiles. Gender-determined variations in given age categories were tested with non-parametric Wilcoxon test. Differences between the age categories were tested for both genders using Kruskal-Wallis test. A statistically significant difference was set as $p < 0.05$.

Results

Individuals from the analyzed control group were divided into three separate categories based on their age: 1) less than 2 years old, 2) 2–6 years old, and 3) 7–42 years old. The statistically evaluated distribution of ApoC-III sialylated isoforms – including the median, mean values and reference range – determined for the whole group is shown in Figure 3.

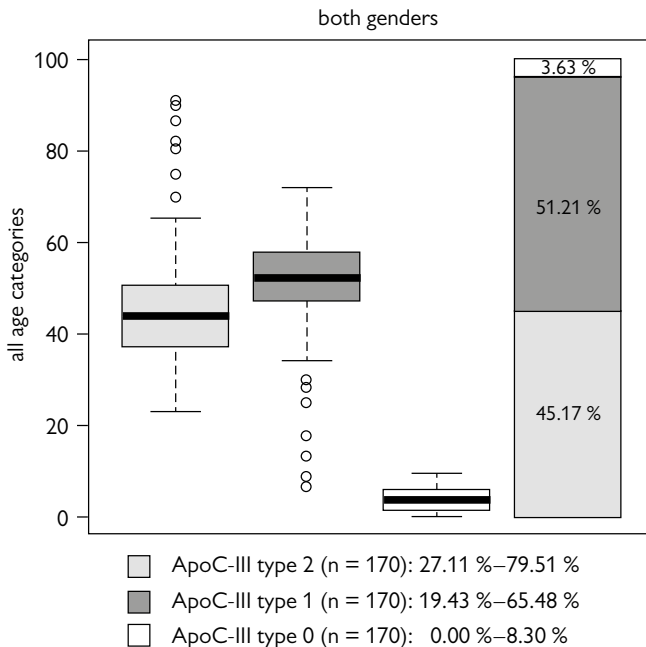


Figure 3 – Distribution of ApoC-III sialylated isoforms separated by isoelectric focusing of serum samples, determined in a group of healthy individuals (n=170) of both genders in the age interval 1 day–42 years. The bold line inside box-plot represents median, the column graph on the right shows mean values. Intervals below are the reference range.

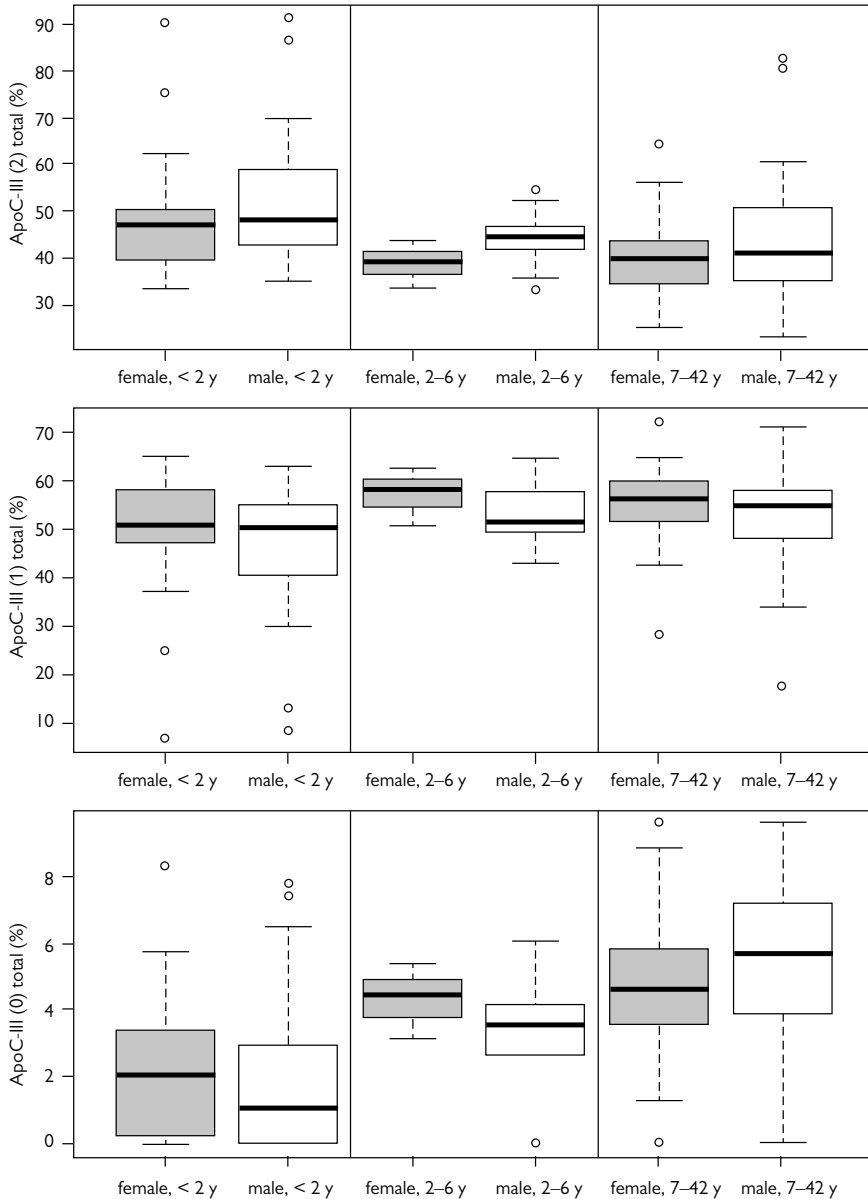


Figure 4 – Evaluation of gender- and age-dependent differences in the distribution of ApoC-III sialylated isoforms separated by isoelectric focusing of serum samples, determined in a group of healthy individuals ($n=170$) of both genders (89 males, 81 females) in three different age categories: 1) < 2 y ($n=70$), 2) 2–6 y ($n=16$) and 3) 7–42 y ($n=84$) (y – years). The bold line inside box-plots represents median. 1) Wilcoxon test results (female vs. male) for a) ApoC-III₂: $p=0.238$ (< 2 y); 0.157 (2–6 y); 0.345 (7–42 y), b) ApoC-III₁: $p=0.226$ (< 2 y); 0.281 (2–6 y); 0.181 (7–42 y) and c) ApoC-III₀: $p=0.522$ (< 2 y); 0.380 (2–6 y); 0.165 (7–42 y). 2) Kruskal-Wallis test results (age dependent differences) for a) ApoC-III₂: $p=0.002$ (female – F); 0.008 (male – M), b) ApoC-III₁: $p=0.041$ (F); 0.110 (M) and c) ApoC-III₀: $p<0.001$ (F); < 0.001 (M).

No statistically significant changes in ApoC-III sialylated isoforms' relative amounts were found between males and females ($p > 0.05$, Figure 4). However, regarding age-dependent differences, we noted a relative increase of ApoC-III₀ with growing age, accompanied by a relative decrease of the ApoC-III₂ isoform. This trend was calculated as statistically significant, for both genders (the lowest value $p < 0.001$ was obtained when comparing ApoC-III₀ content between groups < 2 years and 7–42 years; Figure 4).

Pathological ApoC-III profile was defined as a combination of relatively decreased ApoC-III₂ and relatively increased ApoC-III₁ or ApoC-III₀ compared to controls. Out of the tested non-CDG patients, all showed physiological ApoC-III profile except for three individuals with Prader-Willi s. (PWS; Patients 1, 3 and 7 in Table 1) and a boy with chronic renal dysfunction. As expected, normal O-glycosylation of ApoC-III was found in patients with genetic defects in *PMM2*, *EXT1* and *NGBR*. Multiple serum samples were analyzed from a boy with *PGM1* deficiency, displaying from borderline to pathological pattern, and a slight ApoC-III hypoglycosylation was also seen in patient with *MAN1B1* defect. The abnormal ApoC-III profiles are depicted in Figure 5 and the quantification of all analyzed ApoC-III profiles is shown in Table 2.

Discussion

To establish a screening assay for detecting O-glycosylation abnormalities in serum, we performed separation of ApoC-III sialylated isoforms by isoelectric focusing, followed by a Western blot detection – a method developed by Wopereis et al. (2003) – and determined a reference range of their relative amounts in our control group of 170 healthy subjects. While we found no variations between genders, there was a statistically significant relative decrease of ApoC-III₂ and increase of ApoC-III₀ with growing age. It underlines the need to consider the patient's age when evaluating their profile. This finding was in agreement with previous

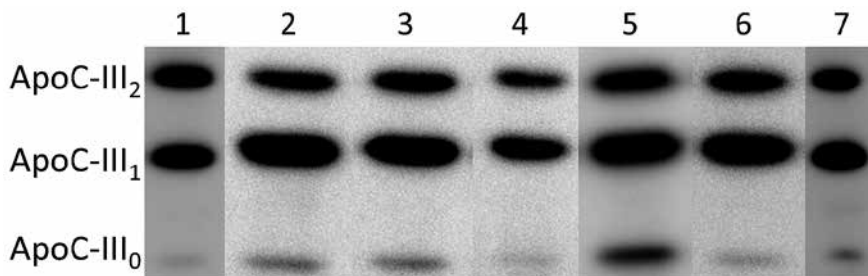


Figure 5 – ApoC-III hypoglycosylation detected in the analyzed group of patients. Serum samples were separated by isoelectric focusing, followed by a Western blot detection of ApoC-III. Relatively decreased ApoC-III₂ and increased ApoC-III₁ and/or ApoC-III₀ compared to a control (lane 1) were seen in three patients with Prader-Willi syndrome (2–4), unexplained chronic renal dysfunction (5), *PGM1* (6) and *MAN1B1* (7) deficiency.

Table 2 – Relative amounts of sialylated ApoC-III isoforms in the analyzed group of patients

	Age	Percentage of total ApoC-III (%)		
		Disialo-(2)	Monosialo-(1)	Asialo-(0)
Reference range	1 d–42 y	27.1–79.5	19.4–65.5	0–8.3
PWS, Patient 1 (lane 2 in Figure 5)	23 y	24.2	73.3	2.5
PWS, Patient 2	27 y	39.9	51.1	9.0
PWS, Patient 3 (lane 3)	20 y	27.3	70.3	2.4
PWS, Patient 4	21 y	37.2	57.4	5.4
PWS, Patient 5	33 y	48.4	48.8	2.9
PWS, Patient 6	17 y	42.6	57.5	ND
PWS, Patient 7 (lane 4)	21 y	28.2	71.9	ND
PWS, Patient 8	18 y	39.2	58.8	2.0
PWS, Patient 9	27 y	35.7	61.3	3.1
PWS, Patient 10	5 m	46.8	51.3	1.9
Chronic renal dysfunction (lane 5)	2 y	25.0	62.3	12.7
Rett syndrome, Patient 1	2 y	40.8	55.2	4.0
Rett syndrome, Patient 2	7 y	34.1	59.4	6.5
Silver-Russell syndrome	18 y	50.8	47.4	1.8
DiGeorge syndrome	12 y	46.6	51.9	1.6
Gapo syndrome	18 y	43.8	51.1	5.2
Schnitzler syndrome	46 y	39.9	57.2	2.9
Marfan syndrome	27 y	55.9	37.7	6.4
Stickler syndrome	32 y	37.2	60.0	2.8
Dyschondrosteosis	32 y	39.0	60.0	1.0
PMM2-CDG	24 y	34.8	59.8	5.4
EXT1-CDG	3 y	59.0	39.2	1.9
NGBR deficiency	11 m	43.1	54.4	2.5
PGM1-CDG (lane 6)	7 y	27.4	71.7	1.0
MAN1B1-CDG (lane 7)	10 y	27.9	69.3	2.8

PWS – Prader-Willi syndrome; d – day; y – years; m – months; ND – not detected

report by Wopereis et al. (2007), who, in addition, found higher relative levels of ApoC-III₂ in premature neonates than in full-term newborns. The observed age-dependent changes of ApoC-III sialylation are, in our opinion, likely downstream consequences of alterations in lipid metabolism associated with development/aging. It is unknown whether they directly hold any implications for the individual's health status, however in a study done by Tertov et al. (1996), it was determined that the circulating immune complexes containing low density lipoprotein (CIC-LDL), present in the blood of patients with coronary atherosclerosis, have considerably (2.1-fold) lower sialic acid content than native LDL.

It has been long known that increased ApoC-III level is associated with elevated triacylglycerols (TAG) in plasma (Kashyap et al., 1981), and is considered a valuable

marker for the risk of coronary heart disease (Sacks et al., 2000). Overexpressing ApoC-III in transgenic mice elevated TAG levels (Ito et al., 1990), while disruption of ApoC-III gene caused hypotriglyceridemia (Maeda et al., 1994). Vice versa, high total plasma TAG and VLDL-TAG in hypertriglyceridemia lead to accumulation of ApoC-III in triglyceride rich lipoproteins (TRL), resulting from both increased transfer of ApoC-III to TRL and increased hepatic production of VLDL ApoC-III (Marcoux et al., 2001). Recently, Savinova et al. (2014) found an increase of total ApoC-III (approx. 1.4-fold) together with its slightly reduced glycosylation in 56 subjects with metabolic syndrome, compared to controls. In their study, VLDL fraction of the patients contained 33% of ApoC-III₂, 58% of ApoC-III₁ and 9% of ApoC-III₀, whereas the controls had 40%, 52% and 8%, respectively. They point out that ApoC-III sialylation is responsive to prescription of metformin, as well as of omega-3 fatty acids and niacin (author's note: these medications are known to lower plasma TAG). Interestingly, some experiments in rats also documented alterations in the relative amounts of ApoC-III sialylated isoforms under different dietary conditions, where carbohydrate-rich diet, accompanied by a rise in plasma TAG levels, induced an increase of plasma ApoC-III₀ (Holdsworth et al., 1982). All the data above suggest a direct relationship between TAG levels and ApoC-III hyposialylation, however the underlying mechanism is currently not clear. At this point we can only speculate whether this is caused by impaired ApoC-III catabolism and consequent rises in relative amounts of its hyposialylated isoforms, or perhaps due to the increased production rate of new ApoC-III molecules and their secretion through Golgi apparatus (where sialylation occurs), the glycosylation machinery is overwhelmed and fails to fully modify all the passing glycoproteins. We confirm an observation of pathological ApoC-III profiles with decreased ApoC-III₂ and increased ApoC-III₁ (> 70%) in 3 individuals (positive) and a borderline profile with increased ApoC-III₀ (9%) in one individual (Patient 2 in Table 1), out of 10 analyzed patients with confirmed PWS. While Munce et al. (2010) found a correlation between abnormal ApoC-III profiles in PWS patients and sleep abnormalities, in our study only one positive patient suffered from a sleep apnoea. They reasoned that the observed glycosylation abnormality could be caused by deficiency in regulating protein degradation, based on their finding of two genes with putative roles as E3 ubiquitin ligases in the common deleted region. No relationship between aberrant ApoC-III and BMI was detected by Munce et al. (2010) or us, however we noted higher TAG (≥ 1.4 mmol/l) in all positive PWS patients compared to the others, supporting our assumption that ApoC-III hyposialylation in PWS is attributable to increased plasma TAG levels. We believe that drug treatments could have affected the observed results in our study, i.e. normalized the possible hyposialylation of ApoC-III through lowering plasma TAG.

Ooi et al. (2011) studied ApoC-III metabolism in subjects with moderate chronic kidney disease and found that they had significantly higher plasma ApoC-III concentrations, and the selected isoform for analysis, ApoC-III₁, had

significantly lower fractional catabolic rate. They hypothesize that elevated ApoC-III sialylation documented by Holdsworth et al. (1982) could render ApoC-III-containing TRL particles less suitable for lipolytic degradation. Moreover, the delayed ApoC-III catabolism could be due to impaired renal function as kidney is partly involved in the removal of ApoC-III from plasma. This contradicts our finding of a hypoglycosylated ApoC-III pattern (\downarrow ApoC-III₂, \uparrow ApoC-III₀) in a patient with chronic renal dysfunction as the predominant symptom. We cannot exclude the potential effect of elevated TAG level as it was not measured in the analyzed serum. Interestingly, hypoglycosylation linked to renal dysfunction is well documented in IgA nephropathy (IgAN), characterized by specific undergalactosylation of IgA1 O-glycans (Narita and Gejyo, 2008). They suggest that there is no primary abnormality in O-galactosylation pathway in B lymphocytes, but the IgA1 glycosylation defect is rather secondary to aberrant immunological reaction with IgA1 overproduction. In addition, recent studies have found decreased expression of *GALNT2* (the corresponding enzyme polypeptide N-acetylgalactosaminyltransferase initiates mucin type O-glycosylation) modulated by miRNA in IgA1-producing cells of IgAN patients (Serino et al., 2015). The finding is intriguing, since decreased *GALNT2* expression was also detected in circulating blood cells of obese diabetic patients, probably triggered by their hyperglycemia (Marucci et al., 2013). Moreover, certain SNPs in *GALNT2* gene were found to be associated with plasma TAG and cholesterol levels (Kathiresan et al., 2008). Thus, altered *GALNT2* activity might be linked to various conditions of metabolic derangement. While our patient did not present with features of IgAN, the observed ApoC-III hypoglycosylation could be secondary to yet unrecognized metabolic factor associated with his severe phenotype.

PGM1 deficiency indirectly lowers the intracellular concentration of UDP-Gal (Tegtmeyer et al., 2014), one of the substrates needed for mucin type 1 O-glycosylation, what could possibly explain our finding of reduced ApoC-III sialylation in the analyzed patient. However, the extent of detected hypoglycosylation was variable in serum samples withdrawn at different periods and sometimes the abnormal changes were rather subtle. Xia et al. (2013) performed LC/MS-MS analysis to quantify selected plasma O-glycan structures in various CDG subtypes and, interestingly, their PGM1-CDG patient had increased T/ST-antigen ratio (Gal-GalNAc/Sia-Gal-GalNAc) similar to those reported in galactosemia. The other analyzed PGM1-CDG patient who was on galactose treatment showed normal pattern, supporting the idea that the observed glycosylation disturbances in PGM1-CDG result from reduced UDP-Gal pool, which was also reported in galactosemic patients (Ng et al., 1989). Borderline ApoC-III hyposialylation was detected in our patient with pathogenic mutation in *MAN1B1* gene. Its deficiency disturbs Golgi morphology and impairs Golgi anterograde trafficking as studied in *MAN1B1*-depleted cells (Péanne et al., 2014), likely affecting both N- and O-glycosylation.

Conclusion

We determined a reference range and assessed gender- and age-dependent differences of the distribution of serum apolipoprotein C-III sialylated isoforms detected by Western blot after isoelectric focusing. Besides finding a mild ApoC-III hypoglycosylation in some individuals with Prader-Willi syndrome what had already been documented elsewhere, we suggest it is linked to plasma triacylglycerol levels. We also show, for the first time, slightly reduced O-glycosylation of ApoC-III in patients with PGM1 and MAN1B1 deficiency. Thus, we conclude the established method is sufficiently sensitive and suitable for screening of mucin type 1 O-glycosylation disturbances. Our results also demonstrate the importance of multiple analyses in the same individual. Further studies should be done to elucidate how patients' medication and diet might influence the outcome of the analysis.

Acknowledgements: The authors thank to Václav Čapek, PhD., for executing the statistical analyses.

References

- Christiansen, M. N., Chik, J., Lee, L., Anugraham, M., Abrahams, J. L., Packer, N. H. (2014) Cell surface protein glycosylation in cancer. *Proteomics* **14**(4–5), 525–546.
- Foulquier, F., Vasile, E., Schollen, E., Callewaert, N., Raemaekers, T., Quelhas, D., Jaeken, J., Mills, P., Winchester, B., Krieger, M., Annaert, W., Matthijs, G. (2006) Conserved oligomeric Golgi complex subunit 1 deficiency reveals a previously uncharacterized congenital disorder of glycosylation type II. *Proc. Natl. Acad. Sci. U. S. A.* **103**(10), 3764–3769.
- Foulquier, F., Ungar, D., Reynders, E., Zeevaert, R., Mills, P., García-Silva, M. T., Briones, P., Winchester, B., Morelle, W., Krieger, M., Annaert, W., Matthijs, G. (2007) A new inborn error of glycosylation due to a Cog8 deficiency reveals a critical role for the Cog1-Cog8 interaction in COG complex formation. *Hum. Mol. Genet.* **16**(7), 717–730.
- Freeze, H. H., Chong, J. X., Bamshad, M. J., Ng, B. G. (2014) Solving glycosylation disorders: Fundamental approaches reveal complicated pathways. *Am. J. Hum. Genet.* **94**(2), 161–175.
- Gardeitchik, T., Mohamed, M., Korenke, C., Van Asbeck, E., Van Kraaij, S., Monique, V. S., Lefeber, D., Wevers, R., Morava, E. (2014) A novel genetic defect connecting cutis laxa to congenital disorders of glycosylation. *J. Inherit. Metab. Dis.* **37**, 163 (Suppl. 1).
- Holdsworth, G., Stocks, J., Dodson, P., Galton, D. J. (1982) An abnormal triglyceride-rich lipoprotein containing excess sialylated apolipoprotein C-III. *J. Clin. Invest.* **69**(4), 932–939.
- Huchtagowder, V., Morava, E., Kornak, U., Lefeber, D. J., Fischer, B., Dimopoulou, A., Aldinger, A., Choi, J., Davis, E. C., Abuelo, D. N., Adamowicz, M., Al-Aama, J., Basel-Vanagaite, L., Fernandez, B., Grealley, M. T., Gillissen-Kaesbach, G., Kayserili, H., Lemyre, E., Tekin, M., Türkmen, S., Tuysuz, B., Yüksel-Konuk, B., Mundlos, S., Van Maldergem, L., Wevers, R. A., Urban, Z. (2009) Loss-of-function mutations in ATP6V0A2 impair vesicular trafficking, tropoelastin secretion and cell survival. *Hum. Mol. Genet.* **18**(12), 2149–2165.
- Ito, Y., Azrolan, N., O'Connell, A., Walsh, A., Breslow, J. L. (1990) Hypertriglyceridemia as a result of human apo CIII gene expression in transgenic mice. *Science* **249**(4970), 790–793.
- Kashyap, M. L., Srivastava, L. S., Hynd, B. A., Gartside, P. S., Perisutti, G. (1981) Quantitation of human apolipoprotein C-III and its subspecies by radioimmunoassay and analytical isoelectric focusing:

- Abnormal plasma triglyceride-rich lipoprotein apolipoprotein C-III subspecies concentrations in hypertriglyceridemia. *J. Lipid Res.* **22(5)**, 800–810.
- Kathiresan, S., Melander, O., Guiducci, C., Surti, A., Burt, N. P., Rieder, M. J., Cooper, G. M., Roos, C., Voight, B. F., Havulinna, A. S., Wahlstrand, B., Hedner, T., Corella, D., Tai, E. S., Ordovas, J. M., Berglund, G., Vartiainen, E., Jousilahti, P., Hedblad, B., Taskinen, M. R., Newton-Cheh, C., Salomaa, V., Peltonen, L., Groop, L., Altshuler, D. M., Orho-Melander, M. (2008) Six new loci associated with blood low-density lipoprotein cholesterol, high-density lipoprotein cholesterol or triglycerides in humans. *Nat. Genet.* **40(2)**, 189–197.
- Kodera, H., Ando, N., Yuasa, I., Wada, Y., Tsurusaki, Y., Nakashima, M., Miyake, N., Saitoh, S., Matsumoto, N., Saito, H. (2015) Mutations in COG2 encoding a subunit of the conserved oligomeric Golgi complex cause a congenital disorder of glycosylation. *Clin. Genet.* **87(5)**, 455–460.
- Lübbehusen, J., Thiel, C., Rind, N., Ungar, D., Prinsen, B. H., De Koning, T. J., Van Hasselt, P. M., Körner, C. (2010) Fatal outcome due to deficiency of subunit 6 of the conserved oligomeric Golgi complex leading to a new type of congenital disorders of glycosylation. *Hum. Mol. Genet.* **19(18)**, 3623–3633.
- Maeda, N., Li, H., Lee, D., Oliver, P., Quarfordt, S. H., Osada, J. (1994) Targeted disruption of the apolipoprotein C-III gene in mice results in hypotriglyceridemia and protection from postprandial hypertriglyceridemia. *J. Biol. Chem.* **269(38)**, 23610–23616.
- Marcoux, C., Tremblay, M., Fredenrich, A., Davignon, J., Cohn, J. S. (2001) Lipoprotein distribution of apolipoprotein C-III and its relationship to the presence in plasma of triglyceride-rich remnant lipoproteins. *Metabolism* **50(1)**, 112–119.
- Marucci, A., Di Mauro, L., Menzaghi, C., Prudente, S., Mangiacotti, D., Fini, G., Lotti, G., Trischitta, V., Di Paola, R. (2013) GALNT2 expression is reduced in patients with type 2 diabetes: Possible role of hyperglycemia. *PLoS One* **8(7)**, e70159.
- Munce, T., Heussler, H. S., Bowling, F. G. (2010) Analysis of N- and O-linked protein glycosylation in children with Prader-Willi syndrome. *J. Intellect. Disabil. Res.* **54(10)**, 929–937.
- Narita, I., Gejyo, F. (2008) Pathogenetic significance of aberrant glycosylation of IgA1 in IgA nephropathy. *Clin. Exp. Nephrol.* **12(5)**, 332–338.
- Ng, W. G., Xu, Y. K., Kaufman, F. R., Donnell, G. N. (1989) Deficit of uridine diphosphate galactose in galactosaemia. *J. Inherit. Metab. Dis.* **12(3)**, 257–266.
- Ooi, E. M., Chan, D. T., Watts, G. F., Chan, D. C., Ng, T. W., Dogra, G. K., Irish, A. B., Barrett, P. H. (2011) Plasma apolipoprotein C-III metabolism in patients with chronic kidney disease. *J. Lipid Res.* **52(4)**, 794–800.
- Paesold-Burda, P., Maag, C., Troxler, H., Foulquier, F., Kleinert, P., Schnabel, S., Baumgartner, M., Hennet, T. (2009) Deficiency in COG5 causes a moderate form of congenital disorders of glycosylation. *Hum. Mol. Genet.* **18(22)**, 4350–4356.
- Pan, S., Cheng, X., Sifers, R. N. (2013) Golgi-situated endoplasmic reticulum α -1, 2-mannosidase contributes to the retrieval of ERAD substrates through a direct interaction with γ -COP. *Mol. Biol. Cell* **24(8)**, 1111–1121.
- Péanne, R., Rymen, D., Jurisch-Yaksi, N., Foulquier, F., Annaert, W., Matthijs, G. (2014) MAN1B1-CDG: How stressed-out can the Golgi be? *Glycobiology* **24(11)**, 1105.
- Pérez, B., Medrano, C., Ecay, M. J., Ruiz-Sala, P., Martínez-Pardo, M., Ugarte, M., Pérez-Cerdá, C. (2013) A novel congenital disorder of glycosylation type without central nervous system involvement caused by mutations in the phosphoglucomutase 1 gene. *J. Inherit. Metab. Dis.* **36(3)**, 535–542.
- Sacks, F. M., Alaupovic, P., Moye, L. A., Cole, T. G., Sussex, B., Stampfer, M. J., Pfeffer, M. A., Braunwald, E. (2000) VLDL, apolipoproteins B, CIII, and E, and risk of recurrent coronary events in the cholesterol and recurrent events (CARE) trial. *Circulation* **102(16)**, 1886–1892.
- Savinova, O. V., Fillaus, K., Jing, L., Harris, W. S., Shearer, G. C. (2014) Reduced apolipoprotein glycosylation in patients with the metabolic syndrome. *PLoS One* **9(8)**, e104833.

- Serino, G., Sallustio, F., Curci, C., Cox, S. N., Pesce, F., De Palma, G., Schena, F. P. (2015) Role of let-7b in the regulation of N-acetylgalactosaminyltransferase 2 in IgA nephropathy. *Nephrol. Dial. Transplant.* (Epub ahead of print)
- Spaapen, L. J., Bakker, J. A., van der Meer, S. B., Sijstermans, H. J., Steet, R. A., Wevers, R. A., Jaeken, J. (2005) Clinical and biochemical presentation of siblings with COG-7 deficiency, a lethal multiple O- and N-glycosylation disorder. *J. Inherit. Metab. Dis.* **28(5)**, 707–714.
- Tegtmeyer, L. C., Rust, S., Van Scherpenzeel, M., Ng, B. G., Losfeld, M. E., Timal, S., Raymond, K., He, P., Ichikawa, M., Veltman, J., Huijben, K., Shin, Y. S., Sharma, V., Adamowicz, M., Lammens, M., Reunert, J., Witten, A., Schrapers, E., Matthijs, G., Jaeken, J., Rymen, D., Stojkovic, T., Laforêt, P., Petit, F., Aumaitre, O., Czarnowska, E., Piraud, M., Podskarbi, T., Stanley, C. A., Matalon, R., Burda, P., Seyyedi, S., Debus, V., Socha, P., Sykut-Cegielska, J., Van Spronsen, F., De Meirleir, L., Vajro, P., DeClue, T., Ficicioglu, C., Wada, Y., Wevers, R. A., Vanderschaege, D., Callewaert, N., Fingerhut, R., Van Schaftingen, E., Freeze, H. H., Morava, E., Lefeber, D. J., Marquardt, T. (2014) Multiple phenotypes in phosphoglucomutase 1 deficiency. *N. Engl. J. Med.* **370(6)**, 533–542.
- Tertov, V. V., Sobenin, I. A., Orekhov, A. N., Jaakkola, O., Solakivi, T., Nikkari, T. (1996) Characteristics of low density lipoprotein isolated from circulating immune complexes. *Atherosclerosis* **122(2)**, 191–199.
- Van Scherpenzeel, M., Timal, S., Rymen, D., Hoischen, A., Wuhrer, M., Hipgrave-Ederveen, A., Grunewald, S., Peanne, R., Saada, A., Edvardson, S., Grønborg, S., Ruijter, G., Kattentidt-Mouravieva, A., Brum, J. M., Freckmann, M. L., Tomkins, S., Jalan, A., Prochazkova, D., Ondruskova, N., Hansikova, H., Willemsen, M. A., Hensbergen, P. J., Matthijs, G., Wevers, R. A., Veltman, J. A., Morava, E., Lefeber, D. J. (2014) Diagnostic serum glycosylation profile in patients with intellectual disability as a result of MAN1B1 deficiency. *Brain* **137(Pt 4)**, 1030–1038.
- Wopereis, S., Grünewald, S., Morava, E., Penzien, J. M., Briones, P., Garcia-Silva, M. T., Demacker, P. N., Huijben, K. M., Wevers, R. A. (2003) Apolipoprotein C-III isofocusing in the diagnosis of genetic defects in O-glycan biosynthesis. *Clin. Chem.* **49(11)**, 1839–1845.
- Wopereis, S., Abd Hamid, U. M., Critchley, A., Royle, L., Dwek, R. A., Morava, E., Leroy, J. G., Wilcken, B., Lagerwerf, A. J., Huijben, K. M., Lefeber, D. J., Rudd, P. M., Wevers, R. A. (2006a) Abnormal glycosylation with hypersialylated O-glycans in patients with Sialuria. *Biochim. Biophys. Acta* **1762(6)**, 598–607.
- Wopereis, S., Lefeber, D. J., Morava, E., Wevers, R. A. (2006b) Mechanisms in protein O-glycan biosynthesis and clinical and molecular aspects of protein O-glycan biosynthesis defects: a review. *Clin. Chem.* **52(4)**, 574–600.
- Wopereis, S., Grünewald, S., Huijben, K. M., Morava, E., Mollicone, R., Van Engelen, B. G., Lefeber, D. J., Wevers, R. A. (2007) Transferrin and apolipoprotein C-III isofocusing are complementary in the diagnosis of N- and O-glycan biosynthesis defects. *Clin. Chem.* **53(2)**, 180–187.
- Xia, B., Zhang, W., Li, X., Jiang, R., Harper, T., Liu, R., Cummings, R. D., He, M. (2013) Serum N-glycan and O-glycan analysis by mass spectrometry for diagnosis of congenital disorders of glycosylation. *Anal. Biochem.* **442(2)**, 178–185.
- Zeevaert, R., De Zegher, F., Sturiale, L., Garozzo, D., Smet, M., Moens, M., Matthijs, G., Jaeken, J. (2013) Bone dysplasia as a key feature in three patients with a novel congenital disorder of glycosylation (CDG) type II due to a deep intronic splice mutation in TMEM165. *JIMD Rep.* **8**, 145–152.

Title: ApoC-III hypoglycosylation in glycogen storage diseases: the role of UDP-GalNAc depletion?

Authors' names and institutional affiliations:

¹Nina Ondruskova, ¹Tomas Honzik, ¹Hana Kolarova, ¹Jiri Zeman, ¹Hana Hansikova

¹Department of Pediatrics and Adolescent Medicine, First Faculty of Medicine, Charles University in Prague and General University Hospital in Prague, Ke Karlovu 2, 12808, Prague 2, Czech Republic

Corresponding author: Hana Hansikova, hana.hansikova@lf1.cuni.cz, Department of Pediatrics and Adolescent Medicine, First Faculty of Medicine, Charles University in Prague and General University Hospital in Prague, Ke Karlovu 2, 12808, Prague 2, Czech Republic

Word counts: Text: 2915 words; Summary: 249 words

Number of figures and tables: 2 figures, 2 tables

A summary:

Apolipoprotein C-III (ApoC-III) is a mostly liver-derived serum O-glycoprotein, which is used, along with N-glycoprotein transferrin (TRF), as a marker in the biochemical screening of congenital disorders of glycosylation (CDG). However, it is increasingly evident that secondary glycosylation abnormalities might occur in other, non-CDG metabolic diseases (such as type 2 diabetes), generally reflecting the severity of their disease course. The recent re-classification of phosphoglucomutase 1 (PGM1) deficiency to PGM1-CDG from what was originally designated as glycogen storage disease (GSD) type XIV has inspired us to examine the possible glycosylation disturbances in the serum from our group of 30 patients with various types of GSD. Interestingly, isoelectric focusing and SDS-PAGE analysis revealed mild to significant ApoC-III hypoglycosylation in types Ia, non-Ia, III, VI and IX. The most profound alterations in the relative amounts of ApoC-III sialylated isoforms were found in GSD type III, with the mean values of asialoApoC-III: 11.3 %, monosialoApoC-III: 68.7 % and disialoApoC-III: 20.1 % (vs. the reference range of 3.3 %, 53.3 % and 43.4 %, respectively). The extent of the detected reduced O-glycosylation in GSD Ia and non-Ia seemed to be associated with some parameters of metabolic compensation, while hypertriglyceridemia alone was excluded as the causative factor. We hypothesize a potential role for the reduced availability of the nucleotide-monosaccharides, specifically UDP-GalNAc, in the glycosylation reactions in patients with GSD III, VI and IX. We also suggest another possible mechanism through the decreased expression of the *GALNT2* gene, in response to a currently unknown metabolic factor.

Synopsis: Glycogen storage disease types Ia, non-Ia, III, VI and IX present with mild to profound serum apolipoprotein C-III hypoglycosylation.

Details of the contributions of individual authors:

Nina Ondruskova (realization of experimental part, manuscript preparation), Tomas Honzik (patients recruitment, samples and clinical data collection, manuscript preparation and revision), Hana Kolarova (samples collection, laboratory and clinical data collection), Jiri Zeman (patients recruitment, samples collection, manuscript revision), Hana Hansikova (experimental part supervision, manuscript preparation and revision)

Name of one author who serves as guarantor: Hana Hansikova

Competing interests: none

Details of funding: This study was supported by the grants IGA MZ CR NT-12166-5/2011 (H.H. and N.O.), RVO-VFN 64165/2012 (T.H.), UNCE 204011 (N.O.), SVV UK 260148/2015 (N.O. and H.K.) and Grant Agency of Czech Republic, GACR 14-36804G, Centre of mitochondrial biology and pathology (MITOCENTRE) (J.Z.). The authors confirm independence from the sponsors; the content of the article has not been influenced by the sponsors.

Details of ethics approval: The study was approved by Ethical committee of the First Faculty of Medicine, Charles University in Prague and General University Hospital in Prague.

A patient consent statement: Informed consent form was signed by each participant or their parents.

Keywords: glycogen storage disease; glycosylation; apolipoprotein C-III; congenital disorders of glycosylation; hypertriglyceridemia

Abbreviations (not explained in the text):

Glc - glucose, Gal - galactose, Man - mannose, Fru - fructose, Glc-1(6)-P - glucose-1(6)-phosphate, Gal-1-P - galactose-1-phosphate, Man-6-P - mannose-6-phosphate, Fru-6-P - fructose-6-phosphate, GlcNAc - N-acetylglucosamine, GalNAc - N-acetylgalactosamine, Neu(5)Ac - neuraminic acid (sialic acid), UDP-Gal - uridine diphosphate galactose; UDP-GlcNAc - uridine diphosphate N-acetylglucosamine, UDP-GalNAc - uridine diphosphate N-acetylgalactosamine, CMP-Neu5Ac - cytidine monophosphate neuraminic acid; SNPs - single nucleotide polymorphisms

Introduction

Apolipoprotein C-III (ApoC-III) is a serum core 1 mucin type O-glycoprotein that is produced in the liver and intestine, and its main functions are to promote VLDL assembly and inhibit lipoprotein lipase activity. There is a strong positive correlation between ApoC-III and triacylglycerols (TAG) serum concentrations (Marcoux et al., 2001). Because it carries the most common form of O-glycan in humans, it is used, along with serum N-glycoprotein transferrin (TRF), as a marker in screening for congenital disorders of glycosylation (CDG) (Wopereis et al., 2007). Due to the multi-systemic, non-specific and extremely variable clinical manifestation of CDG syndromes (currently, there are more than 100 types, and the number is rapidly expanding (Hennet and Cabalzar, 2015)), an accurate biochemical analysis is crucial for a correct diagnosis.

However, a number of studies have emerged lately reporting complex dysregulation of plasma glycoprotein glycosylation in various unrelated, non-CDG metabolic diseases, such as type 2 diabetes, metabolic syndrome, malnutrition, rheumatic diseases, IgA nephropathy (IgAN) or Prader-Willi syndrome (Allen, 1995, Bilen et al., 2014, Chrostek et al., 2014, Munce et al., 2010, Savinova et al., 2014, Testa et al., 2015). The causes for the observed secondary glycosylation abnormalities remain largely unexplained and are likely specific for each condition, but, in general, a greater extent of metabolic derangement is associated with more prominent glycosylation disturbances.

Recently, aberrant TRF glycosylation was found in phosphoglucomutase 1 (PGM1; EC 5.4.2.2) deficiency (OMIM: 614921), a monogenic metabolic disease originally labelled as glycogen storage disorder (glycogenosis, GSD) type XIV (Stojkovic et al., 2009), which led to its novel classification as a congenital disorder of glycosylation (PGM1-CDG) (Timal et al., 2012). Glycogenoses are a group of rare inborn defects in glycogen metabolism that are characterized by a histological finding of either an increased cellular accumulation of glycogen molecules, with a normal or an abnormal structure, or its depletion. GSD types are mostly denoted by roman numerals that are further subdivided based on the causative genes, the affected tissue (muscle, liver or both) and the onset of the disease (Kilimann and Oldfors, 2015). Clinically, the majority of patients with GSD show exercise intolerance, hypotonia or muscle cramps, while hepatic involvement typically manifests with hepatomegaly and episodes of hypoglycemia. In addition to fasting hypoglycemia, laboratory abnormalities often include lactic acidosis, hyperlipidemia (particularly

hypertriglyceridemia), hyperuricemia, increased creatine kinase and hepatic transaminases. Similar to PGM1-CDG, where the detected protein hypoglycosylation is caused by insufficient UDP-Gal as a substrate for galactosylation reactions (Morava, 2014), UDP-Gal levels were found to be reduced in the liver of patients with galactosemia (Ng et al., 1989). Although the primary complications of galactosemia are attributed to the toxic accumulation of Gal-1-P, multiple studies have confirmed that the patients harbor N- and O-glycans abnormalities (Liu et al., 2012, Sturiale et al., 2005) which qualify galactosemia as a glycosylation-related disorder. The above examples imply that it should not be unexpected to find glycosylation alterations in some of the other monogenic disorders of carbohydrate metabolism.

The aim of our study was to examine serum N- and O-glycosylation in our group of patients with various types of confirmed glycogenoses to determine whether there is a broader biochemical overlap between the CDG and GSD syndromes.

Material and methods

Patients and material

The analyzed group consisted of patients diagnosed with various types of glycogen storage diseases (total: n = 30; 2x type 0 (OMIM: 240600), 7x Ia (OMIM: 232200), 3x non-Ia (OMIM: 232220), 6x II (OMIM: 232300), 7x III (OMIM: 232400), 1x VI (OMIM: 232700), 4x IX (OMIM: 306000); 46 serum samples altogether), 2 subjects with hypertriglyceridemia due to familial lipoprotein lipase (LPL) deficiency (OMIM: 238600), one patient with suspected Berardinelli-Seip congenital lipodystrophy (BSCL) and one individual with hypertriglyceridemia of unknown origin; for the selected clinical and laboratory data, see Table 1 (patients suffering from GSD type II are not included in Table 1 due to their biochemically distinct presentation, compared to other GSD). All of the GSD patients were treated with uncooked cornstarch according to standard guidelines. Additionally, all of the subjects with GSD type Ia or non-Ia required continuous nocturnal gastric drip-feeding to prevent hypoglycemia. Glucose blood levels were monitored before feeding. No marked hyperglycemias were detected during our follow-ups in any of the analysed GSD patients. Patients were defined as having poor glycemic control when ≥ 2 hypoglycemias per 1 week were registered during the house monitoring. Blood was obtained from the tested patients with informed consent from each participant or their parents. Serum was separated by centrifugation (630 g, 10 min) and stored at -20 °C until analysis.

Isoelectric focusing (IEF), sodium dodecyl sulphate polyacrylamide gel electrophoresis (SDS-PAGE) and Western blot of serum ApoC-III, TRF and alpha-1-antitrypsin (AAT)

IEF of ApoC-III and Western blotting was carried out as described previously, and the profiles were evaluated using the determined reference range in (Ondrušková et al., 2015). IEF of TRF and SDS-PAGE of ApoC-III was performed according to Wopereis et al. (Wopereis et al., 2005) and the Western blotting of ApoC-III as in (Ondrušková et al., 2015). Neuraminidase treatment of ApoC-III in a control sample was performed by mixing 4 μ l of serum with 1 μ l of neuraminidase, followed by overnight incubation at laboratory temperature. SDS-PAGE and Western blot of AAT was performed as follows: serum was centrifugated (6600 g for 2 min), the clear middle fraction was diluted 100-fold with distilled water and this was then diluted 10-fold with fresh made sample buffer (10 mM Tris/HCl pH 8.0, 1 mM EDTA, 2.5 % SDS, 2 % DTT and 0.01 % bromophenol blue), followed by protein denaturation at 95 °C for 5 min; after SDS-PAGE using the PhastSystem™ Electrophoresis

System (GE Healthcare) with a separation time of 180 volthours, the Western blotting was performed analogically to (Ondrušková et al., 2015), using an antibody to alpha-1-antitrypsin. The acquired profiles of the proteins' glycosylated isoforms were quantified densitometrically using AlfaDigiDoc for TRF and Quantity One for ApoC-III. TRF glycosylated profiles were labelled as normal, borderline or pathological according to our internal reference range that was determined for the method (and validated by external quality control testing ERNDIM-CDG).

Resources

Antibodies: ApoC-III (06501707, Biotrend, 1:1000), AAT (A0409, Sigma, 1:1000), TRF (A0002, Dako, 1:1000); Enzymes: neuraminidase (Roche, 11585886001, 10 U/ml); Software: AlfaDigiDoc (Alpha Innotech), Quantity One (Bio-Rad).

Results

A significant change in ApoC-III O-glycosylation, with markedly reduced disialo-(ApoC-III₂) and elevated mono- (ApoC-III₁) and/or asialoform (ApoC-III₀), was detected repeatedly in all of the 7 patients with GSD type III (mean values: ApoC-III₀: 11.3 %, ApoC-III₁: 68.7 %, ApoC-III₂: 20.1 % vs. ref. range: 3.3 %, 53.3 % and 43.4 %, respectively). Similarly, a profound ApoC-III hypoglycosylation was observed in all but one of the tested GSD IX individuals and in the patient with type VI. Mild to pronounced hypoglycosylation was also seen in types Ia and non-Ia, while type 0 had no pathological changes. SDS-PAGE confirmed ApoC-III hypoglycosylation, revealing an additional band at a lower molecular weight (M_w) in the patients with pathological IEF profile (selected profiles shown in Fig. 1). To determine whether this represents ApoC-III with a shortened glycan chain (without two terminal sialic acid residues) or whether it is ApoC-III without any glycan at all, we ran a control sample that was previously incubated with neuraminidase and, based on its position, concluded that the lower band is aglycosylated. The quantification of the ApoC-III sialylated isoforms' relative amounts in the analyzed samples is summarized in Table 2.

We then compared the available laboratory data from all of the GSD patients with our results and noted that a majority of patients with pathological ApoC-III had increased serum triacylglycerols (TAG), as shown in Table 2. Thus, we decided to analyse the subjects with non-GSD hypertriglyceridemia to test whether high TAG alone could be the causative factor. Whereas the LPL deficient patient with a higher TAG (14.1 mmol/l) also had a slightly higher ApoC-III₀ than the one with a TAG of 6.7 mmol/l (controls: 1.0-1.64), both of their ApoC-III glycosylated profiles were evaluated as borderline/normal, as were the profiles from the patients with suspected Berardinelli-Seip congenital lipodystrophy and hypertriglyceridemia of unknown origin.

In parallel, serum N-glycosylation was assessed by IEF of TRF, and interestingly, some samples that were drawn from GSD type III and VI patients (P15 P19, P20) at younger age (up to 2 years) showed TRF hyposialylation; however, this normalized with age (see Table 2). Borderline TRF hypoglycosylation was also detected in three older patients (P6, P17, P22). Nevertheless, no profound general defect in N-glycosylation was found by the SDS-PAGE analysis of AAT, which in N-glycosylation disorders, such as PMM2-CDG (deficiency of phosphomannomutase 2, EC 5.4.2.8; OMIM: 212065), shows a distinguishable pathological pattern (results not shown).

Discussion

The status of serum ApoC-III and TRF glycosylation is a subject of physiological interindividual variability (e.g., due to gene polymorphisms) and intraindividually undergoes age-dependent changes, which need to be considered first before it can be used as a marker to indicate any pathological processes. In our experience, healthy children below 2 years of age often present with an abnormal relative increase of fully glycosylated ApoC-III and, on the contrary, hypoglycosylated TRF, that both normalize with age. A good example is our finding in the serum withdrawn from P20 (GSD type VI) at the age of 2 who had seemingly normal ApoC-III, yet showed a pathological TRF glycosylated profile, and who later, at the age of 3, showed a normal TRF but a markedly pathological ApoC-III glycosylation. The previously described physiological increase of ApoC-III₀ percentage with age (Wopereis et al., 2003) was clearly evident and can be seen in 3 chronologically different samples from GSD III patients P13 or P15 (see Table 2). Thus, the use of different reference ranges determined for the corresponding age categories and repeated analyses in the same individual at various chronological stages are recommended.

Our analysis of ApoC-III by isoelectric focusing revealed mild to profound ApoC-III hyposialylation in GSD types Ia, non-Ia, III, VI and IX. Based on our previous detection of ApoC-III hypoglycosylation in patients with Prader-Willi syndrome where a connection to increased serum TAG levels was found (Ondrušková et al., 2015), we originally reasoned that concomitant increased synthesis of ApoC-III could be the culprit (i.e., not having enough time to get properly modified due to the rapid passage through Golgi). However, because of normal/borderline ApoC-III glycosylation in non-GSD hypertriglyceridemic subjects, we presume this cannot be the causative factor.

GSD type III is caused by mutations in the *AGL* gene, coding for the debranching enzyme with catalytic activities of amylo-alpha-1,6-glucosidase (EC 3.2.1.33) and 4-alpha-glucanotransferase (EC 2.4.1.25). Dysfunctional debranching enzyme fails to break down glycogen at the branching points and thus blocks the subsequent action of glycogen phosphorylase (EC 2.4.1.1), which would normally produce approximately 10 molecules of Glc-1-P for each free glucose released by amylo-1,6-glucosidase. The same metabolic conversion (glycogen to Glc-1-P) is affected in types VI and IX, which have defective enzymatic functions of glycogen phosphorylase and its activating partner phosphorylase

kinase (EC 2.7.11.19), respectively. One potential cause of the detected significantly hypoglycosylated ApoC-III in these GSD types could be the decreased flux of precursors in the direction to form UDP-GlcNAc, a substrate needed for CMP-Neu5Ac synthesis, as well as for producing UDP-GalNAc (see Fig. 2). This would be in agreement with the observed normal to borderline N-glycosylation status of transferrin (produced mainly in liver, like ApoC-III), which contains terminal sialic acid residues but no GalNAc in its glycan structure. In contrast, the relatively decreased UDP-Gal level occurring in phosphoglucomutase 1 deficiency has different hypoglycosylation patterns, including rather slight ApoC-III hypoglycosylation, but clearly defective transferrin N-glycosylation.

It is important to note that a glycosylation defect, involving both the N- and O-glycome, was already described in neutrophils from patients with GSD type Ib (non-Ia) and with *G6PC3* defect (OMIM: 612541) (Hayee et al., 2011). *G6PC3* is an isoform of *G6PC*; however, the mutations in *G6PC3* are not associated with GSD type Ia but lead to severe neutropenia and neutrophil dysfunction (Jun et al., 2012). Mass spectrometry analysis of the neutrophils in the analysed patient with *G6PC3* deficiency showed reduced incorporation of galactose, especially into complex N-glycans and to a lesser extent into core 2 O-glycans (however, the galactosylation of core 1 was normal), and the authors hypothesize that this could be a result of an insufficient UDP-Gal concentration in the Golgi. They suggest that the detected aberrant glycosylation of gp91^{phox}, a NADPH oxidase component, could account for the diminished respiratory burst seen in *G6PC3*-deficient cells, and they also note that in both *G6PC3*-deficient and GSD Ib neutrophils, ER stress-related events might play a role in their pathophysiology. In another study by Raval et al., induced pluripotent cells (iPSC) were generated by reprogramming fibroblasts from patients with infantile-onset acid alpha-glucosidase deficiency (GSD type II) and were differentiated into cardiomyocytes (CM), in order to study the molecular basis of hypertrophic cardiomyopathy in Pompe disease (Raval et al., 2015). Unexpectedly, they discovered that the lysosomal-associated membrane proteins LAMP1 and LAMP2 had higher electrophoretic mobilities compared to a control and consequently established abnormal glycan processing in the Pompe iPSC-CM model. The observed hypoglycosylation of N-linked glycans was global and manifested with a deficiency of higher complexity bisecting bi-antennary and multi-antennary glycans. They speculate that these changes are secondary to the disturbed glycogen metabolism, which, by disproportional consumption of UTP and Glc-6-P (to produce glycogen), limits the availability of these

substrates for glycosylation reactions. It is still unknown, however, how the abnormal glycosylation detected in the iPSC-CM model of Pompe disease relates to cardiomyopathy. In comparison, our group of GSD type II patients all displayed normal serum ApoC-III glycosylation. Taken together, the above studies and our analyses demonstrate that glycosylation defects in GSD are complex and both type- and tissue-specific, and we need to take this into consideration when designing studies to determine their impact on physiological function.

O-glycosylation of ApoC-III occurs at Thr₉₄, and this site was validated as specific for the action of polypeptide N-acetylgalactosaminyltransferase 2 (ppGalNAc-T2, coded by *GALNT2*) (Schjoldager and Clausen, 2012). Recent genome-wide association studies report that certain SNPs in the *GALNT2* gene are linked to TAG and cholesterol levels (Kathiresan et al., 2008). Interestingly, in a study conducted by Holleboom et al., they provide evidence that the reduced catalytic activity of ppGalNAc-T2 due to mutation in *GALNT2* in the two studied probands is responsible for their elevated HDL and low TAG and that this effect occurs via underglycosylated ApoC-III (relatively increased ApoC-III₀), which is less potent at inhibiting LPL (Holleboom et al., 2011). On the other hand, Marucci et al. suggest that, based on their experiments, the decreased expression of *GALNT2* detected in patients with type 2 diabetes is secondary to hyperglycemia because in U937 cells exposed to high glucose concentrations, there was a reduction of *GALNT2* mRNA levels (Marucci et al., 2013). Overall, it is evident that a primary defect in glycosylation can lead to altered metabolic profiles, and vice versa, certain metabolic parameters might regulate the expression of genes involved in glycosylation.

In the case of GSD Ia and non-Ia, it seems likely that hypoglycosylated ApoC-III could be a consequence of altered *GALNT2* expression during the time of metabolic decompensation. However, up until now, the main factor (molecular link) has remained unidentified. This is partly supported by our analysis of the patients with multiple samples tested (P3, P10, P11). The ApoC-III glycosylation profile became more pathological after P3 experienced frequent hypoglycemia in the period of short-term non-compliance (sample 2 in Table 2) and when P10 showed severe metabolic decompensation at the time of diagnosis (sample 1, see Table 1 and 2) compared to when they were better compensated on a strict diet regime. There was no deterioration in terms of glycemic control, triglyceridemia, hepatopathy and hepatomegaly between the two measurements in P11 (6 months period; Table 1 and 2), which could be

associated with the worsening of his ApoC-III glycosylation. Nevertheless, it is worth mentioning that the latter presents with multiple complications (Crohn-like disease, recurrent infections, nephrotic syndrome, autoimmune thyroiditis, osteopenia, growth retardation and pubertal delay) with continuing long-term clinical disease progression. These results suggest that perhaps the glycosylation status of ApoC-III could be used, prospectively, as an alternative marker for monitoring the disease progression, up-to-date metabolic condition or therapeutic efficacy in GSD types Ia and non-Ia, but obviously further studies are required to characterize how ApoC-III glycosylation responds to specific metabolic changes.

Lastly, we cannot exclude the possible involvement of sialic acid cleaving/transferring enzymes in the circulation (neuraminidases (D'Avila et al., 2013), trans-sialidases (Tertov et al., 2001)) in the patients, or altered catabolism of ApoC-III glycoforms related to GSD pathophysiology. Further studies need to be performed to identify the underlying mechanism for the observed ApoC-III hypoglycosylation and to determine its implications for the disease course in patients.

Conclusion

Our study is the first to report mild to profound hypoglycosylation of serum ApoC-III, a predominantly liver-derived O-glycoprotein, in patients with glycogen storage diseases Ia, non-Ia, III, VI and IX. We hypothesize a role for insufficient levels of nucleotide-monosaccharides, nominally UDP-GalNAc, in the etiology of the glycosylation defect in GSD III, VI and IX. Our data also suggest that particularly in types Ia and non-Ia, ApoC-III glycosylation might be connected to the extent of their metabolic decompensation. Certain diseases, including GSD, likely present with a unique serum glycosylation pattern, which could serve as a valuable tool in the diagnostic process. Moreover, if the glycosylation status reflects metabolic dysbalances, as was indicated by our ApoC-III analysis in GSD Ia and non-Ia patients, it might be potentially applied for monitoring the course of their disease.

References

- Allen AC (1995) Abnormal glycosylation of IgA: is it related to the pathogenesis of IgA nephropathy? *Nephrol Dial Transplant* 10: 1121-1124.
- Bilen O, Altun Z, Arslan N, Onvural B, Akan P, Coker C (2014) The effect of malnutrition on protein glycosylation in children. *Iran J Pediatr* 24: 273-279.
- Chrostek L, Cylwik B, Gindzienska-Sieskiewicz E, Gruszewska E, Szmitkowski M, Sierakowski S (2014) Sialic acid level reflects the disturbances of glycosylation and acute-phase reaction in rheumatic diseases. *Rheumatol Int* 34: 393-399.
- D'Avila F, Tringali C, Papini N et al. (2013) Identification of lysosomal sialidase NEU1 and plasma membrane sialidase NEU3 in human erythrocytes. *J Cell Biochem* 114: 204-211.
- Hayee B, Antonopoulos A, Murphy EJ et al. (2011) G6PC3 mutations are associated with a major defect of glycosylation: a novel mechanism for neutrophil dysfunction. *Glycobiology* 21: 914-924.
- Hennet T, Cabalzar J (2015) Congenital disorders of glycosylation: a concise chart of glycolyx dysfunction. *Trends Biochem Sci* 40: 377-384.
- Holleboom AG, Karlsson H, Lin RS et al. (2011) Heterozygosity for a loss-of-function mutation in GALNT2 improves plasma triglyceride clearance in man. *Cell Metab* 14: 811-818.
- Jun HS, Cheung YY, Lee YM, Mansfield BC, Chou JY (2012) Glucose-6-phosphatase- β , implicated in a congenital neutropenia syndrome, is essential for macrophage energy homeostasis and functionality. *Blood* 119: 4047-4055.
- Kathiresan S, Melander O, Guiducci C et al. (2008) Six new loci associated with blood low-density lipoprotein cholesterol, high-density lipoprotein cholesterol or triglycerides in humans. *Nat Genet* 40: 189-197.
- Kilimann MW, Oldfors A (2015) Glycogen pathways in disease: new developments in a classical field of medical genetics. *J Inherit Metab Dis* 38: 483-487.
- Liu Y, Xia B, Gleason TJ et al. (2012) N- and O-linked glycosylation of total plasma glycoproteins in galactosemia. *Mol Genet Metab* 106: 442-454.
- Marcoux C, Tremblay M, Fredenrich A, Davignon J, Cohn JS (2001) Lipoprotein distribution of apolipoprotein C-III and its relationship to the presence in plasma of triglyceride-rich remnant lipoproteins. *Metabolism* 50: 112-119.
- Marucci A, di Mauro L, Menzaghi C et al. (2013) GALNT2 expression is reduced in patients with Type 2 diabetes: possible role of hyperglycemia. *PLoS One* 8: e70159.
- Morava E (2014) Galactose supplementation in phosphoglucomutase-1 deficiency; review and outlook for a novel treatable CDG. *Mol Genet Metab* 112: 275-279.
- Munce T, Heussler HS, Bowling FG (2010) Analysis of N- and O-linked protein glycosylation in children with Prader-Willi syndrome. *J Intellect Disabil Res* 54: 929-937.
- Ng WG, Xu YK, Kaufman FR, Donnell GN (1989) Deficit of uridine diphosphate galactose in galactosaemia. *J Inherit Metab Dis* 12: 257-266.

- Ondrušková N, Honzík T, Kytarová J, Matoulek M, Zeman J, Hansíková H (2015) Isoelectric Focusing of Serum Apolipoprotein C-III as a Sensitive Screening Method for the Detection of O-glycosylation Disturbances. *Prague Med Rep* 116: 73-86.
- Raval KK, Tao R, White BE et al. (2015) Pompe disease results in a Golgi-based glycosylation deficit in human induced pluripotent stem cell-derived cardiomyocytes. *J Biol Chem* 290: 3121-3136.
- Savinova OV, Fillaus K, Jing L, Harris WS, Shearer GC (2014) Reduced apolipoprotein glycosylation in patients with the metabolic syndrome. *PLoS One* 9: e104833.
- Schjoldager KT, Clausen H (2012) Site-specific protein O-glycosylation modulates proprotein processing - deciphering specific functions of the large polypeptide GalNAc-transferase gene family. *Biochim Biophys Acta* 1820: 2079-2094.
- Stojkovic T, Vissing J, Petit F et al. (2009) Muscle glycogenesis due to phosphoglucomutase 1 deficiency. *N Engl J Med* 361: 425-427.
- Sturiale L, Barone R, Fiumara A et al. (2005) Hypoglycosylation with increased fucosylation and branching of serum transferrin N-glycans in untreated galactosemia. *Glycobiology* 15: 1268-1276.
- Tertov VV, Kaplun VV, Sobenin IA, Boytsova EY, Bovin NV, Orekhov AN (2001) Human plasma trans-sialidase causes atherogenic modification of low density lipoprotein. *Atherosclerosis* 159: 103-115.
- Testa R, Vanhooren V, Bonfigli AR et al. (2015) N-glycomic changes in serum proteins in type 2 diabetes mellitus correlate with complications and with metabolic syndrome parameters. *PLoS One* 10: e0119983.
- Timal S, Hoischen A, Lehle L et al. (2012) Gene identification in the congenital disorders of glycosylation type I by whole-exome sequencing. *Hum Mol Genet* 21: 4151-4161.
- Wopereis S, Grünewald S, Huijben KM et al. (2007) Transferrin and apolipoprotein C-III isofocusing are complementary in the diagnosis of N- and O-glycan biosynthesis defects. *Clin Chem* 53: 180-187.
- Wopereis S, Grünewald S, Morava E et al. (2003) Apolipoprotein C-III isofocusing in the diagnosis of genetic defects in O-glycan biosynthesis. *Clin Chem* 49: 1839-1845.
- Wopereis S, Morava E, Grünewald S et al. (2005) Patients with unsolved congenital disorders of glycosylation type II can be subdivided in six distinct biochemical groups. *Glycobiology* 15: 1312-1319.

Table 1: Relevant clinical and laboratory data in the group of analysed patients.

Patients [gender, age] (serum sample number, in chronological order)	Diagnosis	BMI [kg/m ²]	Glycemic control	Hepatomegaly [cm below the costal margin] [¶]	Hepatopathy
P1 [F, 1.5 y] (1) [2.5 y] (2)	GSD 0	16.8 (50. P) 18.8 (99. P)	poor good	NP	NP NP
P2 [M, 11.5 y]	GSD 0	14.8 (11. P)	good	NP	NP
P3 [M, 13.5 y] (1) [14 y] (2)	GSD Ia	27.3 (>99. P; +3 SD) 26.7 (>99. P; +2.7 SD)	good good	+3	NP NP
P4 [M, 29 y]	GSD Ia	26	poor	+10	NP
P5 [M, 23 y]	GSD Ia	23.6	good	+4	NP
P6 [F, 8.5 y]	GSD Ia	17.0 (65. P)	good	+4	NP
P7 [M, 22 y]	GSD Ia	21.4	poor	+5	NP
P8 [M, 25 y]	GSD Ia	23.1	poor	+4	2x ↑LFT's
P9 [†] [M, 4 y]	GSD Ia	17.7 (90.6. P)	poor	+10	>5x ↑LFT's
P10 [M, 4 mo] (1) [9.5 y] (2)	GSD non-Ia	17.1 (65. P) 19.8 (90. P)	poor good	+3	1.5x ↑LFT's NP
P11 [M, 19 y] (1) [19.5 y] (2)	GSD non-Ia	26 (>90. P) 24.6	good good	+4	NP NP
P12 [F, 2 mo]	GSD non-Ia	14.3 (4.7. P)	poor	+6	NP
P13 [‡] [F, 1.5 y] (1) [7.5 y] (2) [8 y] (3)	GSD IIIa	16.1 (40. P) 15.9 (50. P) 15.9 (45. P)	good good good	+2	3.8x ↑LFT's 3x ↑LFT's 10.5x ↑LFT's
P14 [F, 17 y] (1) [17.5 y] (2)	GSD IIIa	25.3 (94.8. P) 26.0 (97. P)	poor poor	+9	9.5x ↑LFT's 13x ↑LFT's
P15 [M, 1.5 y] (1) [3 y] (2) [7 y] (3)	GSD IIIa	19.5 (91.7. P) 17.7 (86. P) 16.9 (70. P)	good good good	+10	20x ↑LFT's 63x ↑LFT's 6x ↑LFT's
P16 [§] [M, 6 y]	GSD IIIa	19 (97.6. P)	good	+11	>22x ↑LFT's
P17 [M, 16.5 y] (1) [17 y] (2)	GSD IIIa	NA 21. (45. P)	good good	+5	4x ↑LFT's 3.5x ↑LFT's
P18 [F, 39.5 y]	GSD IIIa	24.7	good	+2	2x ↑LFT's
P19 [M, 2 y] (1) [9.5 y] (2) [10 y] (3) [10.5 y] (4)	GSD IIIb	18.7 (91.5. P) 19.1 (83. P) 19.1 (80. P) 20.5 (90. P)	good good good good	+5	7.5x ↑LFT's NP NP NA
P20 [¶] [M, 2 y] (1) [3 y] (2)	GSD VI	16.9 (55. P) 15.9 (45. P)	good good	+10	16x ↑LFT's 5x ↑LFT's
P21 ^{¶¶} [M, 5 y] (1) [5.5 y] (2) [12 y] (3)	GSD IXa	14.5 (24. P) 14.8 (35. P) 15.9 (20. P)	good good good	NP	NP NP NP
P22 [M, 15.5 y]	GSD IXa	19.5 (35. P)	good	+6	5x ↑LFT's
P23 ^{¶¶} [M, 2.5 y]	GSD IXa	17.3 (79. P)	good	+2	1.5x ↑LFT's
P24 [F, 26.5 y]	GSD IXa	22.9	good	NP	NP

Table 1. Continuation

Patients [gender, age] (serum sample number, in chronological order)	Diagnosis	BMI [kg/m²]	Glycemic control	Hepatomegaly[¶] [cm below the costal margin]	Hepatopathy
HyperTAG controls (HTC)					
HTC1 [F, 8 y]	LPL deficiency	14.7 (25. P)	good	NP	NP
HTC2 [M, 5 y]	LPL deficiency	11.9 (0.6. P)	good	NP	NP
HTC3 [M, 6 mo]	Berardinelli – Seip congenital lipodystrophy	14.1 (6. P)	good	+3	NP
HTC4 [M, 3 y]	hyperTAG of unknown origin	14.6 (17. P)	good	NP	NP

M – male, F – female, mo – months, y – years, LFT's – liver function tests (expressed as multiples of alanine aminotransferase upper reference limit; controls <0.6), LPL – lipoprotein lipase, NA – not available, NP – not present, P – percentile, SD – standard deviation, [¶]only the first measurement is listed (no change over time) [‡]patient treated for growth hormone deficiency, [€] activity of glycogen debrancher enzyme 0.72 nmol/24h/mg Hb (ref. range 8 - 34), [¥] activity of glycogen debrancher enzyme 0.43 nmol/24h/mg Hb, ^Σ activity of glycogen debrancher enzyme 0.3 nmol/24h/mg Hb, ^τactivity of liver glycogen phosphorylase 4.70 umol/min/g protein (ref. range 8 – 35), ^Ωactivity of phosphorylase kinase 0 umol/min/g Hb (controls >100), ^βactivity of phosphorylase kinase 0 umol/min/g Hb (controls >100)

Table 2. Quantification of apolipoprotein C-III sialylation and transferrin glycosylation status related to serum concentration of triacylglycerols and glycemia in the analysed patients.

Patients [gender, age] (serum sample)		Percentage of total ApoC-III [%]			TRF glyco- sylation [†]	TAG [mmol/l] [‡]	Glycemia [mmol/l] [‡]
		Disialo- (2)	Monosialo-(1)	Asialo- (0)			
Reference range (0d-42y)		27.1 – 79.5	19.4 – 65.5	0 – 8.3	N	1.0-1.64 [‡]	3.3-5.8
GSD 0	P1 [F, 1.5 y] (1)	38.8	57.9	3.3	N	1.33	5.3
	[2.5 y] (2)	48.6	47.7	3.7	N	0.44	5.0
	P2 [M, 11.5 y]	28.4	69.9	1.7	N	0.84	5.9
GSD Ia	P3 [M, 13.5 y] (1)	30.8	66.1	3.2	N	3.22	4.7
	[14 y] (2)	28.8	71.2	0	N	4.11	1.9 [€]
	P4 [M, 29 y]	31.4	55.9	12.6	N	7.8	4.7
	P5 [M, 23 y]	26.6	57	16.4	N	6.52	5.1
	P6 [F, 8.5 y]	27.1	65.5	7.4	B	3.13	5.1
	P7 [M, 22 y]	28.1	64.6	7.3	N	9.98	5.3
	P8 [M, 24 y]	27.1	63.1	9.8	N	12.37	5.8
	P9 [M, 4 y]	29.1	54.5	16.4	N	19.28	3.5
GSD non-Ia	P10 [M, 4 mo] (1)	31.9*	66.9	1.2	N	7.52	5.6
	[9.5 y] (2)	32.1	62.9	5	N	1.12	4.8
	P11 [M, 19 y] (1)	39	50.1	10.9	N	4.77	4.5
	[19.5 y] (2)	21.6	68.5	9.8	N	2.38	4.5
	P12 [F, 2 mo]	36.2	63.1	0.7	N	5.11	1.0
GSD III (part I)	P13 [F, 1.5 y] (1)	33.7*	57.2	9.1	N	9.3	6.5
	[7.5 y] (2)	13.7	73.4	12.9	N	2.44	4.2
	[8 y] (3)	21.4	57.7	21	N	4.99	3.9
	P14 [F, 17 y] (1)	16.1	73.5	10.4	N	2.15	5.3
	[17.5 y] (2)	22.3	71.1	6.6	N	2.02	4.1
	P15 [M, 1.5 y] (1)	20.7	69.4	9.9	P	5.18	4.0
	[3 y] (2)	26.8	61.7	11.5	N	4.02	4.8
	[7 y] (3)	14.6	63.4	22	N	4.04	5.3

Table 2. Continuation

Patients [gender, age] (serum sample)		Percentage of total ApoC-III [%]			TRF glyco- sylation [†]	TAG [mmol/l] [‡]	Glycemia [mmol/l] [‡]
		Disialo- (2)	Monosialo-(1)	Asialo- (0)			
Reference range (0d-42y)		27.1 – 79.5	19.4 – 65.5	0 – 8.3	N	1.0-1.64 [‡]	3.3-5.8
GSD III (part 2)	P16 [M, 6 y]	20.7	70.7	8.6	N	2.27	4.5
	P17 [M, 16.5 y] (1)	11.2	68.5	20.4	B	2.44	5.5
	[17 y] (2)	14.1	63.5	22.5	B	1.97	4.2
	P18 [F, 39.5 y]	26.1	69	5	N	1.41	4.6
	P19 [M, 2 y] (1)	31.2*	64.9*	3.9	P	1.21	3.7
	[9.5 y] (2)	14.5	80.5	5	N	0.65	3.7
	[10 y] (3)	17.3	75.4	7.4	N	NA	NA
	[10.5 y] (4)	16.8	78.6	4.6	N	NA	NA
GSD VI	P20 [M, 2 y] (1)	36.5	58.1	5.4	P	4.46	3.4
	[3 y] (2)	15	75.6	9.4	N	3.77	4.1
GSD IX	P21 [M, 5 y] (1)	37.5	59.2	3.3	N	0.75	5.7
	[5.5 y] (2)	30.8*	64.1	5.1	N	1.2	4.4
	[12 y] (3)	40.6	57.3	2.1	N	0.68	5.0
	P22 [M, 15.5 y]	13.4	72	14.7	B	1.33	5.1
	P23 [M, 2.5 y]	16.2	78.1	5.7	N	2.14	6.6
	P24 [F, 26.5 y]	16.3	74.8	9	N	1.33	4.2
GSD II	P25-30 [F/M, 9 mo-34 y]	40.1-61.6	36.1-55.8	1.6-4.2	N	NA	NA
HyperTAG	HTC1 [F, 8 y]	40.4	51.2	8.5	N	14.1	5.0
	HTC2 [M, 5 y]	48.1	48.5	3.4	N	6.66	4.0
	HTC3 [M, 6 mo]	44.8	50.4	4.9	N	8.24	4.5
	HTC4 [M, 3 y]	46.6	50.3	3.1	N	1.7	4.4

M – male, F – female, mo – months, y – years, hyperTAG – hypertriglyceridemia, NA - not available, [†]evaluated as normal (N), borderline (B) or pathological (P), [‡]for children aged 1 - 15 years, for children <1 year the reference range is 0.5 - 2.22, for >15 years 0.68 - 1.7, [‡]average values of measurements made 3 – 0 days prior to ApoC-III isoelectric focusing (ApoC-III biological half-life is approximately 2.5 days), *pathological due to reference range determined for age interval <2 years; [‡]the lowest value measured during hypoglycemia attacks 2-3 days prior to ApoC-III isoelectric focusing

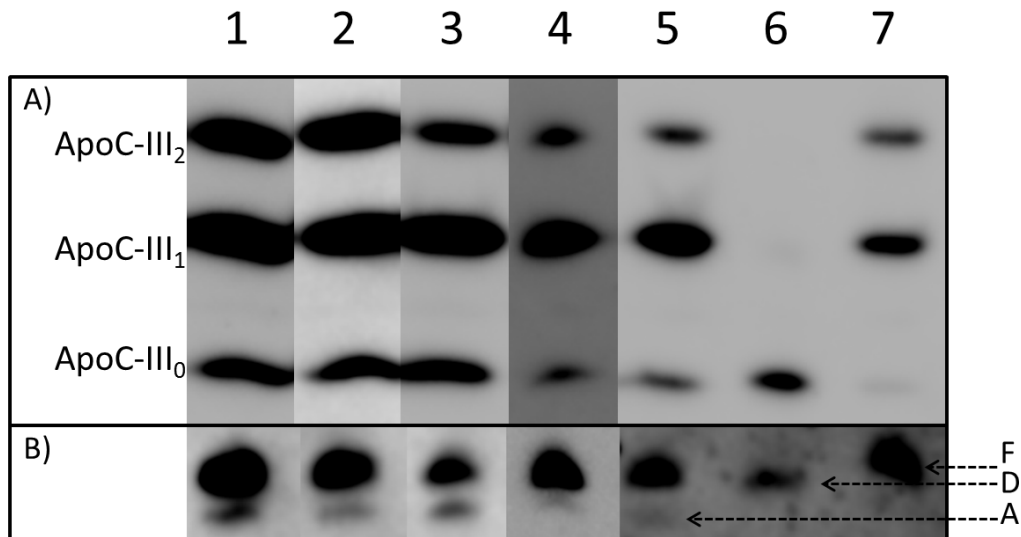


Figure 1: Isoelectric focusing (A) and SDS-PAGE (B) analysis of ApoC-III in selected serum samples from patients with various types of GSD. Lane 1 (GSD type Ia; P4), lane 2 (GSD non-Ia; P11, sample 1), lane 3 (GSD III; P15, sample 3), lane 4 (GSD VI; P20, sample 2), lane 5 (GSD IX; P22), lane 6 (healthy control, serum after neuraminidase treatment), lane 7 (healthy control, serum without neuraminidase treatment). A) Serum was separated by isoelectric focusing, followed by Western blot detection of ApoC-III. Position of the sialylated ApoC-III isoforms (disialo-, monosialo-, asialo-) is indicated on the left. B) Serum samples were separated by SDS-PAGE (20 % gel, PhastGel High Density, GE Healthcare), followed by Western blot detection of ApoC-III. Arrows on the right indicate fully glycosylated form (F), desialylated form (D) and aglycosylated form (A) of ApoC-III, as judged by their apparent molecular weight.

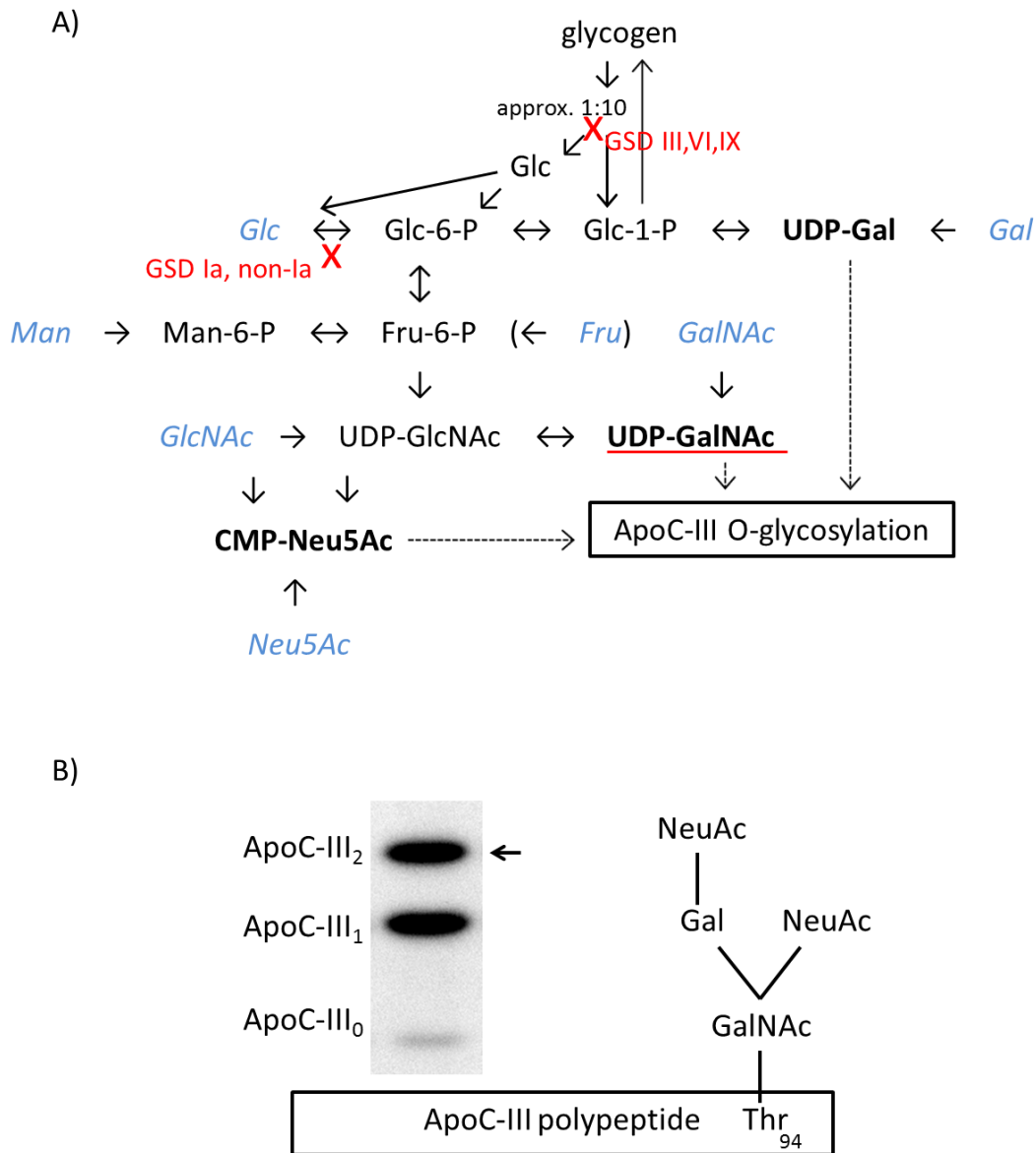


Figure 2: Schematic overview of the biosynthesis of substrates for ApoC-III glycosylation in liver. A) The biosynthesis of the substrates for ApoC-III O-glycosylation. Blue italic represents monosaccharides derived from dietary (extracellular) sources and/or salvage pathways, red cross indicates position of the defect within metabolic pathway. UDP-GalNAc, whose availability is hypothesized to be reduced in GSD types III, VI and IX, is underlined in red. A shortened version of the reactions is shown. B) The structure of fully glycosylated ApoC-III O-glycan. The arrow points to ApoC-III disialoform separated by isoelectric focusing, corresponding to the depicted structure.